The Environmental Fate of Cadmium in the Soils of the Waste Water Irrigation Area of Braunschweig

- Measurement, Modelling and Assessment -

Von der Gemeinsamen Naturwissenschaftlichen Fakultät

der Technischen Universität Carolo-Wilhelmina

zu Braunschweig

zur Erlangung des Grades eines

Doktors der Naturwissenschaften

(Dr. rer. nat.)

genehmigte

D i s s e r t a t i o n

von

Joachim Ingwersen

aus Bargum

1. Referent: Prof. Dr. T. Streck

2. Referent: Prof. Dr. O. Richter

eingereicht am: 11.12.2000

mündliche Prüfung (Disputation) am: 26.03.2001

Druckjahr 2001

“So eine Arbeit wird eigentlich nie fertig, man muß sie für fertig erklären, wenn man nach Zeit und Umständen das Möglichste getan hat.“

Goethe in Caserta 16. März 1787

Vorveröffentlichungen der Dissertation

Teilergebnisse aus dieser Arbeit wurden mit Genehmigung der Gemeinsamen Naturwissenschaftlichen Fakultät, vertreten durch den Mentor der Arbeit, in folgenden Beiträgen vorab veröffentlicht:

Publikationen

- Ingwersen, J., Streck, T. & Richter, J. Cadmium-Verlagerung in den Böden des Abwasserverregnungsgebietes Braunschweig. Mitteilgn. Dtsch. Bodenkundl. Gesellsch. 85: 249-252 (1997).
- Ingwersen, J., Streck, T. & Richter, J. Verfahren zur regionalen Bewertung der Cadmiumeinträge in die Böden des Abwasserverregnungsgebietes Braunschweig. In: Renger, M., F. Alaily und G. Wessolek (Hrsg.) Mobilität & Wirkung von Schadstoffen in urbanen Böden. Heft 26: 152-163 (1998).
- Ingwersen, J., Streck, T. & Richter, J. Verlagerung und Pflanzenaufnahme von Cadmium im regionalen Maßstab – eine Fallstudie. In: Flake, M., R. Seppelt und D. Söndgerath (Hrsg.) Dynamik natürlicher und anthropogener Systeme und ihre Wechselwirkungen. 175-182 (1999).
- Ingwersen, J., Streck, T. & Richter, J. Ein transpirationsbasiertes Modell zur Prognose der pflanzlichen Cd-Aufnahme. Mitteilgn. Dtsch. Bodenkundl. Gesellsch. 91/III: 1466-1469 (1999).
- Ingwersen, J., Streck, T., Utermann, J. & Richter, J. Ground water preservation by soil protection: Determination of tolerable total Cd contents and Cd breakthrough times. J. Plant Nutr. Soil Sci. 163: 31-40 (2000).

Tagungsbeiträge

- Ingwersen, J., Streck, T. & Richter, J. Cadmium-Verlagerung in den Böden des Abwasserverregnungsgebietes Braunschweig. (Poster) Jahrestagung der Deutschen Bodenkundlichen Gesellschaft, Konstanz (1997).
- Ingwersen, J., Streck, T. & Richter, J. Verfahren zur regionalen Bewertung der Cadmiumeinträge in die Böden des Abwasserverregnungsgebietes Braunschweig. (Vortrag) Abschlußtagung "Mobilität & Wirkung von Schadstoffen in urbanen Böden", Berlin (1998).
- Ingwersen, J., Streck, T., Utermann, J. & Richter, J. Determination of Tolerable Total Cd Contents in Soils. (Vortrag) 2nd Symposium: Heavy Metals in the Environment and Electromigration Applied to Soil Remediation, Lyngby (1999).
- Ingwersen, J. Streck, T., Utermann, J. & Richter, J. Grundwasserschutz durch Bodenschutz: Ermittlung von tolerierbaren Cd-Gesamtgehalten and Cd-Durchbruchszeiten (Vortrag) 111. VDLUFA-Kongress, Halle (1999).
- Ingwersen, J., Streck, T. & Richter, J. Verlagerung und Pflanzenaufnahme von Cadmium im regionalen Maßstab – eine Fallstudie. (Vortrag) Geoökon`99, Braunschweig (1999).
- Ingwersen, J., Streck, T. & Richter, J. Ein transpirationsbasiertes Modell zur Prognose der pflanzlichen Cd-Aufnahme. (Vortrag) Jahrestagung der Deutschen Bodenkundlichen Gesellschaft, Hannover (1999).
- Ingwersen, J., Streck, T. & Richter, J. Prognose und Bewertung des Umweltverhaltens von Cd in den Sandböden des Abwasserverregnungsgebietes Braunschweig. (Vortrag) HydroGeoEvent 2000, Heidelberg (2000).

Table of Contents

1 Introduction

Particularly in the 1970s and the early 1980s the concern about significant pollution of soils, plants and ground water by heavy metals led to a boost in the research on heavy metals. Since the German Soil Protection Act (BBodSchG, 1998) has come into force in 1998, modelling of the environmental fate of heavy metals, particularly with regard to the forecast of heavy metal concentrations in seepage water, has made a comeback. In this context Cadmium (Cd) is of special importance. It is one of the most mobile and bioavailable heavy metals in soil and may cause human- and ecotoxicological impacts even at low concentrations. Poisonous effects of Cd, especially at chronic loads, were more or less unknown until the middle of the 20th century. With regard to the human intake, the most important pathway is food. Cd is characterized by a very long biological half-life (10-30 yr). Therefore it accumulates in organs like the liver or the kidney, which might cause functional disorders. For example, protenurie has been observed at a Cd content of the kidney-cortex higher than 200 µg kg^{-1} (Marquardt and Schäfer, 1994). The WHO (1972) has recommended that food may not contain more than 0.1 mg Cd kg^{-1}. This value corresponds to a provisional tolerable weekly intake (*PTWI*) of 400-500 µg Cd. At this intake rate the Cd concentration of the kidney-cortex should never exceed the critical concentration of 200 µg kg^{-1} during a normal human life. Nowadays the average Cd intake by food is in general significantly smaller than the *PTWI* (Table 1). Food with low Cd concentration but high consumption rate, like wheat or potato, is the major part of the weekly Cd intake.

The soil is one of the most important environmental compartments in the biogeochemical cycle of heavy metals. Soils are natural buffers and filters and mainly control the transfer of heavy metals to the adjacent compartments ground

water and plants. Since the industrial revolution the Cd input in soils has continuously increased. For instance, from data by Jones et al. (1987) it follows that from 1895 to 1950 the Cd input in soils at Rothamsted Experimental Station (U.K.) increased nearly linearly at a rate of 0.1 g ha yr^{-1} from 1.1 g ha yr^{-1} to 6.5 g ha yr^{-1}. After 1950, Cd inputs increased more steeply at a rate of about 0.5 g ha yr^{-1}. In 1980, the annual Cd input was about 21.7 g ha^{-1}.

Table 1: Estimated weekly Cd intake by food as calculated by Diehl and Boppel (1985). According to the WHO (1972) the provisional tolerable weekly intake (PTWI) of Cd is 400-500 µg.

Food	**Consumption**	**Cd concentration**	**Cd intake**
	— kg wk^{-1} —	**— µg kg^{-1} —**	**— µg wk^{-1} —**
Wheat	1.58	56 ± 51	89
Potato	1.23	48 ± 51	59
Beer	6.99	3.9 ± 7.9	27
Drinking water	4.55	2	9
Leaf vegetable	0.11	72 ± 194	8
Eggs	0.36	12 ± 14	4
Coffee	0.18	17 ± 12	3
Wine	0.61	5	3
Pork	0.39	12 ± 20	5
Kidney (pork)	0.004	692 ± 849	3
Root vegetable	0.08	245 ± 430	20
Milk	1.25	2.9 ± 3.9	4
Total Cd Intake			234

Cd enters agricultural soils mainly via atmospheric deposition, fertilization, sewage sludge or compost. During the last decade the atmospheric deposition of Cd in the Federal Republic of Germany (*FRG)* has markedly decreased. In 1985, the Cd emissions amounted to 45 t and decreased by 34 t to 11 t in 1995 (Umweltbundesamt, 1997). Emissions are predominantly caused by power stations, industrial production facilities, motor vehicles and domestic heating. In 1995, 2.53 Mio t sewage sludge was applied in the *FRG*. The major part of the

sewage sludge was dumped or burned (1.15 Mio t). 0.95 Mio t was recycled by use in agriculture. The remaining 0.43 Mio t was reused in horticulture, fruit-growing, recultivation etc. The recycling of sewage sludge in agriculture is likely to increase in the next years. According to the Technical Guidelines on Domestic Waste (TA-Siedlungsabfall, 1993) the dumping of sewage sludge will not be allowed by 2004 and the burning of sewage sludge is very expensive. After the Waste Avoidance, Recycling and Disposal Act (KrWAbfG, 1994) came into force in 1996 the amount of compost strongly increased. This law prescribes the non-thermal recycling of organic wastes provided that material recycling is environmentally sound. According to an estimation by Kehres (1994) the annual amount of compost will be 2.6 to 4.1 Mio t in the *FRG* after installing an all over composting system.

Table 2: Cd balance for a rural and an urban district in Germany. The Cd input by compost and sewage sludge was calculated from maximum permitted application rates (Hackenberg and Wegener, 1999).

	Gießen District	**Recklinghausen District**
	— g ha^{-1} yr^{-1} —	**— g ha^{-1} yr^{-1} —**
Cd input		
Fertilizer	1.40	1.48
Compost	2.00	6.44
Sewage Sludge	2.67	3.34
Atmospheric Deposition	1.25	3.32
Sum	7.32	14.58
Cd output		
Harvest material	0.79	0.90
Seepage water	0.60	0.60
Soil erosion	n.a. [§]	n.a. [§]
Sum	1.39	1.50
Cd accumulation	5.93	13.08

[§] not available

Whether Cd accumulates in soil depends on its balance, i.e. on the relationship between sink, source and buffer terms. As sinks are considered the withdrawal

with harvest material, leaching and loss by soil erosion. Hackenberg and Wegener (1999) performed Cd balances for an urban and a rural district in Germany (Table 2). At maximum permitted application rates in both districts the sources are higher than sinks, that is, Cd accumulates in soil. The Cd input via compost, sewage sludge and atmospheric deposition in the urban district is twice as high as in the rural district. In both districts the current Cd output via harvest material and leaching is 5 to 10 times lower than the total Cd input.

After entering the soil, Cd is mainly sorbed on the surface of organic compounds or clays. Only a minor fraction stays in solution. However, the latter fraction is the key variable in controlling bioavailability and leaching of Cd (Allen, 1993). Cd in soil solution can be displaced towards ground water and Cd in soil solution can be transferred to plants. The relationship between sorbed and dissolved phase depends on soil properties like *p*H, organic carbon (*OC*) content, clay content etc.

To sum up, when we investigate the environmental fate of Cd we have to focus on displacement, plant uptake and the sorption properties of soil. Hence, the present study concentrates on these issues which are introduced in more detail in Chapter 3.

2 Objectives and Outline

To verify and expand our understanding of the processes governing the environmental fate of heavy metals in the "real world" we are forced to make investigations under field conditions and at scales larger than a soil column. Not many of such studies, however, have been published so far. Examples are the studies by Boekhold and Van der Zee (1992), Streck and Richter (1997a,b) and Tiktak et al. (1998). Boekhold and Van der Zee (1992) predicted Cd contents along a 200 m transect in a field using an extended Freundlich equation that accounts for soil *p*H, organic carbon and Cd concentration in soil solution. Predictions showed a good agreement with the observed spatial pattern. Tiktak et al. (1998) studied the heavy metal accumulation in Ap horizons of Dutch soils at the national scale (40,000 km^2). They developed a simple process-oriented model which successfully predicted the Cd content in topsoils. Streck and Richter (1997a,b) investigated the Cd displacement at the field scale (about 0.01 km^2). For their investigation they chose a sandy and acidic soil with low organic matter content within the waste water irrigation area (*WIA*) of Braunschweig. This soil had undergone high loads of heavy metals by irrigation of municipal waste water for about 30 years. These conditions led to a measurable Cd displacement and a solute transport model was successfully applied to predict the measured concentration profiles.

The present study takes up the encouraging results and experiences of this field scale study. It was carried out within the same investigation area and used the same analytical methods. Moreover, the environmental fate model developed is based on the one-dimensional solute transport model of Streck and Richter (1997b). The present study, however, takes the work of these authors further in that it

- was carried out at the scale of the whole *WIA* (43 km^2) and
- includes the uptake of Cd by plants.

The main objectives of the study are

- to monitor the displacement of Cd in soil and to measure the current uptake of Cd by different crops
- to determine the soil properties which govern the mobility and bio-availability of Cd
- to develop an environmental fate model for Cd which describes both displacement and plant uptake at the regional scale and
- to develop simple tools to assess the effect of soil Cd on ground water and food quality

The dissertation has the following structure: Chapter 3 introduces the theoretical background of the key processes leaching, sorption and plant uptake. Moreover, this chapter gives a short introduction to the geostatistical methods of block kriging and conditional simulation. In Chapter 4, the waste water irrigation system of Braunschweig is described in detail. Emphasis is given to the irrigation technique applied during the last 40 years. Materials and Methods are listed in Chapter 5. Chapter 6 gives a detailed description of the environmental fate model *SEFAH (Simulating the Environmental FAte of Heavy metals)*. Chapter 7 presents the results of the field observations between 1996 and 1999, i.e. the current status of Cd concentrations in soil, displacement and plant uptake. In addition, the sorption characteristics of soils are described and pedotransfer functions are derived. Chapter 8 presents simulations of the environmental fate of Cd in the soils of the *WIA*. After validation by means of hindcast

simulations, the model is used to calculate several retrospective and prospective scenarios. Finally, Chapter 9 introduces two simple tools to assess the effect of soil Cd on food and ground water quality.

3 Theoretical Background

3.1 Solute Leaching in Soil

The solute transport at the local scale (i.e. soil column) is traditionally described by the convection-dispersion equation (*CDE*) (e.g. Biggar and Nielsen, 1976):

$$\frac{\partial \rho C_T}{\partial t} = \frac{\partial}{\partial z}\left(D_S \frac{\partial C}{\partial z} \right) - \frac{\partial qC}{\partial z} - \phi \tag{1}$$

where C_T (kg kg^{-1}) denotes the total concentration of the solute, C (kg m^{-3}) the concentration in soil solution, D_S (m^2 s^{-1}) the apparent dispersion coefficient, q (m s^{-1}) the volumetric water flux density and ρ (kg m^{-3}) the bulk density. ϕ (kg m^{-3} s^{-1}) is a sink term for solutes which accounts, for example, for the uptake of solutes by plant roots. t (s) and z (m) are time and space coordinates, respectively.

The *CDE* is derived by combining a mass balance equation with flow equations for each phase of the solute (cf. Jury et al., 1991, p. 218-222). Assuming solute flow in z direction only and ignoring the vapour phase the mass balance equation in one dimension is

$$\frac{\partial \rho C_T}{\partial t} = -\frac{\partial I_l}{\partial z} - \phi \tag{2}$$

where I_l (kg m^{-2} s^{-1}) is the total flux of dissolved solute:

$$I_l = I_{ld} + I_{lc} + I_{lh} \tag{3}$$

Here, I_{ld} (kg m^{-2} s^{-1}) is called the liquid diffusion flux, I_{lc} denotes the convection of dissolved solute (kg m^{-2} s^{-1}) and I_{lh} (kg m^{-2} s^{-1}) is the hydrodynamic dispersion flux. I_{ld} is given by

$$I_{ld} = -D_{ls} \frac{\partial C}{\partial z} \tag{4}$$

where D_{ls} ($m^2\ s^{-1}$) is the soil liquid diffusion coefficient. I_{lc} may be written formally as

$$I_{lc} = qC \tag{5}$$

q describes the average water flux over many soil pores only. The tortuous convective movement of solute is represented by I_{lh}. If the time and distance required for solutes in pores of different velocity to mix along a direction normal to the direction of mean convection is short compared to the time required for solutes to move through the volume by mean convection I_{lh} may be written as

$$I_{lh} = -D_{lh} \frac{\partial C}{\partial z} \tag{6}$$

where D_{lh} ($m^2\ s^{-1}$) is the hydrodynamic dispersion coefficient. Inserting equations (4), (5) and (6) into Equation (3) the total flux of dissolved solute is

$$I_l = -D_{ls} \frac{\partial C}{\partial z} - D_{lh} \frac{\partial C}{\partial z} + qC \tag{7}$$

which is usually summarized as

$$I_l = -D_S \frac{\partial C}{\partial z} + qC \tag{8}$$

Here, the wheel turns full circle. Combining Equation (2) and (8) results in the *CDE* introduced at the beginning of this section (Equation (1)).

Assuming stationary water regime and a homogeneous medium the *CDE* simplifies to

$$\rho \frac{\partial C_T}{\partial t} = D_S \frac{\partial^2 C}{\partial z^2} - q \frac{\partial C}{\partial z} - \phi \tag{9}$$

For non-sorbing solutes the total concentration is given by

$$C_T = \frac{\theta}{\rho} C \tag{10}$$

where θ (% by volume) signs the volumetric water content. For sorbing solutes, like heavy metals, C_T has to be extended by the sorbed phase concentration S (kg kg^{-1})

$$C_T = \frac{\theta}{\rho} C + S \tag{11}$$

Inserting Equation (11) into Equation (9) and applying the chain rule leads to

$$\frac{\partial C}{\partial t} = \frac{D}{R} \frac{\partial^2 C}{\partial z^2} - \frac{v}{R} \frac{\partial C}{\partial z} - \frac{\phi}{\theta R} \tag{12}$$

with the retardation factor R

$$R = 1 + \frac{\rho}{\theta} \frac{\partial S}{\partial C} \tag{13}$$

the effective dispersion coefficient D (m^2 s^{-1})

$$D = D_S / \theta \tag{14}$$

and the pore water velocity v (m s^{-1})

$$v = q / \theta \tag{15}$$

The sorbed phase concentration is generally a function of the concentration in soil solution. If the time scale of sorption and desorption is much smaller than the time scale of the transport process the relationship between C and S can be

formally handled similar to an equilibrium reaction. Most heavy metals undergo non-linear sorption and equilibrium between C and S can often be described by the Freundlich isotherm

$$S = kC^m \tag{16}$$

where k ($kg^{-m}\ m^{3m}$) is the Freundlich coefficient and m (1) the Freundlich exponent. The Freundlich coefficient k can be seen as a measure for the sorption strength of a solute. In case of heavy metals k is generally a function of soil properties like pH, organic carbon (OC) content, clay content etc.. It can be determined experimentally in the lab (Filius et al., 1991; Schulte and Beese, 1994; Springob and Böttcher, 1998a). Alternatively, it can be estimated by so-called pedotransfer functions (*PTF*) (Van der Zee and Van Riemsdijk, 1987; Streck and Richter, 1997a; Springob and Böttcher, 1998b; Elzinga et al., 1999). A frequently used *PTF* is

$$\hat{k} = k^* OC^{\,b}\left(H^+\right)^{-a} \tag{17}$$

where k^* ($kg^{-m}\ m^{3m}$) denotes the intrinsic Freundlich coefficient, (H^+) the proton activity and b and a are empirical parameters, which are generally determined by means of multiple linear regression. Heavy metals usually have a Freundlich exponent m smaller than one, that is, sorption of these solutes is non-linear and the sorption isotherm is convex. Hence, at low concentrations Cd is more strongly sorbed than at high concentrations.

From a theoretical analysis Streck and Piehler (1998) have shown that the sensitivity of the mean travel time of a solute to an error in θ crucially depends on the sorption strength of solute. The relative sensitivity R_{SI} of the mean travel time of a linearly sorbing solute to a change in θ is given by

$$R_{S1} = \frac{1}{R} \tag{18}$$

where R is the retardation factor, that is, the stronger sorption, the less sensitivity. As an example, if ρ = 1.5 kg L^{-1} and k = 50 L kg^{-1}, using volumetric water contents of 0.25 and 0.125, the two calculated mean travel times differ by 0.2% only, while for a non sorbing solute the difference is 50%. Streck and Piehler (1998) concluded that the solute transport of strongly sorbing solutes can be modelled without knowledge of the exact value of the water content. Even if their analysis refers only to linearly sorbing solutes, it can be expected that the conclusions also apply to non-linearly sorbing solutes.

The *CDE* was originally developed to describe the solute transport at the local scale. But what happens if we change the modelling scale? Does the mathematical description developed at the local scale apply to the larger scale? If not, how can we describe the process at the larger scale? According to Beven et al. (1999) the latter question is referred to as the scaling problem. The *CDE* is very well suited for illustrating this problem: In soil, local displacement velocities are in general laterally correlated over some distance. Displacement velocities in the vicinity to each other are more likely to be similar than those farther away. The distance within which travel velocities are similar is called their correlation length. The solute needs a certain distance, which is called the mixing distance, to explore this zone of similarity. Only if the convection distance, under field conditions most often restricted to the water table, is much larger than the mixing distance, then the transport process is convective-dispersive. In contrast, if the convection distance is much smaller than the mixing distance, then the local dispersion can be neglected and the transport process is stochastic-convective. Thus, whether the solute transport process is convective-dispersive or stochastic-convective depends crucially on the relationship between mixing distance, convection distance and applied model grid scale.

If a transport process is approximately stochastic-convective, a field or a region can be pictured as an ensemble of vertically parallel non-interacting soil columns. Solute transport in each soil column is described either as piston flow (Dagan and Bresler, 1979) or as convective-dispersive flow (Ammoozegar-Fard et al., 1982; Streck and Richter, 1997b; Djurhuus et al., 1999). In the latter case the solute transport process is actually a hybrid between the convective-dispersive and the stochastic-convective model. However, if local dispersion is small compared to field-scale dispersion, as shown, for instance, by Streck and Richter (1997b) for Cd transport at the field scale, the solute transport is approximately stochastic-convective.

3.2 Uptake of Ions by Plants

Due to the extremely slow movement of Cd through soil, the response of concentration in ground water to Cd inputs may be delayed for decades or even centuries (Gäth, 1996). This is different for plants, which are instantly affected by Cd dissolved in soil solution. Cd in soil solution is readily taken up by plants and may accumulate at high levels in different parts of plants. Because of its impact to the human food chain, heavy metal uptake by plants has been becoming a widespread issue in environmental research.

It is generally agreed that heavy metals like other ions reach the root surface from soil by way of the soil solution (Bowling, 1976, p. 24). Ions are supplied to plant roots by mass flow, diffusion and interception (Barber et al., 1963). Mass flow and diffusion are considered to be the most important supply mechanism for ions in soil. Mass flow means that ions dissolved in soil solution are transported via the transpiration flux to the roots. If the uptake by roots is greater than can be supplied by mass flow, then ion concentration will be lowered at the root surface and diffusion will become increasingly important. For macro-

nutrients like potassium or phosphate it has been shown that plants are able to deplete the direct vicinity of their roots (Hendriks et al., 1981). According to Barber (1976) interception, defined as uptake of ions due to a direct contact between root and soil, contributes only a few per cent of the total nutrition demand.

Ions that find their way into the root arrive first in the "free space" of the apoplast of the cortex. The entry of ions to the apoplast is an unspecific process. According to Mengel (1991, p. 223) the apoplast can be regarded as a continuation of soil solution. However, the pathway from the apoplast to the xylem involves the crossing of biological membranes. It is generally assumed, even if the ions traverse the cortex in the cell walls, that the Casparian strip is an effective barrier to further cell wall movement (Vázquez et al., 1992). Thus, the membranes of the endodermis must be passed. In general, biological membranes can be passed both in a passive and in an active manner. Passive means that ion motion is driven by an energy gradient. In contrast, for an active uptake the plant has to supply energy.

Experimental studies with excised roots (e.g. Epstein, 1966; Barber, 1984) have shown that the active uptake of various chemicals across biological membranes can be described by Michaelis-Menten kinetics:

$$V = \frac{V_{\max} C}{C + K_M} \tag{19}$$

Here, V (kg m^{-2} s^{-1}) denotes the uptake rate, V_{max} (kg m^{-2} s^{-1}) the maximum uptake rate, C (kg m^{-3}) the concentration of an ion and K_M (kg m^{-3}) the Michaelis constant. Thus, this process is assumed to be analogous to the binding of a substrate to an enzyme.

A number of cations have been found to affect each other with regard to root uptake (Jarvis et al., 1976). For example, the uptake of sodium by barley roots is inhibited by potassium and vice versa. It has also been shown that the *p*H of the external solution markedly affects the rate of ion uptake. For example, Hatch et al. (1988) observed that increasing *p*H from 5 to 7 increased Cd uptake by a factor of 4 in cocksfoot, of 8 in perennial ryegrass and of 10 in lettuce and watercress. The authors concluded that Cd competed with hydrogen ions at low *p*H levels.

Various older experiments with intact plants have shown that under specific conditions a relationship exists between transpiration and ion uptake (Broyer and Hoagland, 1943; Hylmö, 1953; Bowling and Weatherley, 1965; Hooymans, 1969). When the supply of ions from the external solution is sufficient, increasing transpiration generally results in an increasing ion uptake. Under these conditions, for example, Bowling and Weatherley (1965) observed that the potassium taken up by mass flow was completely transferred to the xylem. In a recent study, Grifferty and Barrington (2000) observed at a 2.3 times higher transpiration rate a 3 times higher uptake of Zn by winter wheat plants. On the other hand, Bowling (1968) pointed out that there are conditions in which no relationship between water and ion uptake occurs such as where the concentration of an ion is well below a crucial physiological level.

Various mechanistic nutrient uptake models have been developed during the last decades (Cushman, 1984; Butler and Wheater, 1999). In general, emphasis is given to processes like diffusion, active ion uptake or competition between ions. In some cases these models have even been successfully applied. For example, Barber (1984) has validated the mechanistic model of Cushman (1984) for phosphate and potassium uptake by plants.

Models developed to predict uptake of macronutrients by plants have also been used to evaluate soil and plant parameters influencing the bioavailability of trace elements in soil. Mullins et al. (1986) carried out a sensitivity analysis with a nutrient uptake model and suggested that mass flow could supply a significant proportion of Zn and Cd uptake by corn plants. Christensen and Tjell (1984) introduced a Cd uptake model for crops governed by mass flow. The uptake of Cd by plants was assumed to be proportional to the product of concentration in soil solution and volume of water transpired by the plant. However, the authors could not validate their approach due to a gap in information of several parameters that usually are not determined in sewage sludge application experiments. In contrast, Trapp and Pussemier (1991) have shown that the uptake of the organic compound carbamate, an insecticide, is governed by mass flow. They observed that the uptake of twelve N-methyl-arylcarbamates by bean plants were induced from 85% to 97% by mass flow. Consequently, in the model introduced by Trapp and Pussemier (1991) the total uptake of a chemical into the plants is exclusively governed by the transpiration stream. The translocation within the plant is described by empirical factors like the transpiration stream concentration factor (*TSCF*).

The uptake of ions by plants is a fascinating but complex issue. However, there are hints that under specific conditions mass flow strongly controls the uptake of trace solutes by plants. This notion will be pursued in the following to develop a Cd uptake model applicable at the regional scale.

3.3 Geostatistical Tools

Two geostatistical tools, ordinary block kriging and conditional simulation, are used in the current study. Ordinary block kriging is applied, for example, to visualize the general spatial distribution pattern of soil properties like *p*H, *OC*

etc. This purpose is often more or less qualitative and, for instance, the confidence of an estimated block mean is not really important. But block kriging can also be applied to detect blocks that exceed a given Cd threshold concentration (Chapter 9). At this stage block kriging is quantitatively used and with regard to inference it is particularly important to give an index of the confidence to our estimator. In this context, we have to deal with the "*kriging variance*" and the so-called "*smoothing effect*" induced by kriging. Unlike kriging procedures, which yield best estimators for the different blocks, conditional simulations produce the same spatial structure (variance, covariance, histogram) as the measurements. Therefore, conditional simulations can be applied to give us an idea of the real spatial heterogeneity of a variable. A direct comparison, especially between a kriged and a conditionally simulated region, supplies us with an intuitive impression of how accurate our estimator reproduces spatial variability. In addition, conditional simulations are applied in Chapter 8 to generate three-dimensional random fields to initialize the model *SEFAH* and in the Chapter 9 conditional simulations are used to analyse the effect of sample size on our kriging estimates.

The following section gives only a brief summary of the most important formulas and their practical meaning. For more details see Isaaks and Srivastava (1989) and Journel and Huijbregts (1991).

3.3.1. Ordinary Block Kriging

The technique of kriging is often associated with the acronym B.L.U.E for "best linear unbiased estimator". Kriging is "linear" because its estimates are weighted linear combinations of the available data

$$\hat{Z}(x_0) = \sum_{j=1}^{n} w_j Z(x_j) \tag{20}$$

It is "unbiased" since it aims to have the mean residual error m_R equal to zero

$$m_R = 0 \tag{21}$$

and it is "best" because it aims at minimizing the error variance σ_R^2

$$\sigma_R^2 = \min\left|\sigma^2 + \sum_{j=1}^{n}\sum_{i=1}^{n} w_j w_i C_{ji} - 2\sum_{j=1}^{n} w_j C_{j0}\right| \tag{22}$$

whereby σ^2 denotes the variance of point values, C_{ji} is the covariance between the *j*-th and the *i*-th sample and C_{j0} is the covariance between the *j*-th sample and the unknown value being estimated.

To obtain a zero mean residual error in expectation it is necessary to constrain the sum of weights to one

$$\sum_{j=1}^{n} w_j = 1 \tag{23}$$

The set of weights that minimize the error variance satisfies the following *n* equations

$$\sum_{j=1}^{n} w_j C_{ji} + \mu = C_{i,0} \qquad \forall i = 1,\ldots,n \tag{24}$$

where μ denotes the Lagrange parameter, which is necessary for converting a constrained minimization problem into an unconstrained one. This system of equations can be written in matrix notation as

$$\begin{matrix} C & \cdot & w & = & D \end{matrix}$$

$$\begin{bmatrix} C_{11} & \cdots & C_{1n} & 1 \\ \vdots & \ddots & \vdots & \vdots \\ C_{n1} & \cdots & C_{nn} & 1 \\ 1 & \cdots & 1 & 0 \end{bmatrix} \cdot \begin{bmatrix} w_1 \\ \vdots \\ w_n \\ \mu \end{bmatrix} = \begin{bmatrix} C_{10} \\ \vdots \\ C_{n0} \\ 1 \end{bmatrix} \tag{25}$$

and is often referred to as the ordinary kriging system. The weights are calculated by using the inverse of the left-hand side covariance matrix:

$$w = C^{-1} \cdot D \tag{26}$$

The C^{-1} matrix takes into account the clustering of available data and the *D* vector considers the distances between available data and the point to be estimated.

The minimized estimation variance is expressed as

$$\sigma_R^2 = \sigma^2 - \left(\sum_{j=1}^{n} w_j C_{j0} + \mu\right) \tag{27}$$

and is usually referred to as the kriging variance.

Up to here, we have dealt only with point estimation. The estimation of the average value of a variable within a prescribed local area A (block) is straight forward. The block kriging system is quite similar to the point kriging system. Only the covariance vector D requires a modification for block kriging. For point estimation, these covariances are point-to-point covariances. For block estimation, the covariance values required for the vector D are the point-to-block covariances C_{iA}. Thus, the block kriging system becomes

$$\begin{bmatrix} C_{11} & \cdots & C_{1n} & 1 \\ \vdots & \ddots & \vdots & \vdots \\ C_{n1} & \cdots & C_{nn} & 1 \\ 1 & \cdots & 1 & 0 \end{bmatrix} \cdot \begin{bmatrix} w_1 \\ \vdots \\ w_n \\ \mu \end{bmatrix} = \begin{bmatrix} C_{1A} \\ \vdots \\ C_{nA} \\ 1 \end{bmatrix} \tag{28}$$

and the block kriging variance is given by

$$\sigma_R^2 = C_{AA} - \left(\sum_{j=1}^{n} w_j C_{jA} + \mu\right) \tag{29}$$

where C_{AA} is the average covariance between pairs of locations within A. Assuming a normal distributed estimation error and that a proportional effect[1] does not exist or is negligible, confidence intervals (CI) can be calculated using the block kriging variance

$$CI \pm u_{1-\alpha}\sigma_R \tag{30}$$

whereby the value of $u_{1-\alpha}$ depends on the level of significance (α) and whether a one-tailed or a two-tailed interval is desired.

[1] The proportional effect means that a relationship between the local means and variances exists, i.e. the local variability is not constant in space (Isaaks and Srivastava, 1989).

Kriging assumes stationarity, i.e. that (a) the correlation between two data values $z(x_1)$ and $z(x_2)$ does not depend on their particular position within the region but rather on the distance (x_1-x_2) which separates them and (b) the expectation of the random function does not depend on the location and is constant within the region. In practice, the variogram model is often only used for limited distances. In such cases, the variogram model as well as the mean value need to be only locally stationary.

Finally, it must be pointed out that the entire kriging technique is based just on a model of how a phenomenon behaves at locations where it has not been sampled, namely on the covariance function and variogram model. However, unlike many other methods like inverse distance method, triangulation or polygons, that do not state the nature of their model assumed, kriging clearly states the model on which it is based.

3.3.2. Conditional Simulation

The objective of an estimation procedure like kriging is to provide for each block an estimator which is as close as possible to the true unknown value. However, kriging estimators do not reproduce the spatial variability of the true values. The kriging procedure involves a "*smoothing*" of the true dispersion

$$D^2(v,R) \cong D_K^{2*}(v,R) + \sigma_{Kv}^2 \tag{31}$$

where $D^2(v,R)$ is the dispersion variance of the true content of support v within the region R and $D^{2*}{}_K(v,R)$ is the dispersion variance of the corresponding kriged values. σ^2_{Kv} denotes the mean local estimation variance of a unit v. The amount of smoothing increases as the mean of the local kriging variances increases, i.e. the estimators of the true content become worse.

A conditionally simulated region can be seen as one “possible realization” of a random field, that reproduce the first two experimentally found spatial moments (mean and variogram, as well as the histogram) of the region, i.e. it identifies the main dispersion characteristics of a variable. On the other hand, the simulated value is not the best possible estimator of *z(x)*. The variance of estimation of *z(x)* by conditional simulation is exactly twice the kriging variance. The realizations of a simulation are conditional on the experimental data, i.e. at the sampling points the simulated and observed values are the same.

4 The Waste Water Irrigation Area of Braunschweig

The use of waste water for agricultural irrigation is not very widespread in Germany. According to Lenz et al. (1998) this treatment technique is applied at 73 locations in Germany. Because transport of water over long distances is generally expensive, this technique is concentrated near the cities producing the effluent. Moreover, this technique is restricted to areas with soils of high hydraulic conductivity. Waste water irrigation may require pre-treatment to remove pathogens and to minimize undesirable chemicals. Typically, this is achieved in a sewage treatment plant. A particular benefit of waste water irrigation is the reduction in pollution of surface water. Neither treated nor untreated sewage gets directly into local rivers. The discharge of nutrients, which may cause rivers as well as estuaries to eutrophy, is substantially reduced and the local water and nutrient cycle gets narrower. But indeed, waste water irrigation may be accompanied with an input of organic and inorganic pollutants to soil, plants and ground water. However, as we will see later on, whether input of a pollutant causes adverse ecological effects depends on a variety of factors.

The largest waste water irrigation area in Germany and even in Europe is located in the northwest of Braunschweig, Germany. The *WIA* (43 km^2) is part of the sewage management system of Braunschweig. Today, this system consists of three components: the *WIA*, a sewage farm[2] and a sewage treatment plant (Figure 1). First of all, the entire sewage of Braunschweig arrives at the sewage plant "Steinhof", where it passes a primary settling tank followed by an acti-

[2] In German this term means "Rieselfelder".

vated sludge tank and a final settling tank. In winter and spring the surplus sludge from the final settling tanks is completely removed from the effluent by a sewage press. In the vegetation period the removed surplus sludge is added to the effluent. One third of the effluent is pumped into the sewage farm. The other 2/3 are pumped to the *WIA* where they are used for agricultural irrigation. In 1996, about 15 Mio m^3 were applied which corresponds to an annual irrigation height of about 536 mm.

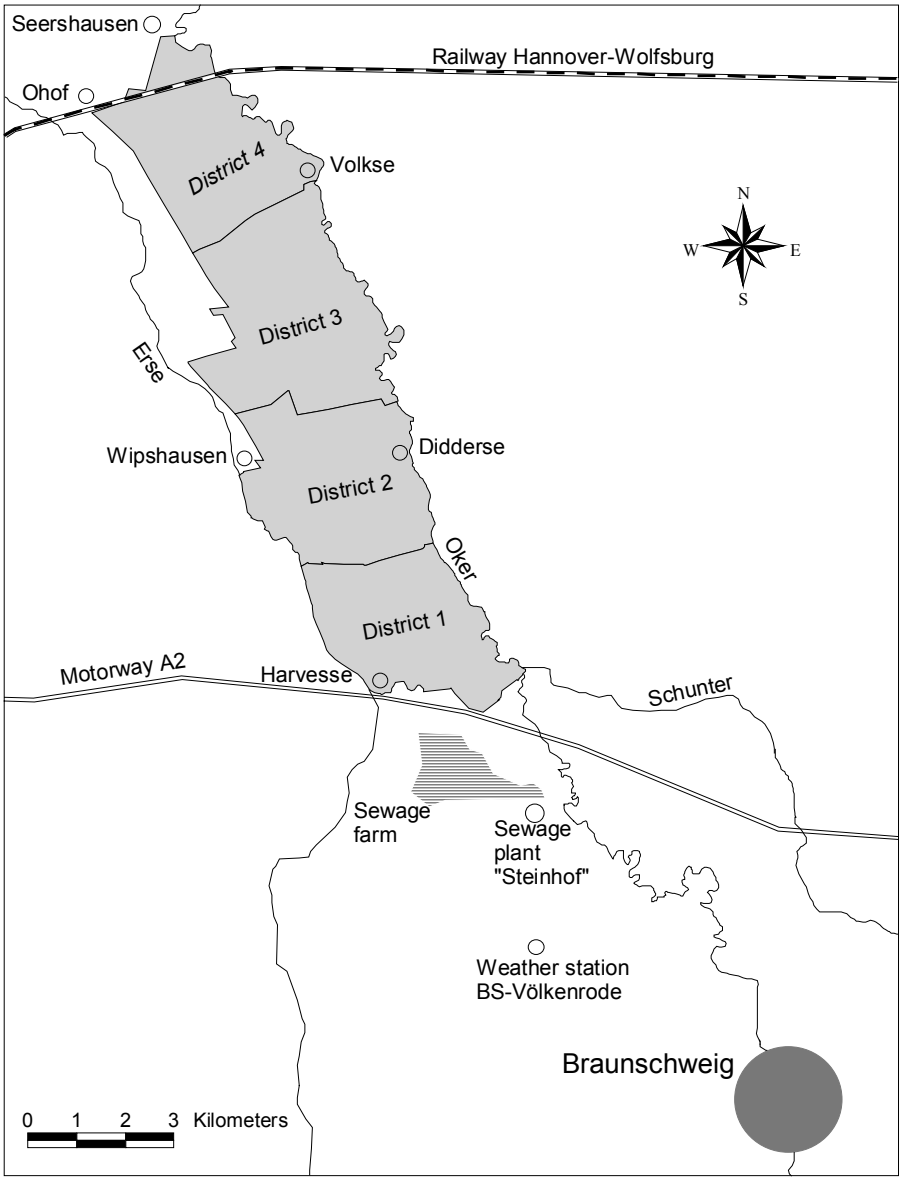

Figure 1: Sketch of the geographical location of the waste water irrigation area of Braunschweig.

The oldest component of the sewage management system is the sewage farm, which started operation as early as 1894. The sewage farm covers today about 200 ha, is bordered by dykes and consists of a system of ditches and ponds which sewage has to pass through before it discharges into the river Oker. Until the beginning of waste water irrigation in 1957 the entire sewage was applied to the sewage farm. Due to the continued population growth the capacity of the sewage farm was already exhausted in the 1920s. Early plannings to extend the sewage treatment system by a *WIA* started in 1935, but due to World War II the project was interrupted. In 1954, the Braunschweig Municipal Waste Water Association (*BMWA*)[3] was founded and the operation started in 1957. Members of the association were the city of Braunschweig and about 550 farmers. At present, the number of farmers is about 300.

The *WIA* of the *BMWA* is located about 10 kilometres north-west of the city centre (Figure 1). The *WIA* contains today about 4,300 ha. In the west it is bordered by the river Erse, in the east by the river Oker, in the south by the motorway A2 and in the north by the railway Hannover-Wolfsburg. About 2,870 ha of the area are in agricultural use. The main crops being sugar beet, potato, winter cereal and summer cereal. The remaining 1,430 ha are mainly forests and villages. The area has got a south to north expansion of about 15 kilometres. The west to east expansion varies between 3 and 5 kilometres. The irrigation area is divided into four areas of approximately equal sizes; the so-called pumping station districts. In 1957, waste water irrigation started in District 1, which is situated in the south of the area. The other three pumping stations started operation within the following nine years. Each district has got a central pumping station, which produces the water pressure necessary for operating the irrigation machines (Figure 2).

[3] This is translated from the German name „Abwasserverband Braunschweig“.

Until the opening of a sewage plant in 1979 raw sewage was used for irrigation. Raw sewage contains high amounts of sludge and particles. To avoid clogging of the nozzles of the irrigation machines each pumping station was equipped with a settling tank, where the major part of sludge was removed by sedimentation. The collected sludge was pumped into nearby sludge basins, where the sludge was composted for a period of 2 to 3 years. The composted sludge was used for fertilization of fields within the *WIA*.

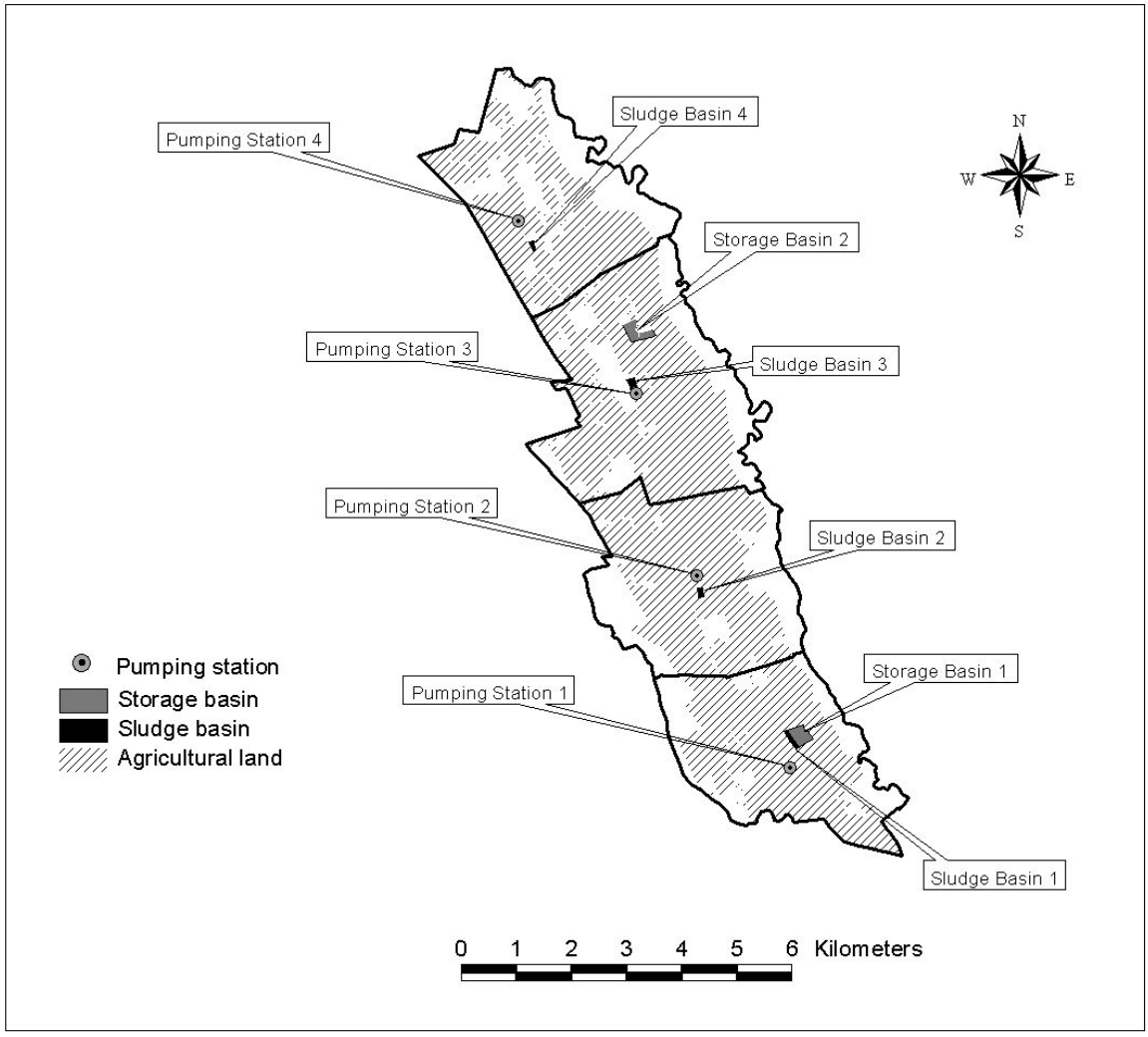

Figure 2: Important installations within the WIA.

Additionally, storage basins of about 4 ha each were installed in District 1 and District 3. Similar to the sewage farm, the two storage basins are bordered by dykes. The storage basins were used for deposit, for example, at weekends or

during frost periods. The annual irrigation heights and therefore the sludge loads were much higher than in other parts of the irrigation area. The accumulated sludge had to be removed from the storage areas several times per year and was used, like the composted sludge, for fertilization. In 1975, new irrigation machines were installed (Figure 3). The machines were equipped with larger nozzles, so higher amounts of sludge could be used for irrigation. Consequently, the sludge basins of the Districts 1 and 2 were shut down. The sludge of these two districts was pumped to Districts 3 and 4, where this additional sludge was composted and applied at the fields of these districts (Abwasserverband, 1979, p. 15).

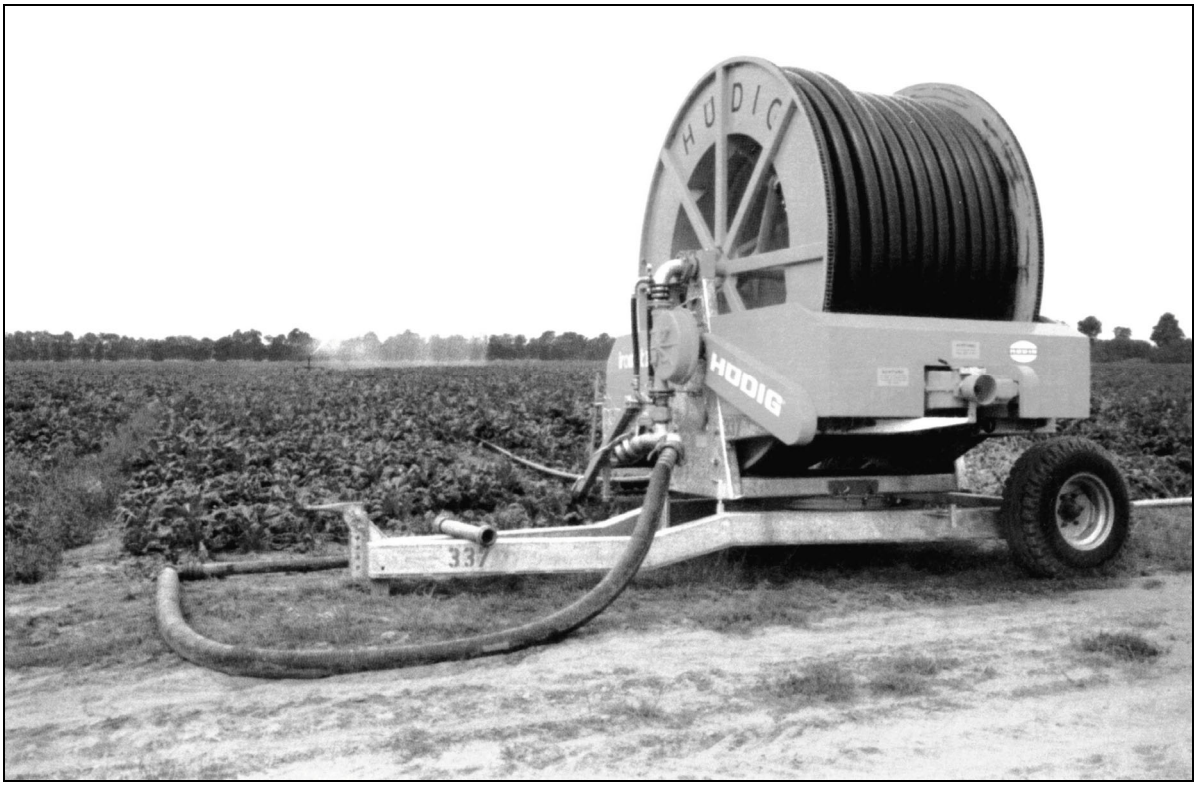

Figure 3: Irrigation machine (Source: Abwasserverband Braunschweig, 1995).

Figure 4: Sprinkling irrigation (Source: Abwasserverband Braunschweig, 1995).

In the past, the waste water irrigation was often accompanied by an unpleasant smell. In the 1970s, the fear of unhealthy germs led to a dwindling public acceptance, in particular by the inhabitants, who had their domiciles in the neighbourhood of the *WIA*. To respond to this precariousness, the sewage plant "Steinhof" was built and put into operation in 1979. At this early stage the sewage was treated mechanically and biologically (primary and secondary treatment). All of the surplus sludge from the secondary treatment was used for sprinkling irrigation within the *WIA*. Consequently, the sludge basins of Districts 3 and 4 were not required anymore and were shut down.

In the early 1980s, concern about heavy metals in food, water and soils gained increasing public attention and in 1983 the German sewage sludge regulation came into force. The *BMWA* also faced this problem. Measurements in the early eighties indicated that up to 200 g Cd per year entered the soils of the *WIA* (Figure 5). Particularly the surplus sludge contained high amounts of heavy

metals. As a response the monitoring of illicit emissions to the municipal sewage canal system was enhanced and the sewage plant was equipped with a sewage press, so that since 1987 the surplus sludge can be removed completely from the irrigation water. Due to these measures Cd loads have been significantly reduced since the late 1980s. As will be shown in Chapter 8.6.1, the impact on food and soil quality would have been tremendous, if the *BMWA* had not taken these steps.

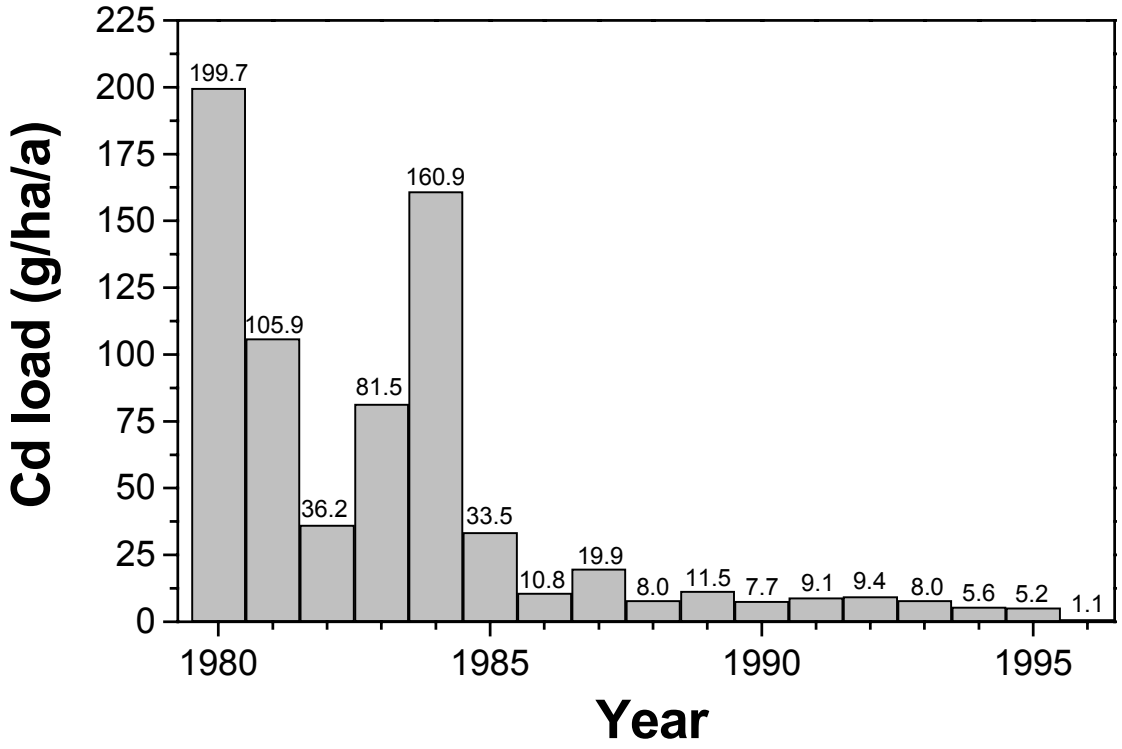

Figure 5: Cd input history of the WIA (Source: Abwasserverband Braunschweig, 1995).

The *WIA* is situated almost completely on the lower terrace of the river Oker which was formed during the Weichsel Glacial (about 10,000 years before present). The area is plain and the elevation drops gradually from 65 to 55 meters above sea level toward the north (Figure 6), which corresponds to a gradient of 0.07%.

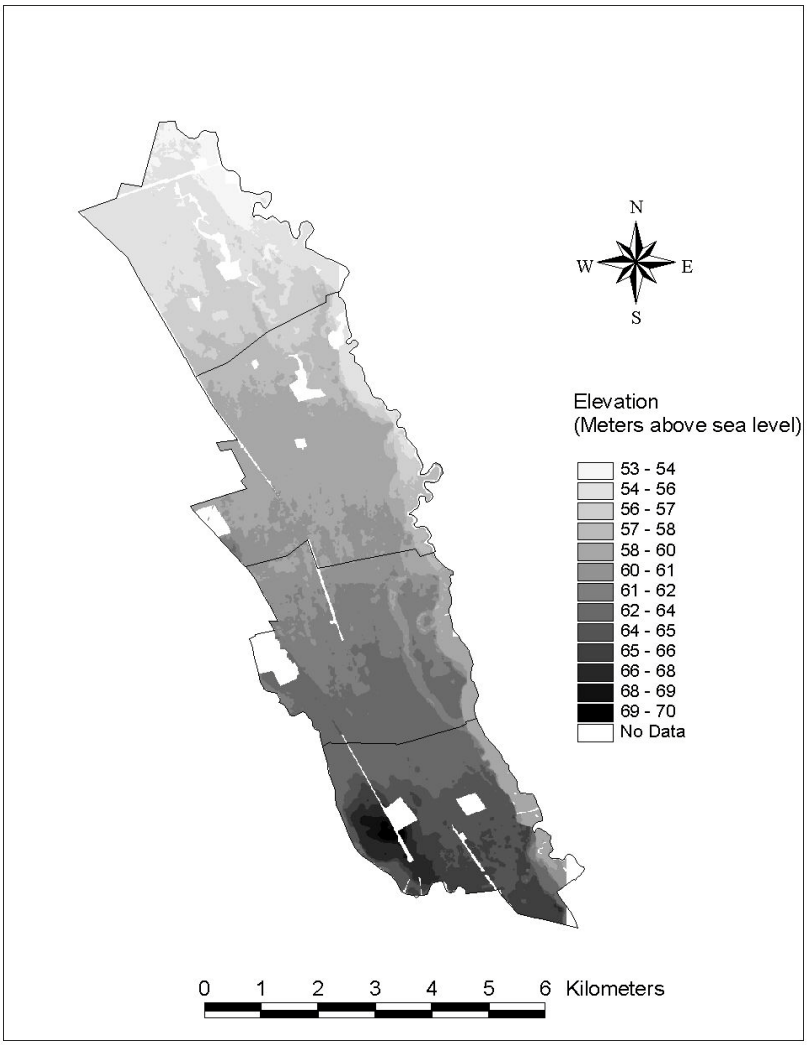

Figure 6: Elevation map of the WIA.[4]

The flood plains of both rivers are situated roughly 3 to 5 m below the surface of the terrace. Soils of the flood plains, which are not subject to this investigation, consist of loamy substrates. Due to the influence of both rivers on landscape genesis the terrace shows a longitudinal arrangement. In the core area the parent material of soils is mainly alluvial sand (< 5% clay), whereas in the south-western and the eastern part larger coherent areas consist of loamy sand (< 8% clay) (Figure 7).

[4] Basisdaten dieser Darstellung: ATKIS-DGM5-Daten der Landesvermessung und Geobasisinformation Niedersachsen -LGN-, Hannover. Mit Erlaubnis des Herausgebers: Landesvermessung und Geobasisinformation Niedersachsen -LGN- vom 13.05.1997 Az.: B2-A 122/97.

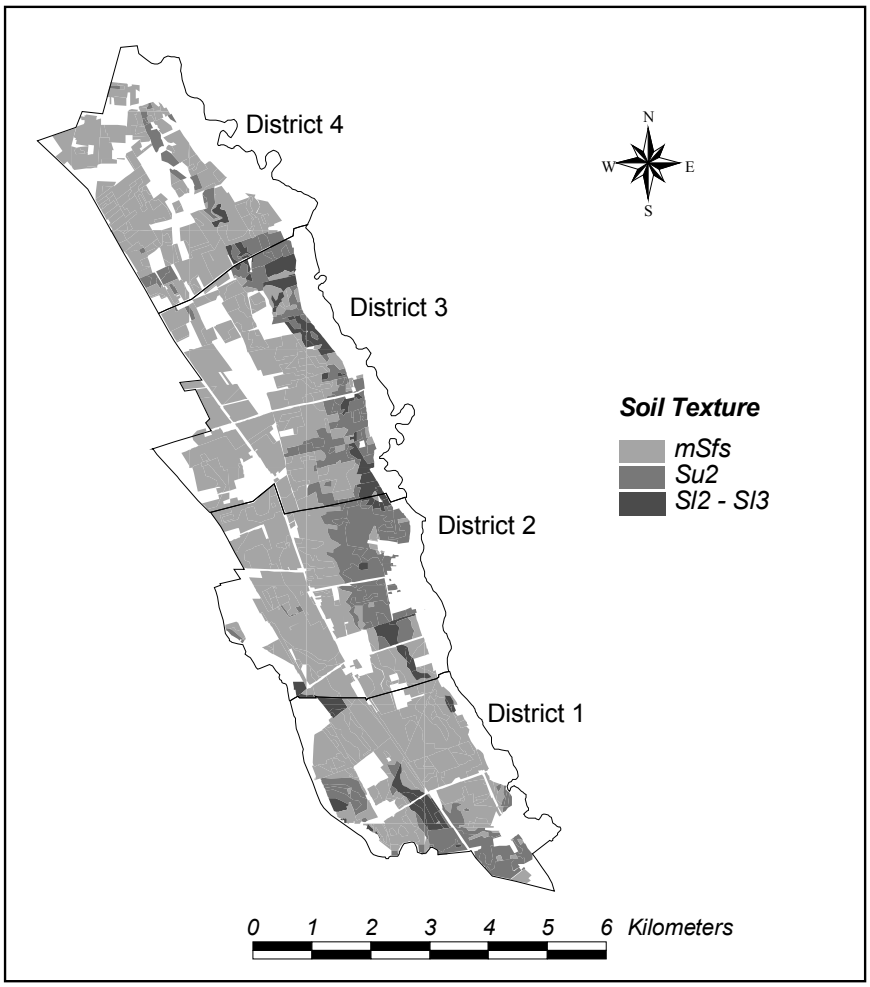

Figure 7: Soil texture map of the WIA.[5]

In the south-western part the site contains partly alluvial sediments of the Drenthe Glacial (about 100,000 years before present). In contrast to all other parts of the terrace these substrates are stony. Until today, the latter deposits have been mined. The more or less continuous strip of loamy sand in the eastern edge probably contains sediments of the river Oker transported to this location either by human activity or floods. In the German classification scheme, the soils consisting of loamy sand were given 25 to 48 points. Soils rated by 14 to 24 are predominantly located in the sandy core area of the *WIA*.

[5] Darstellung auf der Grundlage von Daten des Niedersächsischen Bodeninformationssystems NIBIS, mit Erlaubnis des Niedersächsischen Landesamtes für Bodenforschung Hannover.

Between 1957 and 1996 the average annual precipitation was 626 mm. According to Haude (1955) the potential evapotranspiration is about 532 mm. Thus, the site has an annual average rainfall excess of 94 mm. However, during the main vegetation period water would frequently be short if soils were not irrigated. The average depth of the ground water table is 1.8 m and varies between <1.0 and 6 m (Chapter 8.4.2). About 340 ha of the *WIA* are drained.

As in other sandy areas of the Geest in Lower Saxony, asparagus is cultivated in the *WIA*. In 1996, asparagus fields covered 5.6% of the arable land (161 ha). Before asparagus is planted, the humus and nutrient-rich topsoil is transferred to a depth of 0.3 to 0.6 m by deep ploughing or milling. This procedure leads to a lasting change of the chemical properties of soil. The resulting anthropogenic soil type is labelled Rigosol (R-Ap/R... profile). Deep ploughing will become important in the context of modelling Cd displacement in soils.

5 Material and Methods

5.1 Sampling

Within this study, three sampling campaigns were carried out. The first campaign was executed from September 1996 to November 1996. Soil monoliths were sampled to study the horizontal and vertical variability of the current status of Cd accumulation and the sorption characteristics of soils. The second and the third campaign were carried out from July 1998 to October 1998 and from July 1999 to October 1999, respectively. These two campaigns aimed at studying the plant uptake of Cd by winter wheat (*Triticum aestivum* L.), potato (*Solanum tuberosum* L.) and sugar beet (*Beta vulgaris* L.). The field observations supply the experimental database to initialize and to validate the environmental fate model.

5.1.1. First Campaign

The investigation area was divided into 161 500 m x 500 m blocks (Figure 8). The blocks conform to the topographic map 1:25,000. In each block, a field was randomly selected. First of all, a sample of the Ap horizon was taken separately by digging a 0.5 m x 0.5 m x 0.3 m hole. At the bottom of the hole, we took a soil monolith of 0.07 m diameter and 1.2 m depth with the help of a mechanical soil auger (Cobra, Atlas Copco Inc., Germany). Each monolith was divided into 9 soil layers (0.3-0.4, 0.4-0.5, ..., 1.1-1.2 m) and from the centre of each layer a sample was taken. The large diameter of the probe provided a spreading-free sampling. The samples were stored in plastic cups, dried at 40 °C and passed through a 2 mm sieve. At the field a photograph was taken of each soil monolith and the location of each sampling point was sketched. In the office, the sketch was transferred to a map 1:5,000 and the coordinates were determined. The

accuracy of the coordinates is roughly ± 15 m. Altogether 161 soil monoliths were taken. Eight were drilled outside the irrigation area. Current asparagus cultivations were not sampled.

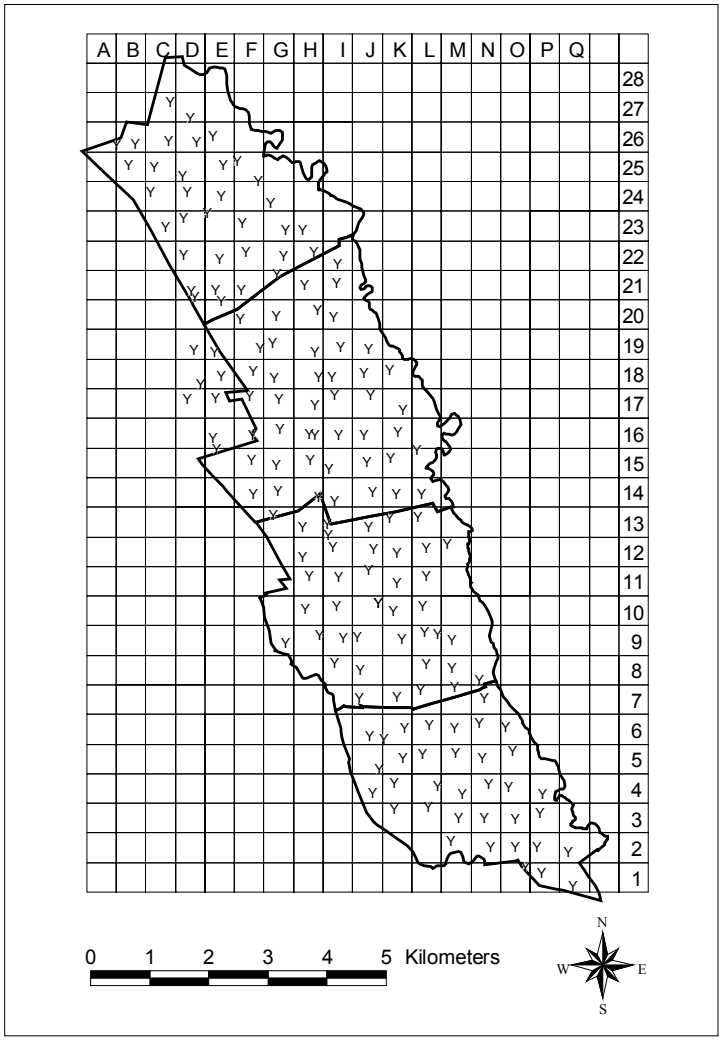

Figure 8: Sampling grid. Within each block (500 m x 500 m) one soil monolith was drilled at a location randomly selected.

5.1.2. Second and Third Campaign

In 1998, we took soil and plant samples from 20 potato and 20 sugar beet fields. At each field a single plant was collected. Within a radius of roughly 0.3 m from the former plant location three soil monoliths were drilled as described above, but without separately sampling the Ap horizon. Soil samples of identical layers

were mixed to a homogeneous sample. The potato plant was divided into straw (stem and leaves) and tuber. The sugar beet was split up into leaf and hypocotyl. In the lab, the plant material was intensively cleaned with distilled water. Particularly, the hollow potato stems were carefully cleaned. Each stem was cut open and checked for the absence of soil material. The potato tubers were peeled and the peel was further prepared separately. Before drying the plant material at 60 °C the total fresh mass was determined. The hypocotyls of sugar beet plants were dried by freezing. Afterwards the dry mass was determined and plant material was ground in a cutting mill followed by a mortar grinder. The samples were stored in plastic cups. Until analysis the cups were kept inside an exsiccator.

Because of logistical problems we could not sample winter wheat plants in 1998. Fortunately, the *BMWA* gave us the data of their long-term control plots (each plot is some hectares). In 1998, winter wheat grain was sampled at 13 control plots[6] along a plot-specific sampling path. The wheat grain was analysed for total Cd content by the laboratory of the *BMWA*. However, no soil samples were taken in the scope of the investigations of the *BMWA*. To close this gap, in September 1998 we resampled each control plot. Along each sampling path six soil monoliths were drilled as described above. Additionally, soil samples were taken from the Ap horizon every 25 m (about 12 Ap horizon samples per plot) and were mixed to a homogeneous soil sample.

In 1999, we again sampled 20 sugar beet and potato fields. In addition, 20 winter wheat fields were examined. A plot of 0.25 m^2 (0.5 m x 0.5 m) was sampled at each site. The wheat stems were cut off roughly 2 cm above ground and the

[6] I2, I3, II3, II5, III1a, III1b, III2a, III2b, III4, III5, IV1, IV4 and IV5. The identification numbers are internally used by the *BMWA*.

plant material was divided into straw and grain. The wheat material was cleaned with distilled water, fresh and dry mass were determined and the material was milled in two stages to a fine "floury" consistency. Soil, potato and sugar beet samples were prepared as described above.

5.2 Measurements

All topsoil samples were analysed for their aqua regia Cd content according to DIN ISO 11466. In accordance with Streck and Richter (1997a), all soil samples were analysed for *p*H, *OC* content, EDTA-extractable Cd content and Cd and Zn concentration in 0.0025 M $CaCl_2$.

It is assumed that the EDTA-extractable content represents the total concentration of a solute, i.e. the fraction which participates in sorption-desorption reactions (Filius et al., 1991; Gäbler et al., 1999). Moreover, it is assumed that a 24 h equilibration of soil with 0.0025 M $CaCl_2$ is suited to determine the concentration in soil solution to a good approximation[7] (Streck, 1993).

The EDTA-extractable content was determined as follows (cf. Zeien and Brümmer, 1989): Duplicate 2 g (samples to 0.5 m depth) or duplicate 10 g (samples below 0.5 m depth) soil were put into acid-rinsed 50-mL polypropylene centrifuge tubes and received 40 mL 0.025 M $(NH_4)_2$-EDTA. The samples were horizontally shaken for 90 min at 140 rpm. Subsequently, the samples were centrifuged for 5 min at 1900 **g**. The supernatant solution was transferred through a filter paper (595½, Ø=70 mm, Schleicher & Schuell Inc., Germany) into acid-rinsed 15-mL polystyrene centrifuge tubes.

[7] At first glance a measurement of the concentraion in soil solution seems to be trivial, but until today it is a quite demanding task to choose or find a suitable method. Unfortunately, the succes of a process-orientated study crucially depends on an adequate choice.

Cd and Zn concentrations in the 0.0025 M $CaCl_2$ background electrolyte were measured as follows (Streck, 1993): Duplicate 30 g soil was weighed into acid-rinsed 50-mL polypropylene centrifuge tubes and 30 mL 0.0025 M $CaCl_2$ was added. Tubes were shaken on a vertically rotating shaker in an air-conditioned room at 20±2 °C and at 30 rpm. After 24 hours of shaking the soil suspension was centrifuged for 10 min at 4200 **g**. The supernatant solution was passed through a filter paper (as above) into acid-rinsed 15-mL polystyrene centrifuge tubes. A possible sorption of dissolved heavy metals to the wall of the centrifuge tubes was prevented by addition of 500 µL 0.8 M $(NH_4)_2$-EDTA.

The 0.025 M EDTA and 0.0025 M $CaCl_2$ extracts were analysed for Cd using a graphite furnace atomic absorption spectrometer with deuterium background compensation (AAS 4001, Perkin Elmer Inc., Germany). Two modifiers were used: (1) a mixture from Palladium(II) chloride, 1 N HNO_3 and Butanol-(1) with a volume ratio of 10:10:1 and (2) 0.015 M $Mg(NO_3)_2 \cdot 6H_2O$. The average detection limit of this method was 0.25 µg Cd L^{-1}. For the analysis of Zn the flame atomic absorption system of the AAS 4001 was used.

The total Cd content of plant material was determined using a microwave assisted extraction. About 0.5 g dry matter received 7 mL 65% HNO_3 and 2 mL 35% H_2O_2 in sealed vessels for microwave digestion (MDS 2000, CEM Inc., USA). Afterwards samples were cooled, transferred into 25 mL volumetric flasks and filled to the mark by adding 65% HNO_3. Cd concentration in the acid digest was measured using graphite furnace atomic absorption spectrometry as described above. For quality control, analytical results of 1999 were checked against those of 1998 and were seen to be in agreement.

The aqua regia extracts were analysed by ICP-OES with axial plasma (ISA Ultrace 166, Jobin Yvon Inc., France). Cd was measured sequentially at 228.8 nm wavelength. The detection limit of this method was 0.1 mg kg^{-1}.

The *p*H values of all soil samples were determined electrochemically (pH 537, WTW Inc., Germany) in a suspension of 20 g soil in 50 mL of 0.01 M $CaCl_2$. The *OC* content (% by mass) of all samples were measured by combustion at 1470 K. Evolving carbon dioxide was measured coulometrically (Coulomat 701, Ströhlein Inc., Germany) in 0.6 M $Ba(ClO_4)_2$ buffered to *p*H 10.2.

5.3 Determination of the Freundlich Coefficient

In general, the Freundlich coefficient k (cf. Equation (16)) can be calculated directly by measurements of the concentration in soil solution C (kg m^{-3}) and the EDTA-extractable content C_{EDTA} (kg kg^{-1}) provided the Freundlich exponent m is known:

$$k = \frac{S}{C^m} = \frac{C_{EDTA} - \theta/\rho\, C}{C^m} \tag{32}$$

where θ/ρ denotes the solution-soil ratio used for the determination of the solution phase concentration. If no experimental data were available, the concentration in soil solution was below the detection limit or sorption characteristics were assumed to be variable in time the Freundlich coefficient was estimated by a *PTF* (Equation (17)).

The parameters of the *PTF* were estimated by fitting the extended Freundlich equation given by Streck and Richter (1997a) to the measured data:

$$S = k^* \, OC^b \, (H^+)^{-a} \, C^m \tag{33}$$

After taking the logarithm the equation is linear in the parameters:

$$\log S = \log k^* + b \log OC - a \log (H^+) + m \log C \tag{34}$$

The coefficients of this linear equation were estimated by multiple regression using the forward selection procedure (SPSS 6.1.2, SPSS Inc., USA). In an alternative approach k^* is assumed to vary horizontally (e.g. Streck and Richter, 1997a)

$$\hat{k} = k^*_{xy}\, OC^b\, (H^+)^{-a} \tag{35}$$

In this case, the "blocking" procedure was used (Draper and Smith, 1966, p. 48). Equation (34) was expanded by N dummy variables Z_i

$$\log S = \log k^* + \sum_{i=1}^{N} \zeta_i Z_i + b \log OC - a \log (H^+) + m \log C \tag{36}$$

where N is the number of soil monoliths sampled. Z_i=1 if the observation is from the i-th soil monolith while Z_i=0 otherwise. After estimating the N+4 parameters in Equation (36) the intrinsic Freundlich coefficient of the i-th soil monolith was calculated by

$$k^*_{xy,i} = 10^{(\log k^* + \zeta_i)} \tag{37}$$

5.4 Statistics and Model Assessment Criteria

Whether the means of two groups were the same was tested by using the two sample Student's *t*-test (*t*-test). Whether the means of more than two groups were the same was tested by a one-way analysis of variance *(ANOVA)* followed by Fisher's *LSD* post hoc test for significant differences. Both procedures were performed as two-tailed tests at the 5% significance level.

The Kolmogorov-Smirnov statistic (*KS*-test) with corrected significance levels according to Lilliefors (1967) was used for testing whether a set of observations

was from a particular population. Unless otherwise stated, all *KS*-tests were performed at the 5% significance level.

With linear regressions the coefficients of determination R^2, defined as the proportion of the total variance explained by the regression, is given. One, two or three asterisks are used to show significance at the 0.05, 0.01 and 0.001 levels, respectively. Multiple regression was applied to estimate the parameters of *PTFs*, as described in the subchapter above. The parameters of non-linear equations were fitted by applying the non-linear regression procedure implemented in SPSS 6.2.1 (SPSS Inc., USA).

For visualization the geographical information system ArcView 3.1 (ESRI Inc., USA) with the extension "Spatial Analyst" was used. For block kriging and conditional simulation the geostatistical software package GStat (Pebesma and Wesseling, 1998) were applied. In case of lognormally distributed variables the following procedure was utilized: 1) transforming the original values *Z(x)* by taking logarithms, 2) kriging the transformed values *Y(x)* and 3) back-transforming them using the formulas given in Journel and Huijbregts (1991, p. 570-572).

Two criteria were applied for model evaluation: the modelling efficiency *EF* (Loague and Green, 1991) and the displacement index *DI*. The modelling efficiency *EF* is defined as the proportion of the total variance of observed data explained by the model:

$$EF = 1 - \sum_{i=1}^{n} (P_i - O_i)^2 \Big/ \sum_{i=1}^{n} \left(O_i - \overline{O}\right)^2 \qquad (40)$$

Here, P_i and O_i denote predicted and observed values, respectively. n is the number of samples and $\overline{O}$ stands for the mean of the observed data. Applying Equation (40) is more appropriate than regressing modelled values on observed ones since a good modelling performance requires that observed and predicted data are identical rather than simply linearly related. Note, however, that the meaning of *EF* is similar to that of the R^2. The *EF* can be seen as the R^2 for a regression line with a slope of unity and an intercept of zero. Thus, the *EF* is a measure of the extent to which predicted values approach a corresponding set of measured observations. If all measured and predicted data are equal *EF* is unity. If *EF* is less than zero the predicted values are less accurate than simply using the observed mean.

As displacement index *DI* we define the ratio between predicted and observed EDTA-extractable Cd in subsoil (0.3 to 1.2 m)

$$DI = \frac{\sum_i h_i \rho_i C^P}{\sum_i h_i \rho_i C^O} \qquad (41)$$

where h_i (m) denotes the thickness of the *i*-th layer in subsoil and ρ_i (kg L^{-1}) is the bulk density of subsoil in the *i*-th layer. C^P (µg kg^{-1}) denotes the predicted EDTA-extractable Cd content and C^O (µg kg^{-1}) the observed EDTA-extractable Cd content. Thus, the *DI* is a measure of the extent to which the model overestimates or underestimates the Cd displacement. If *DI* is less than 100% the model underestimates Cd displacement. If *DI* is higher than 100% the model overestimates Cd displacement.

5.5 Meteorological Data

The meteorological data were taken from the weather station Braunschweig-Völkenrode which is run by the German Meteorological Office. The station is located about 5 km south of the *WIA*. For the period between 1957 and 1998 the station provided air temperature T (°C) and relative humidity rH (%) data in hourly resolution and precipitation P (mm) data in 6-hourly resolution. The annual potential evapotranspiration pET (mm yr^{-1}) was calculated after Haude (1955) using the β-factors given by Heger (1978):

$$pET = \beta \sum_{j=1}^{d} \sum_{i=1}^{24} \Delta e_{ji} \tag{42}$$

whereby Δe_{ji} (Pa) denotes the saturation deficit of the air at the i-th hour of the j-th day of a year. d is the number of days of the year. In accordance with Maidment (1993) Δe_{ji} was calculated by

$$\Delta e_{ji} = 6.108\ (100 - rH_{ji}) \exp\left(\frac{17.27\, T_{ji}}{237.7 + T_{ji}}\right) \tag{43}$$

Here T_{ji} (°C) denotes the air temperature and rH_{ji} (%) the relative humidity at the i-th hour of the j-th day of a year.

5.6 Hydrogeological Data

A map of the depths of water table was produced by overlaying a digital land model (DGM 5) with a ground water elevation map. The digital land model was supplied by the Land Surveying Office Hannover (Germany). Ground water elevation was interpolated from the levels of 26 ground water monitoring wells supplied by the *BMWA*. The data were available for periods between 10 and 33 years in monthly resolution. Time-averaged ground water levels were computed

from all available data. The ground water elevation map was produced by means of Universal Kriging 1.

6 Description of the Model *SEFAH*

The following chapter gives the theoretical background of the environmental fate model *SEFAH*. The first subchapter describing the water regime is followed by two subchapters concerning the displacement of Cd (leaching, annual ploughing and deep ploughing) and the uptake of Cd by plants. Chapter 6 does not deal with the parameterization of the model. This topic is assigned to Chapter 8.4.

6.1 Water Regime

Heavy metal leaching is a very slow process. Depending on sorption behaviour, water flux and distance to the ground water table the time scale of heavy metal leaching may range between decades and centuries. It has been shown that short-term variation of water flux has a negligible effect on heavy metal movement, and thus, the water regime can be simulated under stationary conditions (Swartjes, 1990). The local water balance in one dimension can then be written as (Streck, 1993)

$$\frac{\partial q}{\partial z} + W(z) = 0 \tag{44}$$

where q (m s^{-1}) denotes the water flux density, z (m) the soil depth and $W(z)$ (s^{-1}) the root water uptake. Provided that the root water uptake is proportional to the root length density, $W(z)$ may be written as

$$W(z) = \varpi\, T_P \exp(-\varpi\, z) \tag{45}$$

where ω (m^{-1}) is an empirical parameter which describes the distribution of root length density with depth. T_P denotes the transpiration rate (m s^{-1}). Equation (45) makes sure that

$$\int_0^{\infty} W(z)dz = T_P \tag{46}$$

Integrating Equation (44) and considering Equation (45) gives the water flux density as a function of depth

$$q(z) = q_{\inf} - T_P(1 - \exp(-\varpi\, z)) \tag{47}$$

where q_{inf} denotes the flux density of infiltrating water. Equation (47) may be written as

$$q(z) = P + I - E - T_P(1 - \exp(-\varpi\, z)) \tag{48}$$

where P (m s^{-1}) denotes the precipitation rate (rainfall and snow), I (m s^{-1}) the irrigation rate and E (m s^{-1}) the evaporation rate.

The transpiration rate was computed with an approach of Bierhuizen and Slatyer (1965), who introduced an equation proposed to be applicable for different climatic regions

$$T_P = \frac{\Delta e}{\rho_w k_P} Y \tag{49}$$

where Δe (Pa) is the average saturation deficit of the air during main vegetation period, k_P (Pa) is a crop-specific constant[8], ρ_w (kg m^{-3}) is the density of water and Y is the dry matter production (kg m^{-2} s^{-1}).

6.2 Displacement

6.2.1. Leaching

Cd leaching was computed with the *CDE* introduced in Chapter 3.1.

[8] In plant-physiological studies k_P is generally denoted as k-factor.

$$\frac{\partial \theta C}{\partial t} + \frac{\partial \rho S}{\partial t} = \frac{\partial}{\partial z}\left(D_S \frac{\partial C}{\partial z} \right) - \frac{\partial qC}{\partial z} - \phi \tag{50}$$

Non-linear sorption was described by the Freundlich sorption isotherm (p. 11). The apparent dispersion coefficient D_S ($m^2\ s^{-1}$) can be recognized as the sum of the molecular diffusion D_{ls} ($m^2\ s^{-1}$) and the hydrodynamical dispersion D_{lh} ($m^2\ s^{-1}$) coefficient (p. 9)

$$D_S = D_{ls} + D_{lh} \tag{51}$$

with

$$D_{ls} = a_D D_0 \exp(\theta\, b_D) \tag{52}$$

and

$$D_{lh} = \lambda q \tag{53}$$

The local dispersion length, λ, is generally expected to have no significant effect on modelling heavy metal leaching at the field scale. For example, Streck and Richter (1997b) observed that heavy metal field-scale dispersion could be explained to a high degree by the spatial variability of sorption and that the value of the local dispersion length was unimportant.

The initial condition was chosen as

$$C(z,0) = C_{BG} \qquad z > 0 \tag{54}$$

where C_{BG} denotes the background concentration. The Cd concentration at the upper boundary C_{inf} (kg m^{-3}) was calculated by

$$C_{\inf} = \frac{IC_W + PC_{Pc}}{I + P} \tag{55}$$

where C_W (kg m^{-3}) denotes the Cd concentration in waste water and C_{Pc} (kg m^{-3}) the concentration in precipitation. With a flux type solute input the upper bound-

ary condition for solving the *CDE* for resident concentrations had to be stipulated as (Parker and Van Genuchten, 1984)

$$C(0,t) - \frac{D_S}{q}\frac{\partial C(z,t)}{\partial z}\bigg|_{z=0+} = C_{\inf}(t) \tag{56}$$

The lower boundary condition was set to

$$\frac{\partial C}{\partial z}\bigg|_{z=L} = 0 \tag{57}$$

whereby the depth of the lower boundary L was defined by the depth of water table.

The numerical solution of Equation (50) was achieved by using an implicit-explicit discretization scheme (Smith, 1985). The resulting non-linear system of equations was solved iteratively by means of the Newton-Raphson method (Press et al., 1988). For details see Streck (1993). At the end of each simulation year the sink term ϕ (cf. Chapter 6.3) was calculated and subtracted in each of the n compartments. Afterwards, the new equilibrium between the concentration in soil solution and the sorbed phase concentration was determined by solving the non-linear equation

$$f(C_i) = \frac{\theta_i}{\rho_i}C_i + kC_i^m - C_{T,i} = 0 \qquad i = 0,1,2,3,\ldots,n \tag{58}$$

with the help of the Newton-Raphson method (see above).

6.2.2. Annual Ploughing

Single ploughing does not really lead to soil homogenisation. Only repeated ploughing results in a complete mixing of soil material. However, because heavy metal leaching is extremely slow, ploughing can be regarded as a soil homogenising process (Schimmack and Bunzl, 1986).

Before ploughing the total concentration of Cd in the *i*-th compartment is given by

$$C_{T,i}^{old} = \frac{\theta_i}{\rho_i} C_i^{old} + S_i^{old} \tag{59}$$

After ploughing it is assumed that all *n* compartments of the Ap horizon have the same total concentration (Streck, 1993)

$$C_{T,i}^{new} = \frac{1}{n} \sum_{j=1}^{n} C_{T,j}^{old} \qquad i = 1,2,3,...,n \tag{60}$$

Finally, the new equilibrium between solution and sorbed phase concentration was determined by solving Equation (58).

6.2.3. Deep Ploughing

Deep ploughing in connection with the cultivation of asparagus transfers high amounts of soil material from the Ap horizon (0 to 0.3 m) to a depth of 0.3 to 0.8 m and vice versa. With deep ploughing, more or less continuous soil packages are exchanged rather than mixed. Other than the annual ploughing of the Ap horizon deep ploughing occurs only once at the beginning of each new asparagus cultivation.

The Ap horizon is considered as a homogeneous compartment and is labelled as the *0*-th compartment. Depending on the depth of ploughing *n* compartments below the Ap horizon are affected. After deep ploughing the total concentration in the Ap horizon $C_{T,0}^{new}$ may be written as

$$C_{T,0}^{new} = C_{T,0}^{old} + \frac{1}{h_0 \rho_0} \sum_{i=1}^{n} \alpha_i \left(C_{T,i}^{old} - C_{T,0}^{old} \right) \tag{61}$$

where h_0 (m) denotes the thickness, ρ_0 (kg m^{-3}) the bulk density of the Ap horizon and α_i (kg m^{-2}) stands for the soil exchange rate between the Ap horizon and

the *i*-th compartment. The total concentration in the *i*-th compartment may be calculated by

$$C_{T,i}^{new} = C_{T,i}^{old} - \frac{\alpha_i}{h_i \rho_i}\left(C_{T,i}^{old} - C_{T,0}^{old}\right) \qquad i > 0 \tag{62}$$

Besides Cd also *OC* and H^+ are exchanged between compartments. The exchange of *OC* and H^+ was modelled in analogy to that of Cd. The new Freundlich coefficient of each layer was estimated by a pedotransfer function (cf. Chapter 7.4). Finally, the new equilibrium between solution and sorbed phase concentration was iteratively determined (Equation (58)).

6.3 Plant Uptake

For modelling the uptake of Cd by plants a transpiration-based approach was applied. If the uptake of a solute is governed by mass-flow the uptake rate ϕ (kg m^{-3} s^{-1}) as a function of depth may generally be written as (cp. Equation (45))

$$\phi(z) = \varpi\, \eta\, T_P\, C(z) \exp(-\varpi z) \tag{63}$$

where η is a plant-specific empirical parameter, which accounts for whether the uptake by mass-flow is uncontrolled (η =1), enhanced (η >1) or reduced (η <1).

Since the average Cd content of total dry matter, $\overline{C}$ (kg kg^{-1}), is the quotient between total Cd uptake and total dry matter production *Y* (kg m^{-2} s^{-1}) it can be calculated by

$$\overline{C} = \varpi\, \eta \frac{T_P}{Y} \int_0^\infty C(z) \exp(-\varpi z) dz \tag{64}$$

Applying the relationship between transpiration and dry matter production according to Bierhuizen and Slatyer (1965) (cf. Equation (49)) yields

$$\overline{C} = \varpi\,\eta\,\frac{\Delta e}{\rho_w k_P}\int_0^\infty C(z)\exp(-\varpi z)dz \tag{65}$$

The translocation inside the plant is modelled by means of the plant-specific parameters

$$Q_{HM} = \frac{C_U}{C_P} \tag{66}$$

and

$$Q_Y = \frac{Y_U}{Y_P} \tag{67}$$

where Q_{HM} denotes the Cd content ratio and Q_Y the dry matter yield ratio between unprocessed (e.g. straw) and processed (e.g. grain) plant parts. C_U and C_P denote the Cd content of the unprocessed and processed plant parts, respectively. Y_U and Y_P are the respective dry matter yields. Since the average Cd content of dry matter can be written as

$$\overline{C} = \frac{Y_U C_U + Y_P C_P}{Y_U + Y_P} \tag{68}$$

the Cd content of the processed plant part (e.g. wheat grain) becomes

$$C_P = \frac{\overline{C}(1+Q_Y)}{1+Q_Y Q_{HM}} \tag{69}$$

Combining Equation (65) and Equation (69) leads to

$$C_P = \varpi\,\eta\,\frac{\Delta\Delta e}{\rho_w k_P}\,\frac{1+Q_Y}{1+Q_Y Q_{HM}}\int_0^\infty C(z)\exp(-\varpi z)dz \tag{70}$$

Since the model *SEFAH* divides the soil into n compartments of thickness Δz (m) the sink term ϕ_i (kg m^{-2} s^{-1}) of the i-th compartment is defined as

$$\phi_i = \int_{(i-1)\Delta z}^{i\Delta z}\phi(z')dz' \qquad i = 1,2,3,...,n \tag{71}$$

Integration of Equation (71) yields

$$\phi_i = \eta T_P C_i \exp(-\varpi i \Delta z)\left(\exp(\varpi \Delta z) - 1\right) \tag{72}$$

where C_i (kg m^{-3}) denotes the solution phase concentration in the i-th compartment. Consequently, $\overline{C}$ is

$$\overline{C} = \eta \frac{\Delta e}{\rho_w k_P}\left(\exp(\varpi \Delta z) - 1\right)\sum_{i=1}^{n} \exp(-\varpi i \Delta z) C_i \tag{73}$$

and the Cd content of the processed plant part is given by

$$C_P = \eta \frac{\Delta e}{\rho_w k_P} \frac{1 + Q_Y}{1 + Q_Y Q_{HM}}\left(\exp(\varpi \Delta z) - 1\right)\sum_{i=1}^{n} \exp(-\varpi i \Delta z) C_i \tag{74}$$

7 Field Observations

7.1 Cd Contents and Cd Loads

The most important statistics of the observed EDTA-extractable Cd contents are given in Table 3. EDTA-extractable Cd contents in Ap horizons of the *WIA* were on average 0.285 ± 0.163 mg kg^{-1} and varied over two orders of magnitude. The coefficient of variation (*CV*) was 57%. According to the *KS*-test the EDTA-extractable Cd content was lognormally distributed at α=0.05. In contrast to the results of Mühlnickel et al. (1989), no effect of the different operation periods of districts was observed. The mean EDTA-extractable Cd content did not differ significantly between districts (*ANOVA*, α=0.05). Within all four districts, however, the mean EDTA-extractable Cd content in Ap horizons was significantly higher than outside the irrigation area.

Table 3: Statistics of the EDTA-extractable Cd contents in Ap horizons inside and outside the waste water irrigation area (WIA). Means with the same index are different at the 5% significance level (ANOVA).

	District				***WIA***	**Outside the *WIA***
	1 (N=33)	**2** (N=41)	**3** (N=45)	**4** (N=34)	(N=153)	(N=8)
	mg kg^{-1}					
Mean	0.286[a]	0.239[b]	0.318[c]	0.290[d]	0.285[e]	0.168[abcdef]
SD	0.134	0.107	0.220	0.148	0.163	0.119
min	0.096	0.052	0.034	0.101	0.034	0.053
max	0.690	0.582	1.135	0.872	1.135	0.383

The aqua regia Cd content in Ap horizons of the *WIA* was on average 0.361 mg kg^{-1} (Table 4), and thus clearly below the limit of the sewage sludge regulation of 1.0 mg kg^{-1}. Only at one site was the limit exceeded. This site is situated in the direct vicinity of the former sewage storage basin of District 3.

Table 4: Statistics of aqua regia Cd content in Ap horizons inside and outside the waste water irrigation area (WIA). Means with the same index are different at the 5% significance level (ANOVA).

	District				***WIA***	**Outside the *WIA***
	1 (N=33)	**2** (N=37)†	**3** (N=43)‡	**4** (N=34)	(N=147)	(N=8)
	mg kg^{-1}					
Mean	0.343[b]	0.302[ac]	0.422[ad]	0.365[e]	0.361[f]	0.186[bcdef]
SD	0.157	0.139	0.256	0.152	0.189	0.107
min	0.111	0.100	0.100	0.135	0.100	0.101
max	0.805	0.846	1.485	0.919	1.485	0.418

† The total Cd content in the Ap horizon of soil monoliths J09, K09, L12 and M12 were below the detection limit (<0.1 mg kg^{-1}).

‡ The data of soil monoliths F14 and I19 were missing.

On average 76% of the aqua regia Cd content (C_{AR}) was extractable by means of EDTA. Similar to results by Hornburg (1991), a significant linear relationship (R^2=0.86***) could be derived between both variables (Figure 9).

$$C_{AR} = 1.088\, C_{EDTA} + 0.047 \qquad (75)$$

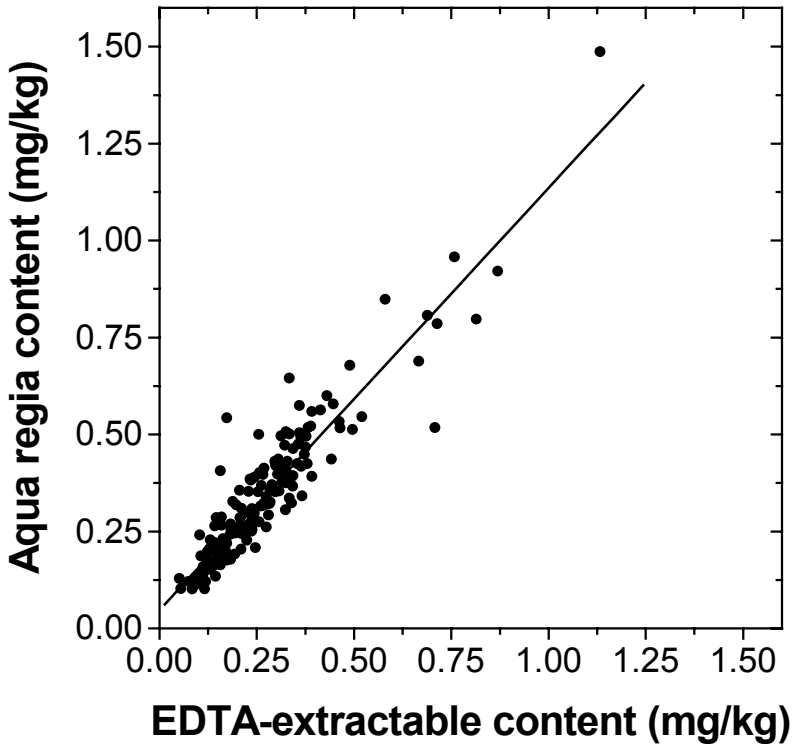

Figure 9: Linear relationship between Cd contents measured by aqua regia digestion and EDTA extraction. The coefficient of determination is 86% (N=155).

Figure 10 shows estimates of the mean aqua regia Cd content (mg kg^{-1}) in Ap horizons within 100 m x 100 m blocks calculated by ordinary block kriging and conditional simulation. After log-transformation an exponential variogram model with a sill of 0.2546 and a practical range[9] of 723 m was fitted to the data and were used for both calculations. There are three major areas with noticeably high Cd contents. The largest area is located in the proximity of the former sewage storage basin of District 3. Smaller areas of high Cd contents are situated in the vicinity of the sewage storage basin of District 1 and at the northern edge of the irrigation area. As already mentioned, sludge was applied not only by irrigation, but also by sludge utilization (cf. p. 25). It is even likely that before 1980

[9] The practical range is the distance at which an asymptotic variogram model reaches 95% of its sill (Journel and Huijbregts, 1978, p. 164)

the latter method was the dominant one. Since 1980, after it had become possible to apply the entire sludge by irrigation, sludge utilization has probably become unimportant. The finding that high Cd loads were observed particularly in the vicinity of the former storage basins indicates that the sludge was preferentially utilized close to the basins.

A comparison of Figure 10A and Figure 10B pictures the smoothing effect induced by ordinary block kriging (cf. Chapter 3.3.2). Kriged block means of aqua regia Cd content are much less variable and spatially more continuous than those using conditional simulation. With ordinary block kriging, the aqua regia Cd content of only 2 blocks (2 ha) exceeds the legal limit of 1 mg kg^{-1}. Applying the method of conditional simulation the Cd content of 9 blocks exceeds the limit.

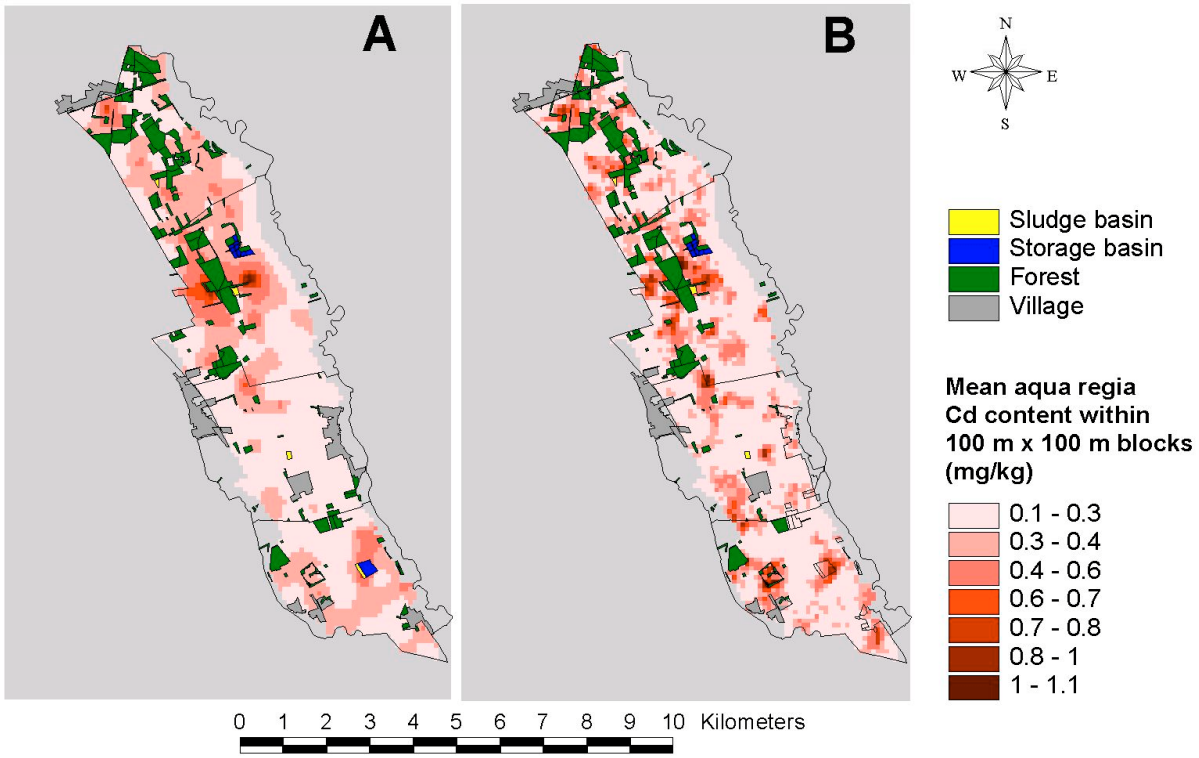

*Figure 10: Estimates of the mean aqua regia Cd content within 100 m x 100 m blocks using **A)** ordinary block kriging and **B)** conditional simulation.*

The Cd load I_{Cd} (kg m^{-2}) of each soil monolith was estimated by

$$I_{Cd} = \int \rho(z) \left(C_{EDTA}(z) - BG_{EDTA}(z)\right) dz \qquad (76)$$

where C_{EDTA} (kg kg^{-1}) and BG_{EDTA} (kg kg^{-1}) denote the measured EDTA-extractable Cd content in 1996 and the estimated EDTA-extractable Cd background content before irrigation started, respectively. $\rho(z)$ (kg m^{-3}) is the soil bulk density as a function of depth (cf. p. 98). BG_{EDTA} was estimated by using the *PTF 1a* assuming a background Cd concentration in soil solution of 0.1 µg L^{-1} (cf. p. 64).

The highest mean Cd load was observed in District 3. Here since the beginning of waste water irrigation an average of 152.9 mg m^{-2} has entered the soils. With 523.5 mg m^{-2}, the highest local Cd load was also measured within District 3. The lowest mean Cd load was found in District 4 with 120.0 mg m^{-2}. The mean Cd loads in Districts 1 and District 2 were 126.5 mg m^{-2} and 133.4 mg m^{-2}, respectively. While Streck (1993) observed Cd loads to be normally distributed at the field scale, Cd loads were observed to be lognormally distributed at the regional scale (*KS*-test, α=0.05).

Though a relationship between operation period and Cd load of a district seems plausible (Mühlnickel et al., 1989), no evidence was found that the Cd load was a function of the operation period. This finding may be explained as follows: In 1975, the sludge storage basins of District 1 and 2 were shut down (cf. p. 26). From 1975 to 1980, the sludge from the settling tanks of these districts was pumped to the pumping stations of District 3 and 4, i.e. sludge and Cd were exported from District 1 and 2 to District 3 and 4. Hence, the effect of operation period on Cd loads may be superimposed by sludge transfer between the districts.

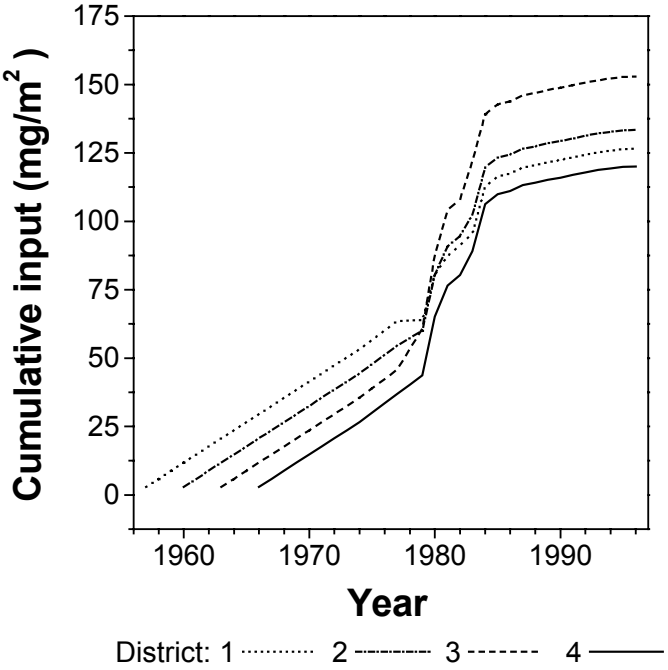

Figure 11: Reconstructed Cd input history of districts. The Cd loads from 1957 to 1979 are estimates. From 1980 to 1996 the Cd loads to the WIA were measured by the BMWA.

For 1980 to 1996, data of Cd loads to the *WIA* were available (cf. Figure 5). Before 1980, however, Cd loads to the *WIA* were not measured. Thus, for 1957 to 1979 a simplified Cd load history was reconstructed from measured soil data (Figure 11). First of all, it was assumed that on average the Cd concentration of waste water C_W (kg m^{-3}) did not differ between districts. If no Cd had been transferred between districts the Cd load to District *i* would have amounted to

$$I_i^* = B_i C_W + I_{80-96} \qquad i = 1,2,3,4 \tag{77}$$

whereby B_i (m^3 m^{-2}) denotes the total amount of waste water irrigated within District *i* until 1979. Due to the differences in the beginning of irrigation B_i differed between districts as follows: B_1=8,726 L m^{-2}, B_2=7,635 L m^{-2}, B_3=6,524 L m^{-2} and B_4=5,423 L m^{-2}. $I_{80\text{-}96}$ (kg m^{-2}) stands for the Cd load to the *WIA* from 1980 to 1996 as calculated from the data of the *BMWA* (76.14 mg Cd m^{-2}).

If I_i^* differed from the measured mean Cd load of District i (I_i), then from 1975 to 1979 either an export ($I_i^* - I_i > 0$) or an import ($I_i^* - I_i < 0$) of Cd was assumed. Moreover, since the sludge from storage basins was composted for 2 to 3 years before agricultural use it was presumed that these exports and imports entered soils evenly partitioned from 1978 to 1982. Because of mass conservation the sum of exports and imports within the *WIA* has to be zero

$$\sum_i (I_i^* - I_i) = 0 \tag{78}$$

Combination of Equation (77) and (78) and rearrangement leads to

$$C_W = \frac{\sum_i I_i - 4I_{80-96}}{\sum_i B_i} \tag{79}$$

Using this approach, from 1957 to 1979 the average Cd concentration in waste water was 8.1 µg L^{-1}. District 1 and District 2 exported 20.0 mg m^{-2} and 4.3 mg m^{-2}, respectively, to District 3 and District 4. The major part of the exported Cd was transferred to District 3 (24.1 mg m^{-2}) and only a minor part (0.2 mg m^{-2}) entered District 4.

The estimated average Cd concentration of waste water from 1957 to 1979 (8.1 µg L^{-1}) is distinctly lower than that reported from Bramm (1976) and as well as that estimated by Streck (1993). Bramm (1976) reported a mean Cd concentration in the waste water of 22 µg L^{-1}. However, Bramm (1976) sampled only 16 waste water probes during 1974 to 1976, therefore this value is obviously not sufficient to represent the average Cd load from 1957 to 1979. Streck (1993) estimated the Cd concentration of waste water from 1962 to 1979 in a procedure similar to the one outlined above, but neglected a possible Cd background content. His estimation resulted in an average Cd concentration in waste water of 15.6 µg L^{-1} from 1962 to 1979. However, Streck (1993) investigated only one

field (about 1 ha) within the *WIA*. Hence, it is likely that the differences can be attributed to an heterogeneous application within the *WIA*.

7.2 Displacement

As noted in Chapter 4 (p. 31) deep ploughing before asparagus cultivation leads to a noticeable change of chemical properties of soil. Soil material and organic matter as well as heavy metals are instantly exchanged between topsoil and subsoil (≈ 0.3 to 0.6 m). Asparagus is cultivated on average for 8 to 10 years in successive years. After this period the plantation has to be used for 15 to 20 years for other crops to regenerate the soil and to avoid diseases and pests. After this recovery phase the crop rotation resumes. Among the 161 soil monoliths drilled, 14 (≈ 9%) were Rigosols[10]. However, these 14 Rigosol sites were not used for asparagus cultivation in 1996, i.e. these sites were probably in their recovery phase. According to the *BMWA* in 1996 about 5.6% of arable land were used for asparagus cultivation. Hence in 1996, approximately 15% of the total agriculturally used area were asparagus sites either in use or in their recovery phase.

The Rigosol sampled within block *H17* may serve as an example for the effect of deep ploughing (Figure 12). Because before drilling the Ap horizon was separately sampled (Chapter 5.1.1) the photograph shows only the subsoil (0.3 to 1.2 m). The *R* horizon is located from 0.3 to 0.6 m depth and is followed by a Bv horizon (0.6 to 0.8 m) and a C horizon (>0.8 m). The arrangement of horizons is mirrored by both the *OC* and EDTA-extractable Cd profiles. Within the *R* horizon high contents of *OC* as well as of EDTA-extractable Cd were measured. This suggests that Cd had been displaced not only by leaching but also by deep ploughing. However, whether and to which extent heavy metals are trans-

[10] Soil monoliths A26, E25, E23, F15, G21, H09, H11, H17, H19, I09, J10, K11, K14 and L12 (cp. Figure 8).

ferred by deep ploughing depends crucially on the time of operation. It is evident that heavy metals can only be transferred with the topsoil material if deep ploughing occurs after the heavy metals entered the Ap horizon. An example for a profile which was deep-ploughed before heavy metal application is given in Figure 13. The soil monolith *I14* shows a distinct *R* horizon, but other than with soil monolith *H17*, Cd contents in the *R* horizon are low.

The amount of soil exchanged due to deep ploughing was estimated on the basis of the measured *OC* profile (Figure 14). First of all, the *OC* profile before deep ploughing was approximately reconstructed. For this it was assumed that the highest *OC* content observed below the Ap horizon is the former *OC* content of the Ap horizon $OC_{0,old}$. The former *OC* content of layers below the Ap horizon $OC_{i,old}$ was set to the *OC* content measured in the layer 0.9-1.0 m. Under these assumptions the soil exchange rate α_i (kg m^{-2}) of layers below Ap horizon can be calculated by

$$\alpha_i = h_i \rho_i \frac{OC_{i,new} - OC_{i,old}}{OC_{0,old} - OC_{i,old}} \tag{80}$$

where h_i (m) is the thickness and ρ_i (kg m^{-3}) the bulk density of layer *i*. The *OC* content of Ap horizon immediately after deep ploughing can be written as

$$OC_{0,new} = OC_{0,old} + \frac{1}{h_0 \rho_0} \sum_{i=1}^{n} \alpha_i \left(OC_{i,old} - OC_{0,old} \right) \tag{81}$$

whereby *n* denotes the number of layers below the Ap horizon affected by deep ploughing.

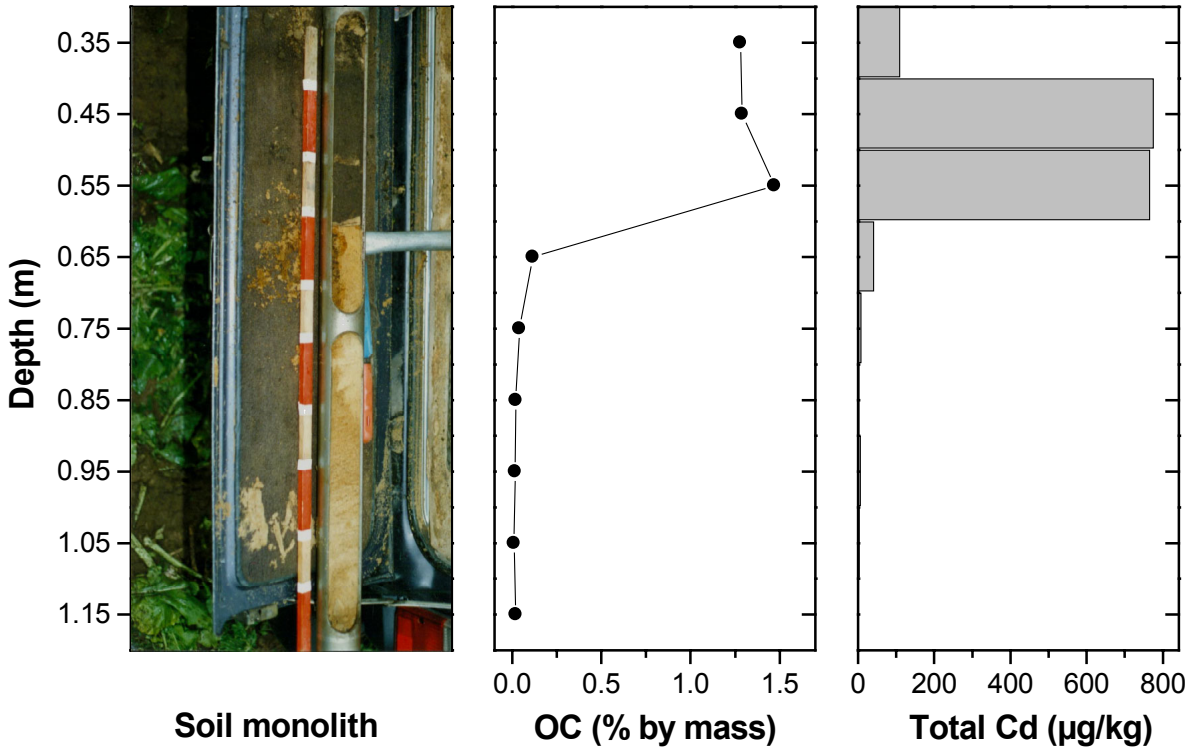

Figure 12: Photograph and profiles of OC and EDTA-extractable Cd content of a Rigosol sampled within block H17. The figure shows only the subsoil (0.3-1.2 m).

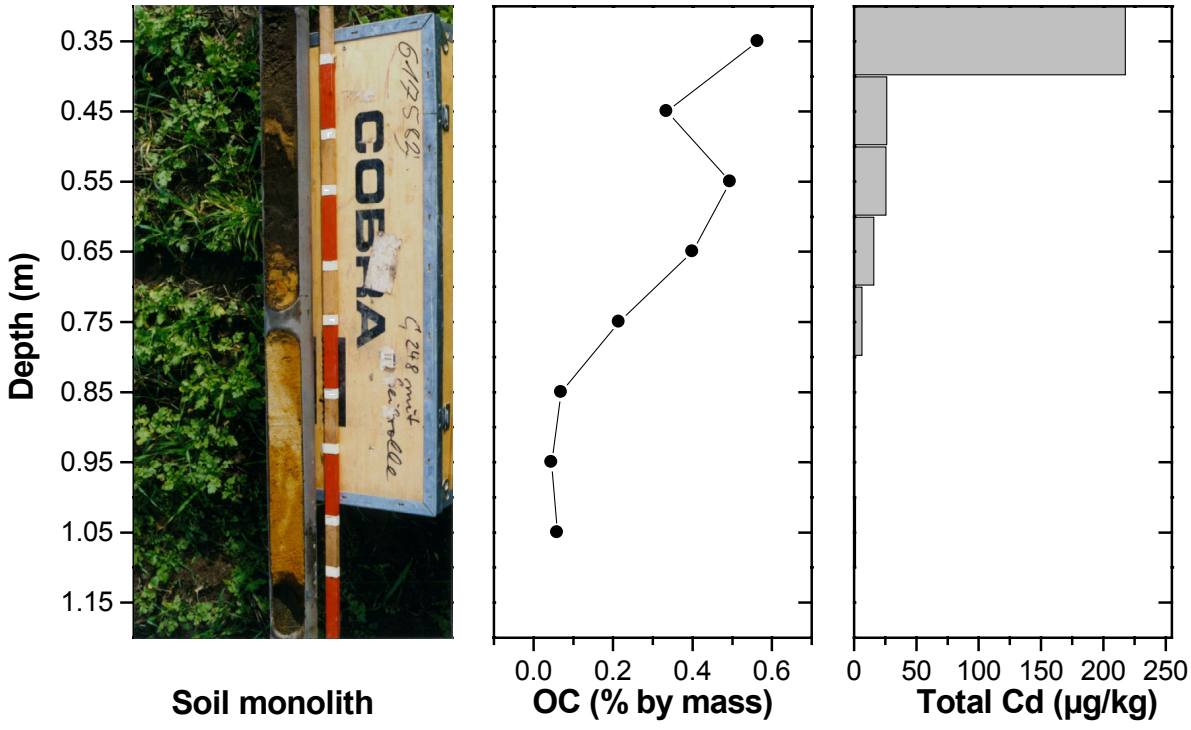

Figure 13: Photograph and profiles of OC and EDTA-extractable Cd content of a Rigosol sampled within block I14. The figure shows only the subsoil (0.3-1.2 m).

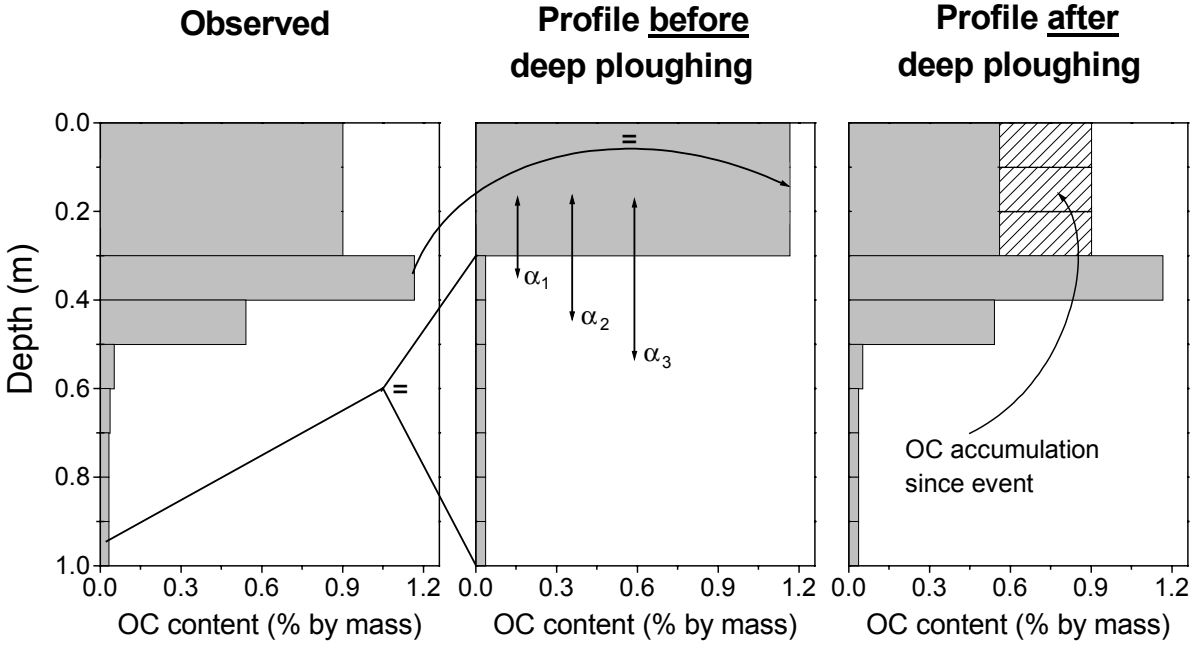

Figure 14: Sketch of the procedure for calculating soil exchange rates by the help of the observed OC profile.

Applying this approach to the 14 Rigosol sites yielded that the average total exchange of soil between Ap horizon and subsoil was 359 kg m^{-2} with a *CV* of 19%. Decreasing quantities of soil were exchanged with increasing depth. For example, on average 44% of the soil exchanged was transferred between the Ap horizon and the layer 0.3-0.4 m. With regard to the layer 0.5-0.6 m this fraction was only 16%. The exchange of soil in deeper layers was enhanced with increasing total exchange (Figure 15). The higher the total exchange the higher the proportion of Ap material transferred to the layer 0.5-0.6 m. In contrast, the higher the total exchange the lower the fraction of Ap material transferred to the layer 0.3-0.4 m. The fraction of Ap material transferred to 0.4-0.5 m was more or less unaffected by the amount of exchanged soil.

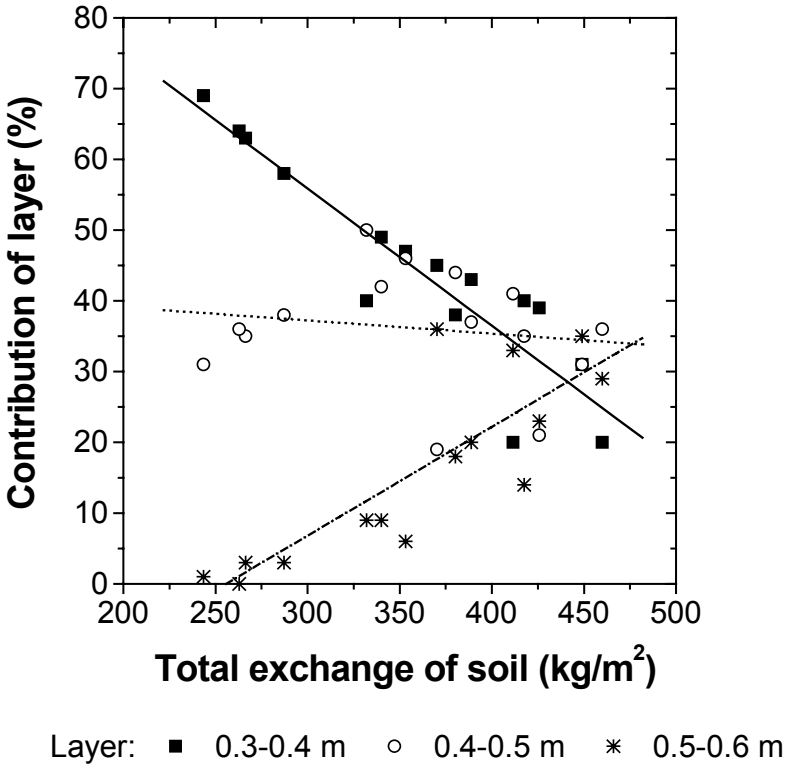

Figure 15: Relationship between the total amount of soil exchanged and the contribution of subsoil layers to total exchange.

Figure 16 shows the averaged EDTA-extractable Cd content profiles for both Rigosols and Non-Rigosols. Not surprisingly, the EDTA-extractable Cd content in the Ap horizon is higher in Non-Rigosols (300.4 µg kg^{-1}) than in Rigosols (130.4 µg kg^{-1}). The Non-Rigosol profile shows continuously decreasing EDTA-extractable Cd contents with depth. In contrast, the Rigosol profile shows highest EDTA-extractable Cd contents in the 0.3 to 0.4 m and the 0.4 to 0.5 m layers.

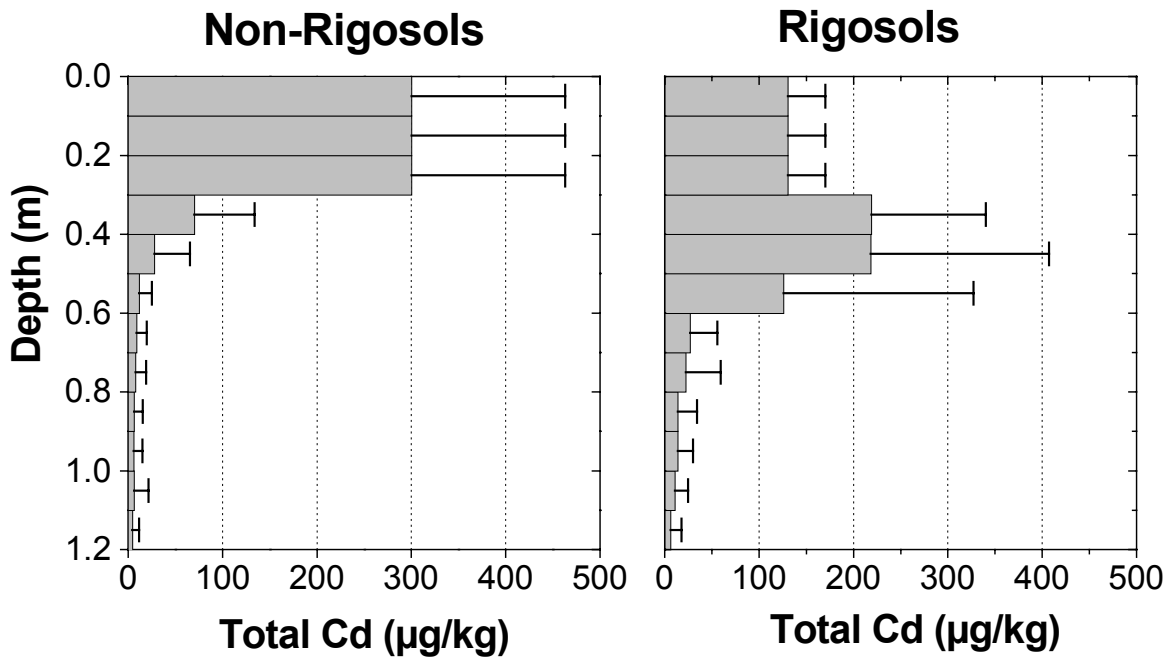

Figure 16: Averaged profiles of the EDTA-extractable Cd contents of Non-Rigosols (N=139) and Rigosols (N=14). Bars indicate standard deviations.

With 994 samples (62%), the Cd concentration in soil solution was below the detection limit. These samples were exclusively subsoil samples. In these cases the concentration in solution was calculated from the EDTA-extractable content, soil *p*H and *OC* content. The Freundlich coefficient *k* was estimated by *PTF* 1a (cf. Chapter 7.4). The equilibrium between solution and sorbed phase concentration was determined by Equation (58) using the Newton-Raphson method.

The averaged profiles of Cd concentration in soil solution are given in Figure 17. The profiles show a similar pattern as those of the EDTA-extractable Cd content. The mean Cd concentration in Ap horizons of Non-Rigosols (1.76 µg L^{-1}) is higher than in those of Rigosols (1.1 µg L^{-1}). The Non-Rigosol profile is characterized by a Cd concentration continuously decreasing with depth. Cd concentrations decrease from 1.76 µg L^{-1} in the Ap horizon to 0.2 µg L^{-1} in the last sampled layer (1.1-1.2 m). In District 4, the district under shortest operation period (30 yr), the Cd concentration in the last sampled layer is on average only

0.1 µg L^{-1}. In the following, this concentration is assumed to be the background concentration of the soils within the *WIA*. In contrast to the Non-Rigosol profile, the Cd concentration of the Rigosol profile increases below Ap horizon and is highest in the 0.4 to 0.5 m layers.

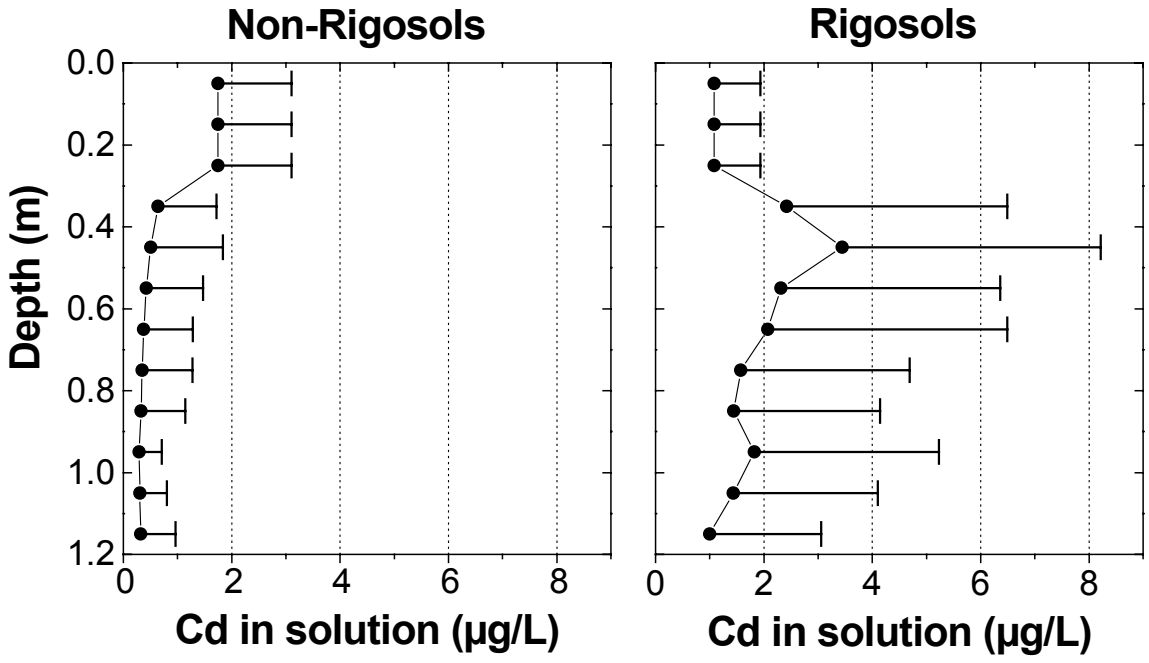

Figure 17: Averaged profiles of Cd solution phase concentrations of Non-Rigosols (N=139) and Rigosols (N=14). Bars indicate standard deviations.

The Cd concentration profiles indicate that, on average, Cd displacement has progressed down to a depth of roughly 0.5 m only. However, Cd displacement is highly variable within the *WIA* (Figure 18). At some sites even after 40 yr of waste water irrigation the Cd displacement seems to be limited more or less to the Ap horizon. In contrast, at some sites Cd has been displaced to below 1.2 m.

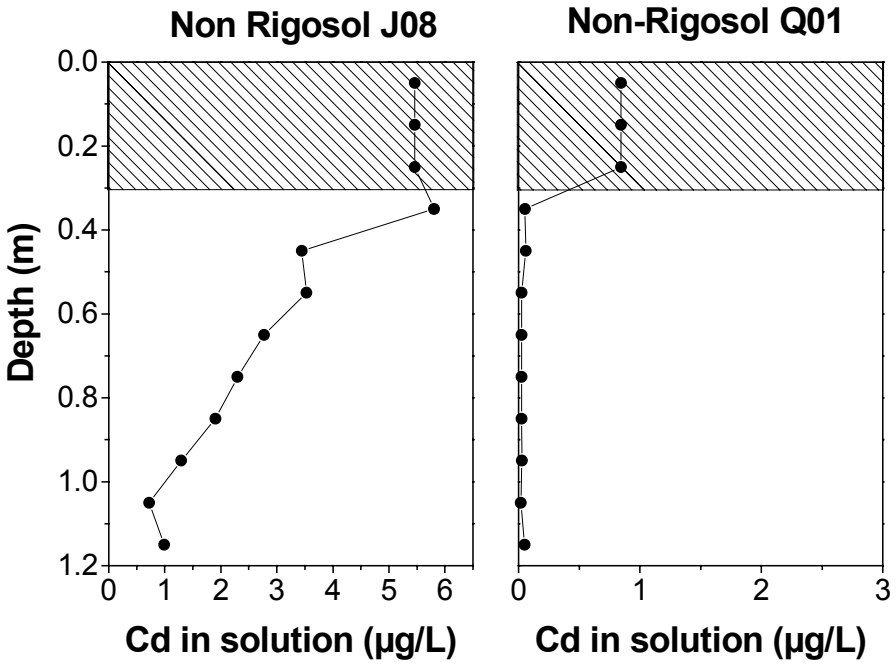

Figure 18: Cd concentrations in solution of soil monoliths J08 and Q01.

7.3 Sorption Characteristics

In Ap horizons of the *WIA* soil *p*H is on average 5.78 with a *CV* of 7% (Figure 19). The range was from 4.8 to 7.0. In subsoils the averaged soil *p*H does not differ distinctly from that in Ap horizons, but subsoil *p*H is more variable than topsoil *p*H. It varies between 3.9 and 7.0, with the *CV* increasing to roughly 12%.

In Ap horizons, soil *p*H decreases from south to north (Figure 19). While in District 1 the soil *p*H is 6.0 on average, in District 3 and 4 it is only 5.7. The same trend was observed in subsoils. In the 0.9 to 1.0 m layer, for example, the mean *p*H in the Districts 1 and 2 is about 5.9 and it decreases to 5.6 in District 3 and 5.7 in District 4.

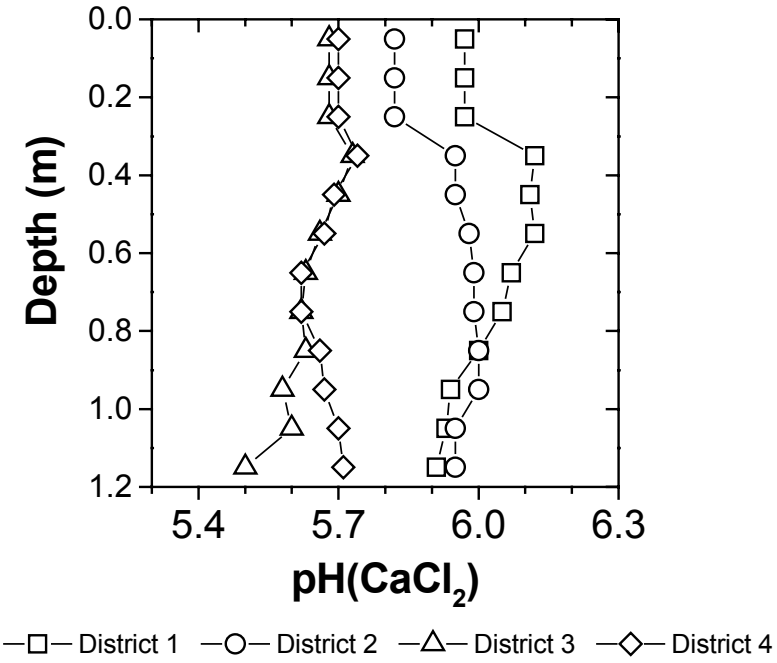

Figure 19: Averaged profiles of soil pH of Districts 1, 2, 3 and 4.

Table 5: Results of the Kolmogorov-Smirnov test for normality of soil pH with corrected significance levels according to Lilliefors (1967). One or two asterisks are used to show significance at the 0.01 or 0.05 level, respectively.

Depth (m)	*WIA*	District 1	District 2	District 3	District 4
0-0.3	**	**	**	*	**
0.3-0.4	*	**	**	*	**
0.4-0.5		**	*	*	**
0.5-0.6		**	**	*	**
0.6-0.7		**	**	**	**
0.7-0.8		**	**	**	**
0.8-0.9		**	**	**	**
0.9-1.0		*	**	*	*
1.0-1.1		**	*		
1.1-1.2		**	*	*	*

Within the *WIA*, only soil *p*H in Ap horizons are normally distributed at α=0.05. In other layers, soil *p*H is neither normally nor lognormally distributed at this significance level (Table 5). *p*H values below 0.4 m show a left-skewed distribution (the mean to the left of the median) (Figure 20). The left skewness

increases with depth. The coefficient of skewness decreases from 0.03 in the 0.3-0.4 m layer to –1.22 in the 1.1-1.2 m layer.

When the test for normality of soil *p*H was separately performed for each district test statistics markedly improved. At α=0.01 the normal hypothesis is only rejected in the 1.0 to 1.1 m layers of District 3 and 4.

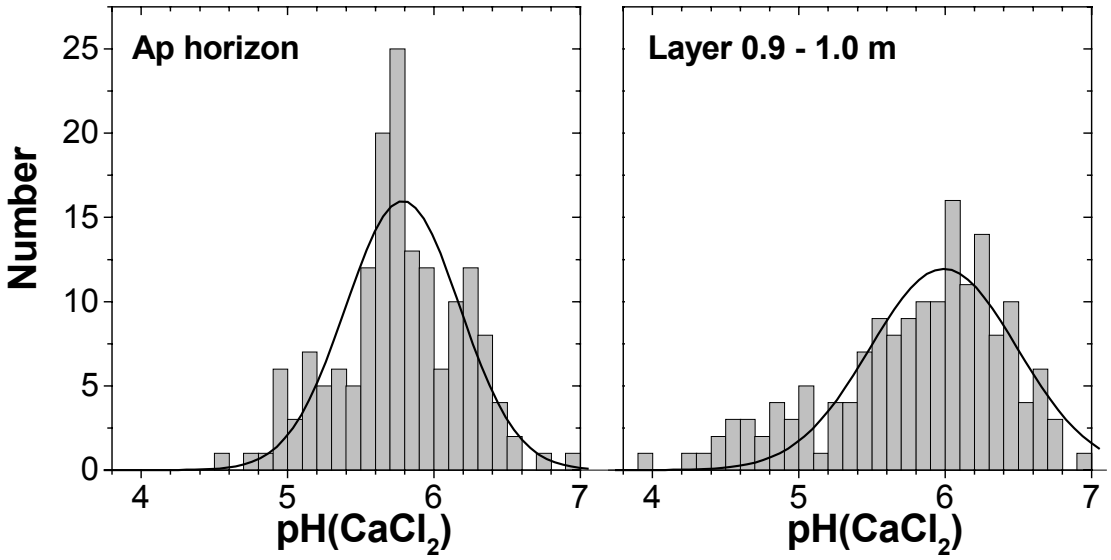

Figure 20: Histograms of soil pH in Ap horizons and 0.9-1.0 m layers. The two plotted curves are fitted normal distributions.

Figure 21 shows the experimental variograms of soil *p*H in the 0 to 0.3 m, 0.6 to 0.7 m and 0.9 to 1.0 m layers. An exponential model was fitted to each variogram. The spatial correlation length increases with increasing soil depth. The practical range of the variogram model is lowest in Ap horizons (505 m) and increases from 1350 m in the 0.5 to 0.6 m layers to 2850 m in the 0.9 to 1.0 m layers. Moreover, Figure 21 shows that also the variability of soil *p*H increases with depth. The semivariance of soil *p*H of the 0.9 to 1.0 m layers is twice as high as the semivariance of soil *p*H in Ap horizons.

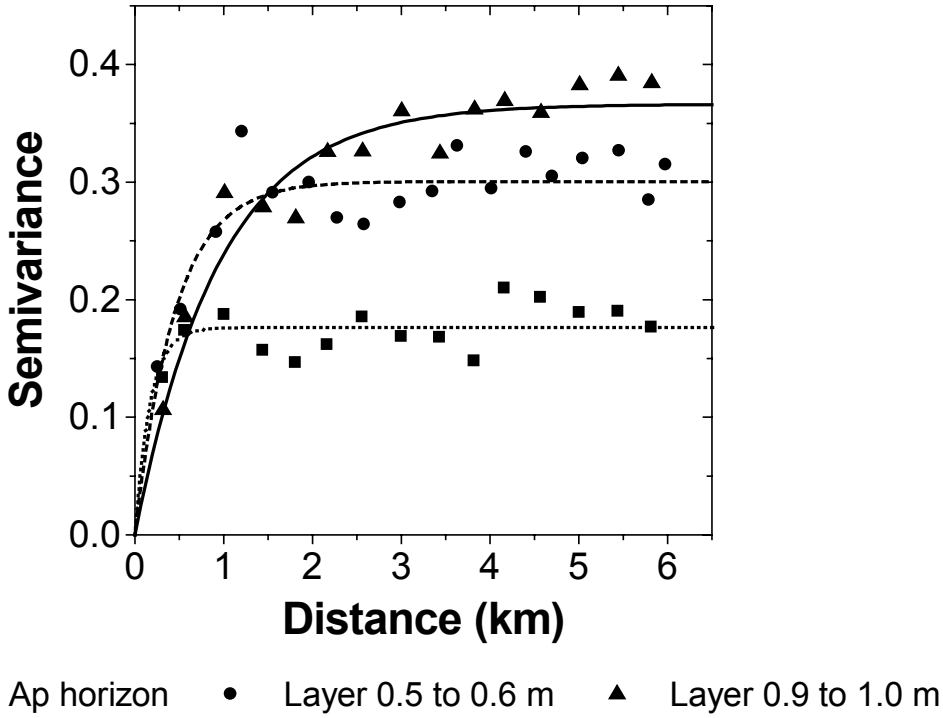

Figure 21: Experimental and fitted semivariograms of soil pH in Ap horizons, 0.5 to 0.6 m layers and 0.9 to 1.0 m layers.

Figure 22 shows estimates of the mean soil *p*H within 100 m x 100 m blocks using ordinary block kriging and conditional simulation. For both procedures the above variogram models were used. Once again the figure clearly demonstrates the smoothing effect induced by kriging. On the basis of the current sampling density block kriging is apparently not suitable to reproduce the "real" spatial variability of *p*H values in Ap horizons. Figure 22 sums up the major previous findings: (1) The *p*H values generally decrease from south to north in both Ap horizons and subsoils and (2) *p*H values in Ap horizons are both less spatially correlated and less heterogeneous than in subsoils.

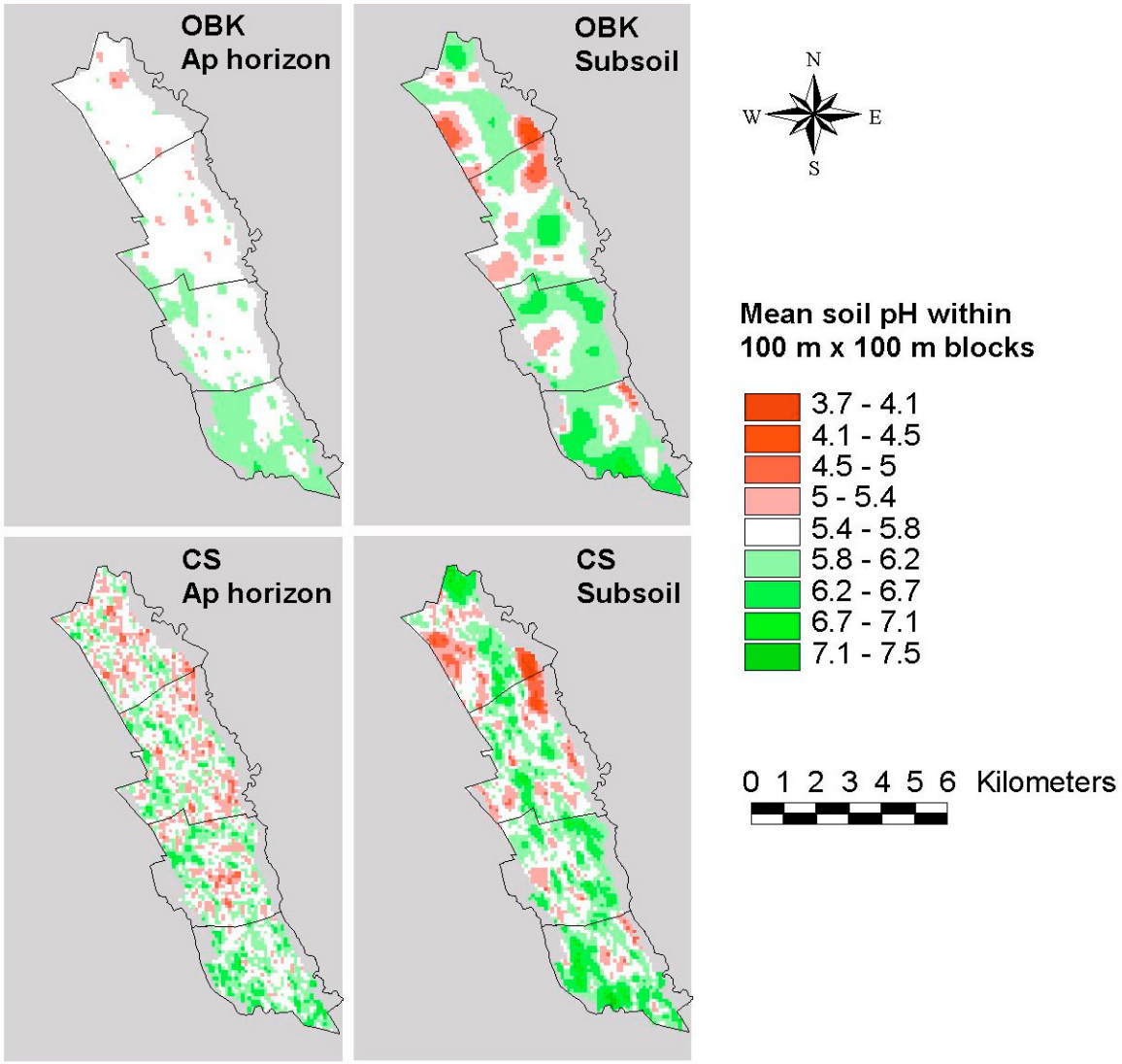

Figure 22: Mean soil pH in Ap horizons and subsoils (0.9 to 1.0 m) within 100 m x 100 m blocks as estimated by ordinary block kriging (OBK) and conditional simulation (CS).

Particularly the latter observation may be interpreted as an indication that the soil *p*H in Ap horizons is mainly controlled by the field-specific agricultural practice (liming, fertilization, crop rotation etc.). With increasing depth soil *p*H is more and more controlled by the original hydro- and geological conditions (depth of water table, parent material etc.). The effect of agricultural cultivation weakens and the correlation length of hydrogeological variables, which may be much higher than several hundred meters, becomes more and more apparent.

In Ap horizons, the mean and the median of *OC* content is 0.99% (by mass) and 0.87% (by mass), respectively, and the *CV* is 50%. In each layer down to 1 m depth, *OC* contents are lognormally distributed at α=0.05. As expected *OC* contents decrease strongly with depth. Below 0.6 m the mean *OC* contents are already smaller than 0.1% (by mass). Due to deep ploughing, the *OC* content in subsoils vary much more than in Ap horizons. For example, in the 0.5 to 0.6 m layers the *CV* increases to 126%.

Within the *WIA*, *OC* contents increase from south to north. The average *OC* content in Ap horizons of District 1 and District 2 is 0.94 and 0.75% (by mass), respectively. The somewhat lower *OC* content in District 2 may be explained by the higher amount of asparagus plantations, particularly in the vicinity of Wipshausen village. In District 3 the average *OC* content is 1.15% (by mass) and increase to 1.40% (by mass) in District 4.

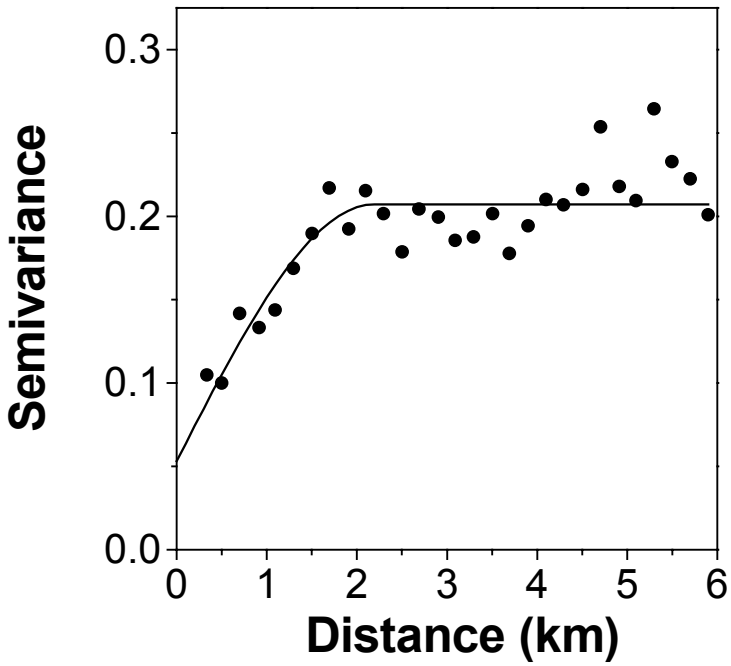

Figure 23: Experimental variogram of OC content in Ap horizons and fitted spherical variogram model. OC contents (% by mass) were transformed by taking logarithms.

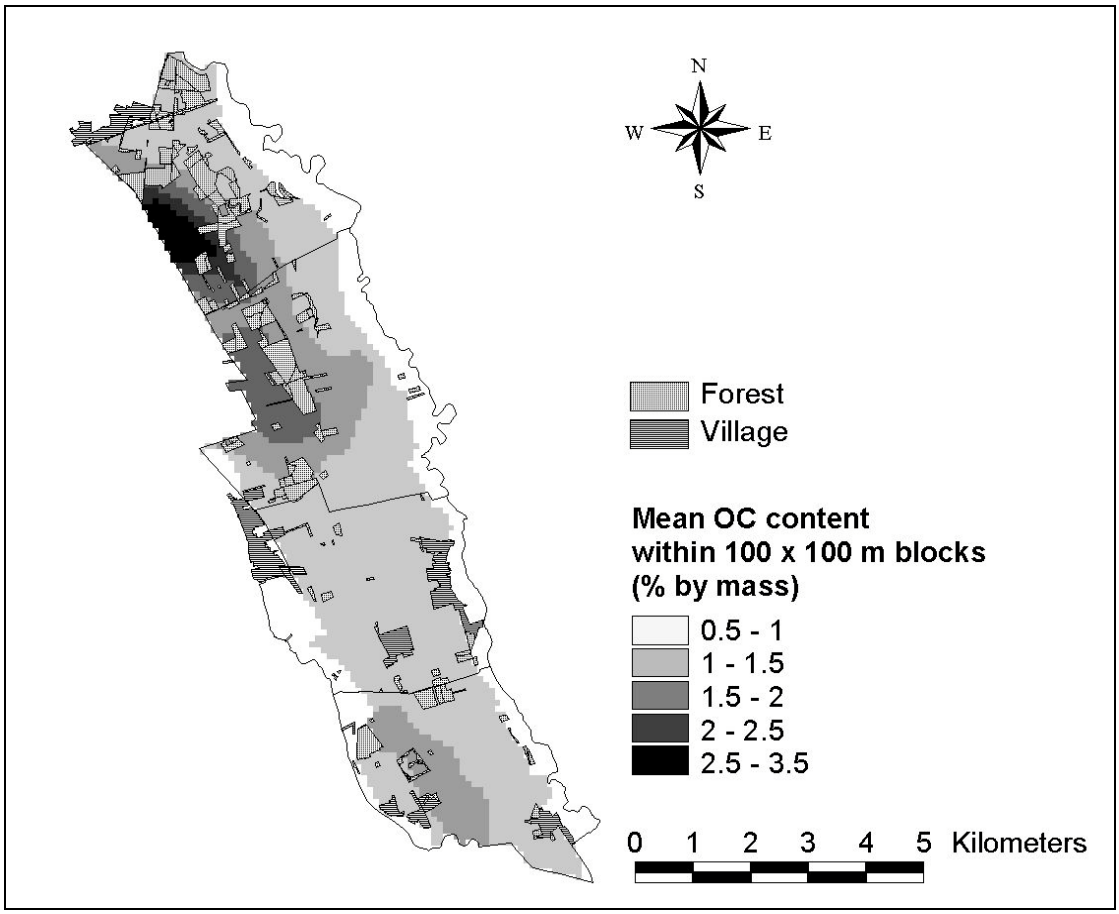

Figure 24: Block kriging estimates of the mean OC content in Ap horizons within 100 m x 100 m blocks.

A nested model, consisting of a nugget model with a sill of 0.053 and a spherical model with a sill of 0.154 and a range of 2192 m, was fitted to the variogram of the log-transformed *OC* contents in Ap horizon (Figure 23). Data from Rigosols were excluded from this calculation. The mean *OC* content in Ap horizons within 100 m x 100 m blocks was estimated by using the ordinary block kriging procedure (Figure 24). In most blocks within the *WIA* the estimated *OC* content ranges between 0.5 and 1% by mass (1788 ha). *OC* contents between 1 and 2% by mass were estimated for 951 ha in large areas of District 3 and also partly for the west of District 1. Highest block means (*OC* > 2% by mass) are found in an area of 128 ha in the west of District 4. In this area heath vegetation grew until the 1950s (Blickwede, pers. comm.).

7.4 Pedotransfer Functions

Under certain circumstances (cf. p. 37) the Freundlich coefficient *k* had to be estimated from the soil properties *p*H and *OC* content by means of a *PTF*. With *PTF 1a* and *PTF 1b*, k^* is constant in space while *PTF 2a* and *PTF 2b* contain the spatially variable coefficient k^*_{xy}. With *PTF 1b* and *PTF 2b*, the regression line was forced through the origin, i.e. the intercept was set to zero. The parameters of the *PTFs* were estimated by using the 616 complete data sets (cf. p. 63).

Table 6: Parameters of different pedotransfer functions (PTF). The parameters were estimated from extended Freundlich equations by multiple regression (N=616).

PTF 1a/1b: $\log S = \log k^* + b \log OC - a \log (H^+) + m \log C$

PTF 2a/2b: $\log S = \log k^* + \sum_{i=1}^{161} \zeta_i Z_i + b \log OC - a \log (H^+) + m \log C$

	Parameters of the *PTF* ‡					
PTF	***a***	***b***	***m***	k^*	k^*_{xy} †	***EF***
	———	———	———	$\mu g^{1-m} L^m kg^{-1}$	$\mu g^{1-m} L^m kg^{-1}$	—%—
1a	0.558 (0.024)	0.740 (0.017)	0.821 (0.025)	0.130	-	87
1b	0.404 (0.003)	0.772 (0.016)	0.746 (0.023)	1	-	86
2a	0.544 (0.021)	0.764 (0.014)	0.796 (0.014)	0.159	1.14 (0.86)#	94
2b	0.409 (0.002)	0.779 (0.013)	0.75 (0.019)	1	0.21 (0.14)#	93

‡ Estimate (± standard error)

† $k^*_{xy,i} = 10^{(\log k^* + \xi_i)}$

In *PTF 2a* and *PTF 2b* the estimated ζ_i were significantly different from zero (α=0.05) only for 37 and 39 soil monoliths, respectively. The mean and the standard deviation of k^*_{xy} was only calculated from these soil monoliths.

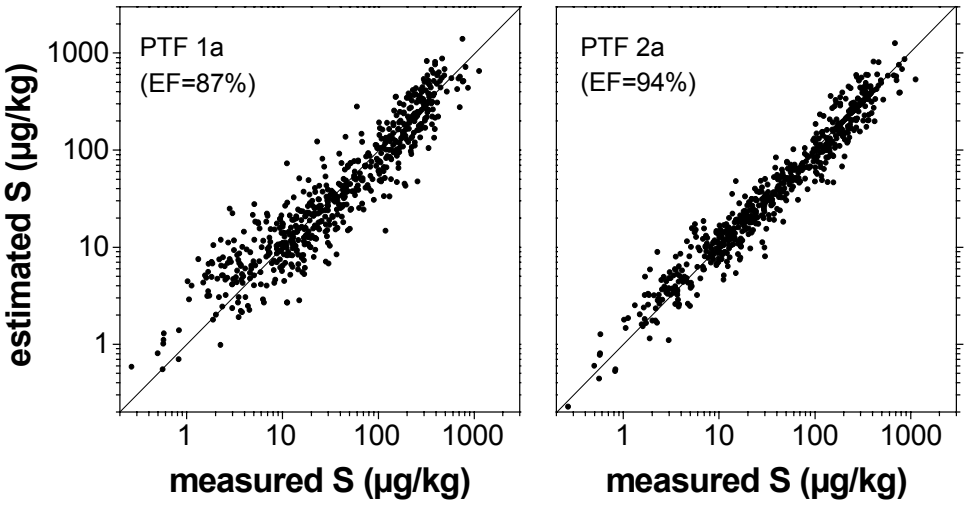

Figure 25: Scatterplot of estimated versus measured sorbed phase concentrations. Estimated concentrations were calculated with constant coefficient k^* (PTF 1a, Equation (34)) or with spatially variable coefficient k^*_{xy} (PTF 2a, Equation (36)).

The estimates of the sorption parameters of the different *PTFs* estimated are given in Table 6. In contrast to the work by Streck (1993) the intercept of *PTF 1a* was significantly different from zero at α=0.05. However, with a non zero intercept a stochastic collinearity was determined between the intercept and the *p*H coefficient *a*. In *PTF 2a* and *PTF 2b* only 37 and 39 of the estimated ζ_i, respectively, were significantly different from zero (α=0.05). The parameters *a* and *b* of *PTF 1b* and *PTF 2b*, which describe the effect of *p*H and *OC*, are similar to the parameters estimated by Streck (1993) (e.g. *PTF 1b* versus Model I by Streck (1993); *a:* 0.40 versus 0.38 and *b:* 0.77 versus 0.71). In both *PTFs*, however, the Freundlich exponent was distinctly smaller than the Freundlich exponent given by Streck (1993) who found a value of 0.85 for *m*. Thus, the sorption isotherm estimated in this study is more curved than that estimated by Streck (1993). The use of a non-zero intercept affected both the parameter *a* and the Freundlich exponent *m*. The parameter *b* was left unchanged. When k^* was allowed to vary horizontally the parameters *a*, *b* and *m* were not significantly different from those with a constant k^*. However, the

modelling efficiencies *EF* (Chapter 5.4) were distinctly improved and were for *PTF 2a* and *PTF 2b* 94% and 93%, respectively. Figure 25 shows two scatterplots of measured sorbed phase concentrations and those estimated by using *PTF 1a* and *PTF 2a.* The figure illustrates that the *PTFs* derived allow an acceptable estimation of sorbed phase concentrations.

In general, pedotransfer functions are not directly transferable to other soils or investigations. For example, Springob and Böttcher (1998b) determined a pedotransfer function for the sandy soils of the „Fuhrberger Feld“ catchment and compared their *k* coefficients estimated with those derived from other models found in the literature. They observed a high deviation between these different pedotransfer functions and suspected that this is probably due to differences in ionic strength and composition of background electrolytes used for generating sorption data. Elzinga et al. (1999) evaluated batch sorption data from the literature as well, but they took into account differences in experimental setups for obtaining sorption data and established general purpose Freundlich isotherms for Cd, Cu and Zn in soils. Freundlich equations were derived based on both total dissolved metal concentration and free metal activities in solution. They found that a comparison of different isotherms based on the free metal activity is expected to be most generally applicable. If we express our results in terms of the free Cd^{2+} activity, the resulting *k* coefficients would be, in a first approximation, about 52% of our *k* coefficients estimated (for details of calculation see: Boekhold et al., 1993).

7.5 Cd Plant Uptake

The following three subchapters on the uptake of Cd by winter wheat, sugar beet and potato have the same structure. In the first section the empirical results of the field observations are presented, and in the second section the plant uptake

model is applied to the data. The model testing was carried out in two steps. First, a model with an independent set of parameters measured or taken from the literature was applied to predict the field observations. Second, when model output was unsatisfactory the model was calibrated by modifying either η or k_P (cf. Equation (74)). It was further tested if model performance could be improved by taking into account the influence of soil *p*H or Zn concentration. The competitive effect of H^+ and Zn^{++} on the uptake of Cd was considered by modifying Equation (73) to

$$\overline{C} = \eta \frac{\Delta e}{\rho_w k_P} (1 - \exp(-\omega \Delta z)) \sum_{i=0}^{n} \frac{V_X C_i}{1 - K_X \log X} \exp(-\omega i \Delta z) \qquad (82)$$

whereby X denotes either the Zn^{++} concentration (mol L^{-1}) or the H^+ activity (1). K_X (L mol^{-1} or 1) and V_X (1) are empirical parameters.

7.5.1. Winter Wheat

Altogether 20 winter wheat sites were sampled. One site (wz*1*) was situated within the former storage basin of District 1. The Cd content of grain and straw was unusually high with 2.735 and 10.063 mg kg^{-1}, respectively. This finding can be traced to the special input history of this location (cf. p. 25). The site *wz1* was excluded from the analysis and the following results are based on the remaining 19 sites.

In 1999, the mean Cd content of winter wheat grain was 0.178 mg kg^{-1} (Table 7). At four sites the Cd content of grain exceeded the limit[11] of 0.24 mg kg^{-1}. These contents agree rather well with data of the *BMWA*. For the period from 1995 to 1998 the *BMWA* observed an average Cd content of winter wheat grain of 0.194 mg kg^{-1}. The Cd content of straw was about twice as high as the Cd

[11] Here defined as twice the German food guideline value of wheat grain (0.12 mg kg^{-1}).

content of grain (Q_{HM}=2.1). Q_{HM} varied between plants and ranged between 1.1 and 4.0. Similar relations between the Cd content of straw and grain have been observed by Lübben (1993, Tab. 56c). The mean dry matter production amounted to 1.615 kg m^{-2}, whereby the dry mass production of straw and grain was similar (Q_Y=0.98).

Table 7: Results of the Cd analysis and dry matter measurements for winter wheat in 1999 (N=19).

	Cd content			**Dry matter**			
	Grain	Straw	Plant	Straw	Grain	Q_{HM}[§]	Q_Y[&]
	mg kg^{-1}			kg m^{-2}			
Mean	0.178	0.376	0.275	0.799	0.816	2.10	0.98
SD	0.094	0.252	0.162	0.178	0.123	0.77	0.15
CV (%)	52.7	67.0	59.0	22.2	15.1	36.8	14.9
Minimum	0.063	0.123	0.09	0.569	0.576	1.10	0.80
Maximum	0.478	1.171	0.79	1.175	1.027	4.02	1.24

[§] Q_{HM} denotes the Cd content ratio between unprocessed (e.g. straw) and processed (e.g. grain) plant parts.
[&] Q_Y denotes the dry matter yield ratio between unprocessed (e.g. straw) and processed (e.g. grain) plant parts.

In both years, a significant linear relationship was observed between the Cd concentration in soil solution and Cd content of grain (R^2=0.84*** in 1998 and R^2=0.70*** in 1999) (Figure 26). According to the model the uptake of Cd should be proportional to the amount of transpired water or the saturation deficit. This means the slope of the regression line should depend on the saturation deficit. The higher the saturation deficit the steeper the regression line. In 1999, the saturation deficit was 33% higher than in 1998 (785 Pa versus 591 Pa). And indeed, in accordance with the plant uptake model, in the year with higher saturation deficit the slope of the regression was 40% higher than in the year with the lower saturation deficit (0.115 ± 0.080 m^3 kg^{-1} versus 0.082 ± 0.039 m^3 kg^{-1}).

However, the difference between both regression slopes was statistically not significant (*t*-test, α=0.05).

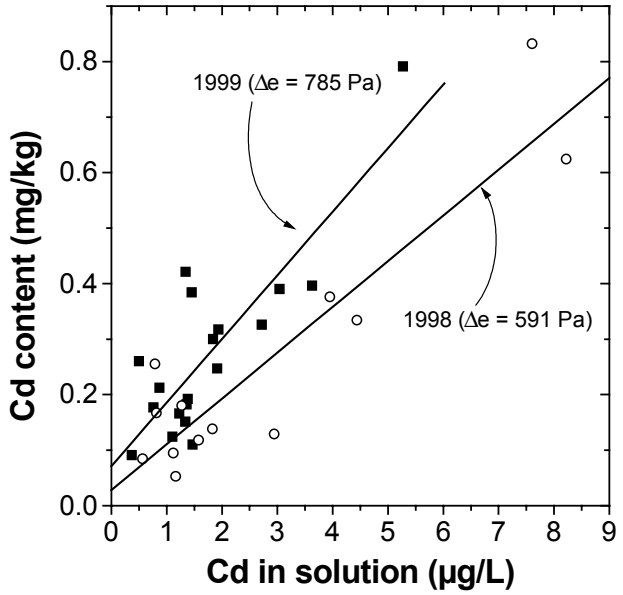

Figure 26: Relationship between Cd concentration in soil solution and Cd content in winter wheat grain in 1998 and 1999.

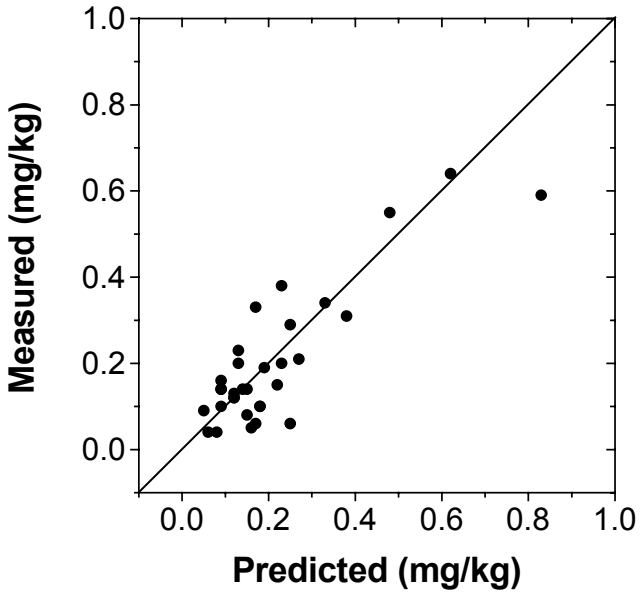

Figure 27: Measured versus predicted Cd contents of winter wheat grain. For the prediction parameters were either measured or taken from the literature. No parameter was fitted.

In 1999, the Cd output by winter wheat harvest amounted to 1.0 g ha^{-1} yr^{-1}. The calculation assumes a grain dry matter yield of 5.8 t ha^{-1} (6.5 t ha^{-1} grain fresh

yield with a water content of 11% by mass) and that the straw remains on the field.

Figure 27 shows the scatterplot of measured versus predicted Cd contents of winter wheat grain. The prediction is fully based on parameters measured or taken from the literature. In view of the fact that no parameters were fitted, the agreement between measured and predicted values is remarkably good (*EF*=68%). The model overestimated the observed Cd contents by 12% on average. By fitting η to the data the *EF* could slightly be increased to 71% , but at the 5% significance level the fitted value (η=0.94 ± 0.06) was not different from unity. The influence of Zn and *p*H competition on Cd plant uptake was tested by fitting of K_X and V_X to the data (Equation (82)). None of the fitted K_X values were significantly different from zero at α=0.05. Thus, competitive effects were negligible under the conditions investigated (*p*H: 4.6-6.6; Zn: 6-344 µg L^{-1}; Cd: 0.5-8.2 µg L^{-1}).

As mentioned above the site *wz1* was excluded from model testing. At this site, the Cd and Zn concentrations in soil solution were 72 µg L^{-1} and 1,987 µg L^{-1}, respectively. The model overestimated the Cd content of wheat by a factor of two (12.18 mg kg^{-1} versus 6.57 mg kg^{-1}). This observation might be an indication that at high concentrations ion competition becomes important.

7.5.2. Sugar Beet

From 1998 to 1999 the mean Cd content of sugar beet hypocotyl was 0.238 mg kg^{-1} (Table 8). This is about half of the forage guideline value for sugar beet (0.5 mg kg^{-1}). At two sites this value was exceeded. The Cd content of hypocotyls was roughly four times lower than the Cd content of leaves (Q_{HM}=4.23). The total dry matter production per plant was 0.382 kg m^{-2} on average, whereby the hypocotyl contributed the major part of dry matter.

Table 8: Results of the Cd analysis and dry matter measurements of sugar beet in 1998 and 1999 (N=40).

	Cd content			**Dry matter per plant**			
	Leaf	Hypocotyl	Plant	Leaf	Hypocotyl	Q_{HM}[§]	Q_Y[$]
	——— mg kg^{-1} ———			——— kg ———		——	——
Mean	0.955	0.238	0.428	102.0	280.3	4.23	0.37
SD	0.663	0.130	0.274	68.2	110.5	1.97	0.16
CV (%)	69.4	54.6	64.0	66.9	39.2	46.6	43.3
Minimum	0.326	0.069	0.148	28.0	101.2	1.46	0.18
Maximum	3.736	0.665	1.591	473.2	560.1	13.16	1.1

[§] Q_{HM} denotes the Cd content ratio between unprocessed (e.g. leaves) and processed (e.g. hypocotyl) plant parts.
[$] Q_Y denotes the dry matter yield ratio between unprocessed (e.g. leaves) and processed (e.g. hypocotyl) plant parts.

Here again, a significant linear relationship was found between Cd concentration in soil solution and Cd content of plant (1998: $R^2=0.84^{***}$; 1999: $R^2=0.65^{***}$) (Figure 28). In 1999, the average saturation deficit during the main vegetation period was 46% higher than in 1998 (898 Pa versus 614 Pa). Similar to winter wheat, the higher saturation deficit yielded a higher slope of regression (0.146 ± 0.113 m^3 kg^{-1} versus 0.086 ± 0.040 m^3 kg^{-1}). Moreover, the two regression slopes were statistically different at α=0.05 (*t*-test). But indeed, it must be stated that the one extreme value in 1998 distinctly affects the result of the *t*-test.

Between 1998 and 1999, the Cd output via sugar beet harvest amounted to 2.4 g ha^{-1} yr^{-1} on average, presumed that the dry matter yield of hypocotyl is 99 dt ha^{-1} (450 dt ha^{-1} fresh matter with a water content 78% by mass) and that the leaves remain on the field.

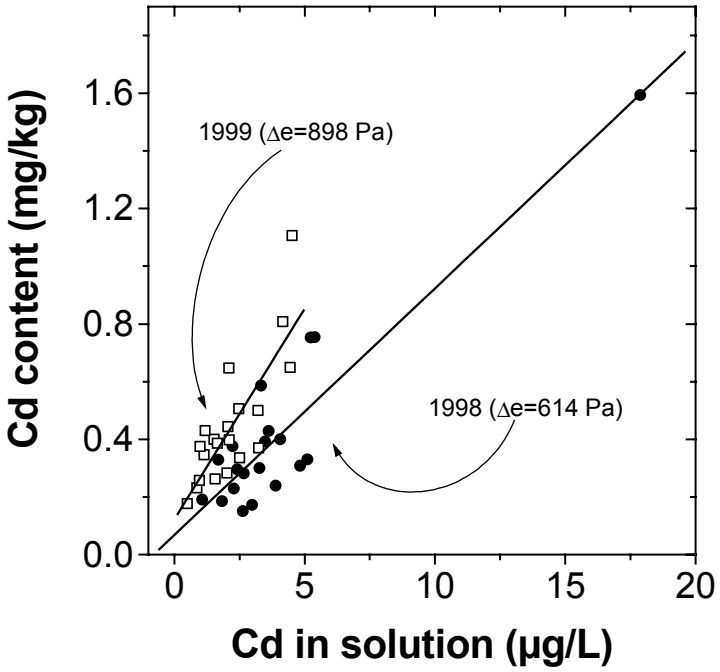

Figure 28: Relationship between Cd concentration in soil solution and Cd contents in sugar beet plants in 1998 and 1999.

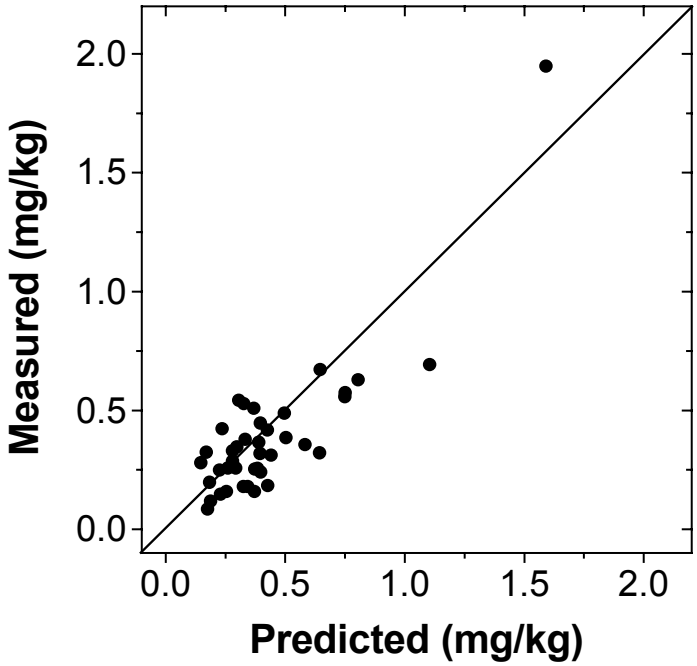

Figure 29: Measured versus predicted Cd contents in sugar beet plants. Only the k_P was fitted. Other parameters were measured or taken from the literature.

In the literature, no unambiguous value could be found for the k_P of sugar beet. Roth et al. (1988), for example, report similar evapotranspiration coefficients[12] of sugar beet (188 L kg^{-1}) and potato (185 L kg^{-1}). However, since the investigations were carried out in different years and the average saturation deficit during the main vegetation period was not documented, it is not clear if the k_P of sugar beet and potato are indeed similar. In the present study k_P was therefore estimated from the field observations, with the result of 5.5 ± 0.3 Pa. The scatterplot of measured versus predicted Cd contents of sugar beet plants (Figure 29) shows acceptable spreading around the bisector (*EF*=66%). Note, however, that it is not possible to estimate both k_P and η simultaneously. An identical *EF* could be achieved by fixing k_P to some other value and fitting η. Thus, the fitted k_P should be interpreted with caution. As already mentioned the high Cd content of about 1.5 mg kg^{-1} strongly affects the result. When this value was ignored the fitted k_P was 4.9 ± 0.3 Pa and the *EF* decreased to 48%. Extending the model to account for competition by soil *p*H and Zn did not improve the model output. Hence, competitive effects appeared to be minor under the experimental conditions of this study (*p*H: 4.6-6.8, Zn: 32-347 µg L^{-1}; Cd 0.5-17.9 µg L^{-1}).

7.5.3. Potato

In 1998, the mean Cd content of potato tuber was 0.127 mg kg^{-1} (Table 9). At none of the sites did the Cd content of tuber exceed the limit[13] of 0.24 mg kg^{-1}. In 1999, the results concerning potato tuber differed very much from those of the previous year. In 1999, the mean Cd content of potato tuber was 0.266 mg kg^{-1} (Table 10), and thus roughly twice as high as in 1998. At 8 sites the Cd

[12] Since data on evapotranspiration are in general more readily available than data on transpiration many studies operate with the evapotranspiration coefficient instead of the transpiration coefficient.

[13] Here defined as twice the German food guideline value for potato (0.12 mg kg^{-1}).

content of tuber exceeded the limit. In contrast to those of tuber and peel, the Cd contents of potato straw measured in 1998 did not differ significantly from those measured in 1999 (*t*-test, α=0.05).

Table 9: Results of the Cd analysis and dry matter measurements of potatoes in 1998 (N=20).

	Cd content					**Dry matter per plant**		
	Tuber	Peel	Tuber + Peel	Straw	Plant	Tuber +Peel	Straw	Plant
	mg kg^{-1}					kg		
Mean	0.127	0.233	0.142	2.939	0.354	0.386	0.037	0.422
SD	0.045	0.097	0.052	1.163	0.141	0.145	0.018	0.145
CV (%)	35.2	41.6	36.7	39.6	39.9	37.5	47.7	37.5
Minimum	0.06	0.083	0.067	1.409	0.183	0.098	0.014	0.115
Maximum	0.214	0.416	0.243	5.122	0.635	0.706	0.073	0.78

Table 10: Results of the Cd analysis and dry matter measurements of potatoes in 1999 (N=20).

	Cd content					**Dry matter per plant**		
	Tuber	Peel	Tuber + Peel	Straw	Plant	Tuber +Peel	Straw	Plant
	mg kg^{-1}					kg		
Mean	0.266	0.479	0.291	2.778	0.588	0.371	0.051	0.422
SD	0.134	0.267	0.150	1.727	0.318	0.133	0.019	0.147
CV (%)	50.4	55.8	51.4	62.2	54.1	35.9	38.0	34.9
Minimum	0.082	0.139	0.087	0.671	0.173	0.181	0.025	0.205
Maximum	0.592	1.232	0.663	7.239	1.435	0.751	0.090	0.828

In both years the Cd content of peel was about two times higher than the Cd content of tuber. The highest Cd contents were found in the potato straw which

was between ten and twenty times higher than the calculated Cd content of tuber plus peel. Comparable results have been observed by Weigel (1991, p.47).

The dry matter production was nearly identical in both years. On average, the dry matter production amounted to 0.422 kg per plant, whereby the dry matter production of the straw was less than 10% of total dry matter production.

In both years, a significant linear relationship was found between Cd concentrations in soil solution and Cd contents of potato (1998: $R^2=0.49^{***}$; 1999: $R^2=0.67^{***}$) (Figure 30). In 1999, the slope of the linear regression model was 118% higher than in 1998 (0.181 ± 0.134 m^3 kg^{-1} versus 0.083 ± 0.090 m^3 kg^{-1}). This difference, which is statistically significant at $\alpha=0.05$, may partly be due to the higher saturation deficit in 1999, which was 33% higher than in 1998 (917 Pa in 1999 versus 692 Pa in 1998). However, additional factors seem to have affected the Cd uptake. For quality control of the chemical analysis, measurements in 1999 were checked against those of 1998 and were seen to be in good agreement (cf. p. 36). Therefore, an error in measurements can be ruled out. Grouping the entire data set into three clusters by eye (in the following *Alpha, Beta* and *Gamma*) reveals that two clusters (*Alpha* and *Beta*) are grouped around the two regression lines while the third cluster (*Gamma*) is located at 2 µg Cd L^{-1} above the regression line of 1999. A simple explanation would be that different types of potatoes with different uptake mechanism for Cd were investigated. However, whether these three clusters can indeed be attributed to different types of potatoes could not be clarified in this study.

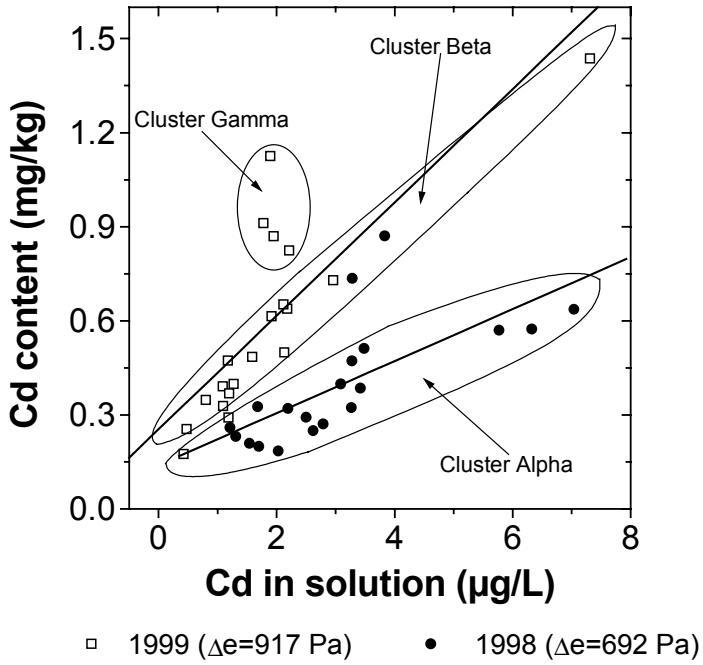

Figure 30: Relationship between Cd concentration in soil solution and Cd content of potato plants.

The Cd output by potato harvest amounted to 1.2 g ha^{-1} yr^{-1} in 1998 and to 2.4 g ha^{-1} yr^{-1} in 1999. The calculation assumes a dry matter yield (tuber plus peel) of 8,360 kg ha^{-1} yr^{-1} (38 t ha^{-1} fresh matter with a water content of 78% by mass) and that the potato straw remains on the field.

Figure 31 shows a scatterplot of measured versus predicted Cd contents of potato plants. For this prediction no parameter was fitted. In 1998, predicted values agreed fairly well with the measured data. In 1999, however, the agreement between measured and independently predicted Cd contents was unsatisfactory. The disagreement between model and measurement was particularly strong at the four sites surrounded by the black line. While predicted values were between 0.26 and 0.32 mg kg^{-1} measured values ranged from 0.82 to 1.12 mg kg^{-1}. At the remaining sixteen sites the model systematically underestimated measured data. Applying the assumption mentioned above, i.e. that different types of potatoes with different uptake mechanisms for Cd had been investigated, distinctly improved the model accuracy (*EF*=81%). For each of the clus-

ters *Alpha* and *Beta* a different value for η was fitted. η of *Alpha* and *Beta* was estimated as 0.98 ± 0.05 and 2.01 ± 0.08, respectively. The Cluster *Gamma* was not considered in the estimation.

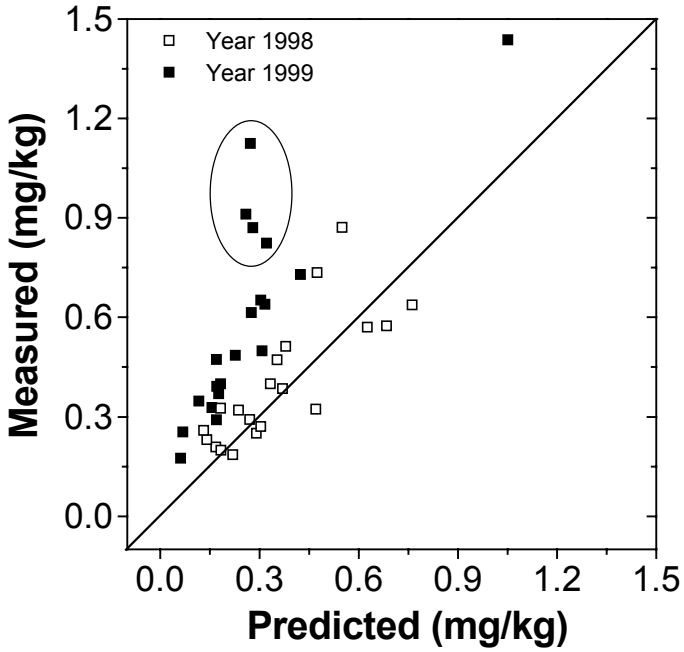

Figure 31: Measured versus predicted Cd contents of potato plants. Predictions are based on parameters either measured or taken from the literature.

Accounting for Zn competition did not improve the model output. The estimated K_{Zn} value was not significantly different from zero at α=0.05. In contrast, grouping the data in two clusters (*Alpha* and *Beta*) and extending the model to account for H^+ competition led to a considerable improvement of the prediction (*EF*=88%) with parameters estimated significantly different from zero at α=0.05 (Figure 32). K_{H+} of *Alpha* and *Beta* amounted to 0.128 ± 0.008 and 0.104 ± 0.020, respectively, and the V_{H+} values of *Alpha* and *Beta* were 0.300 ± 0.051 and 0.444 ± 0.111, respectively.

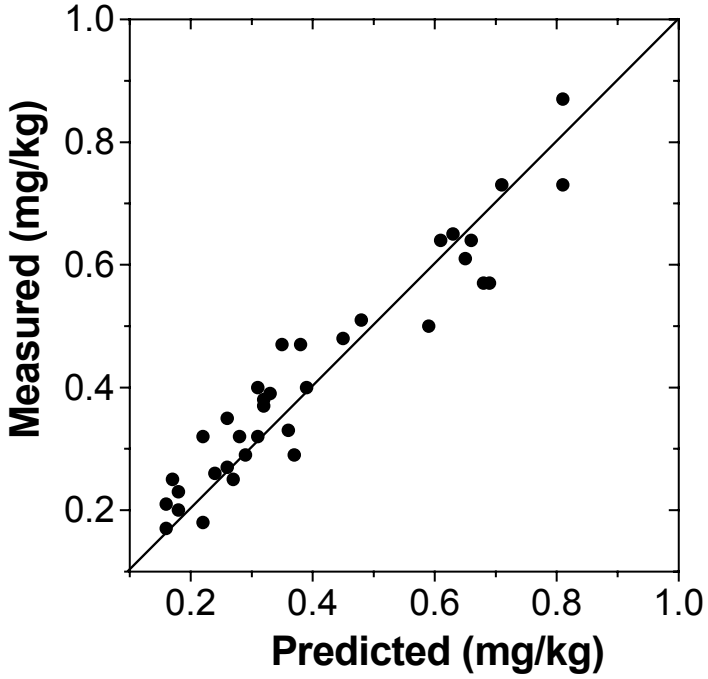

Figure 32: Measured versus predicted Cd contents of potato plants (EF=88%). Data were grouped in two clusters of potatoes with different accumulation behaviour and a competition with hydrogen ions was taken into account.

For Cluster *Alpha* Figure 33A depicts the competitive effect of hydrogen ions on the uptake of Cd in the *p*H range 5 to 7. Similar results were already presented by Hatch et al. (1988). For the calculation a constant Cd concentration of 3 µg L^{-1}, a k_P of 6.2 Pa and an average saturation deficit of the air of 736 Pa were used. Total uptake of Cd is lowest at *p*H 5 and increases by a factor of 3.5 as the soil *p*H increases to 7. The result suggests that the uptake of Cd by potato is markedly suppressed by soil acidification. However, this effect is masked by the increased solubility of Cd in soils with decreasing *p*H (Figure 33B). For the latter calculation a constant EDTA-extractable Cd content of 350 µg kg^{-1}, an *OC* content of 1% by mass, a volumetric water content of 16%, a bulk density of 1.51 kg L^{-1} and the pedotransfer function *PTF 1a* (Chapter 7.4) were applied. Despite the increased competition with hydrogen ions the uptake of Cd is highest at *p*H 5 and decreases by a factor of 6.6 as the soil *p*H increases to 7. Cd concentration in solution is 6 µg L^{-1} at *p*H 5 and decreases by a factor of 23 as soil *p*H increases to 7.

To sum up, the effect of soil *p*H on the bioavailability of Cd is ambiguous. On the one hand, solubility increases as soil *p*H decreases, on the other side, competitive inhibition increases with decreasing soil *p*H. In total, the effect of an increased solubility with decreasing *p*H distinctly prevails at the soils investigated.

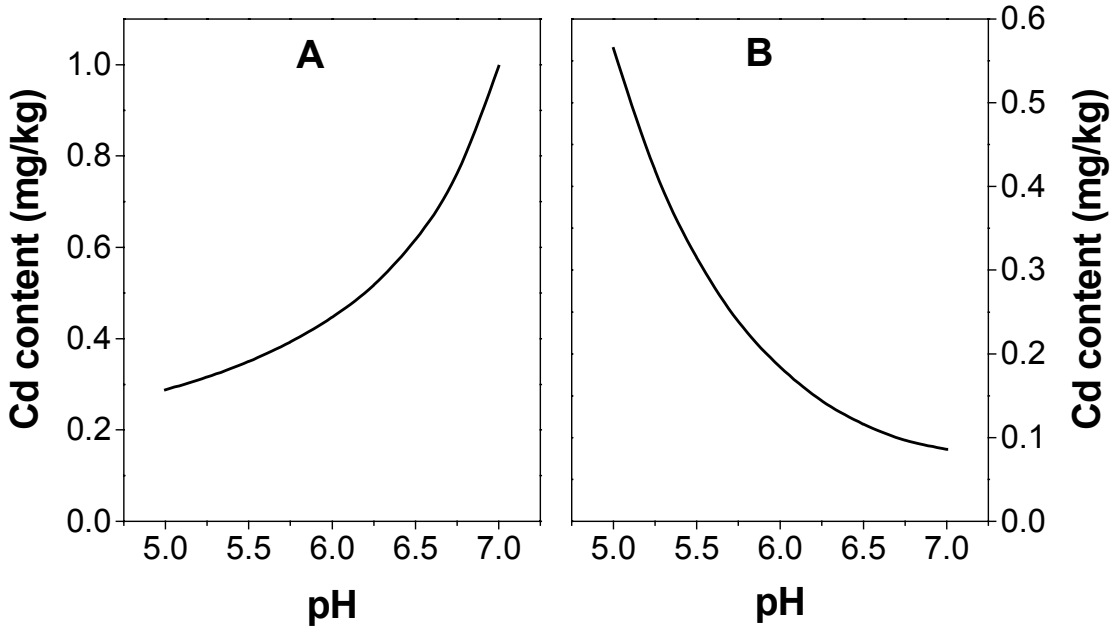

Figure 33: ***A)*** *Competitive effect of hydrogen ions on the uptake of Cd by potato. The Cd concentration was kept constant at 3 µg* L^{-1}. ***B)*** *Competitive effect of hydrogen ion plus increasing solubility of Cd with decreasing soil pH. For the latter calculation a constant EDTA-extractable Cd content of 350 µg* kg^{-1} *was used. For details see text.*

8 Environmental Fate Modelling

8.1 Overview

Basically, two types of modelling approaches are used to simulate the environmental fate of Cd at the regional scale: Deterministic soil column (*DSC*) models and random soil column (*RSC*) models. Both types are parallel soil column models and make use of the local scale model *SEFAH*. Regarding that the effect of local dispersion is very small, hence the solute transport is assumed to be approximately stochastic-convective at the regional scale (Chapter 3.1). However, both modelling approaches differ in the way they account for the spatial variability of model input variables. In the *DSC* modelling approaches the local model *SEFAH* is applied at points of the region where measurements of model input variables were available. An alternative designation for this kind of model is “grid model” as used, for instance, by Streck and Richter (1997b). The *RSC* modelling approaches are based on random input variables and are often shortly labelled Monte-Carlo simulations. Moving from the local scale to the regional scale (scaling) was done in both types by aggregation (Refsgaard and Butts, 1999). Aggregation means that the process equation are used at the scale where they were derived (the *CDE*, for instance, at the local scale) and the regional scale results are then obtained by calculating the spatial mean from the statistical distribution of the model outputs.

The following section is structured as follows: The first three subchapters give a detailed description of the modelling approaches applied. Chapter 8.4 presents the model parameterization. Validation of modelling approaches is described in Chapter 8.5. For validation hindcast simulations were used. It was tested whether the model is suited to reconstruct the present state of Cd in soil using an

independent (non-fitted) set of parameters and boundary and initial conditions. After validation the model is applied to compute several retrospective and prospective scenarios (Chapter 8.6). Finally, the simulation results are discussed in Chapter 8.7.

8.2 Deterministic Soil Column Models

Because in the *DSC* modelling approach the local model *SEFAH* is applied at points in the region where measurements had been carried out, the Freundlich coefficient k can be calculated from given data. If data on the Cd concentration in soil solution, the EDTA-extractable Cd content and the Freundlich exponent m are available the Freundlich coefficients can be determined by Equation (32). If these data were not available, for example, due to concentration below the detection limit, the Freundlich coefficient was estimated from *p*H and *OC* by means of a pedotransfer function (cf. Chapter 7.4). Measurements of these soil properties are available at all locations and all layers. Recall that each soil column consists of 10 layers (0-0.3 m, 0.3-0.4 m, ..., 1.1-1.2 m). The lower boundary of each column was taken from the map of depths water table (Figure 35).

DSC modelling approaches which exclusively use a pedotransfer function to estimate k are labelled as *DSC* plus the label of the *PTF* used. For example, if the Freundlich coefficients are estimated from *PTF 1a* the approach is labelled *DSC 1a*. If measured and estimated Freundlich coefficients were combined, the word *Hybrid* was added to the label.

8.3 Random Soil Column Models

RSC I

The *RSC I* modelling approach uses random model input variables. In accordance with the field observations, the model operates with lognormally distributed *OC* contents and Cd loads. For feasibility reasons the model presumes normally distributed *p*H values in all soil layers, though according to the *KS*-test *p*H values of layers below 0.3 m were not normally distributed at α=0.05 (cf. Chapter 7.3). The depth of water table of each soil column is randomly drawn from the empirical distributions presented in Chapter 8.4.2. Preliminary experiments had shown that at least 400 simulations are necessary to derive stable first and second moments of the model output. For simulation, a set of 500 random soil columns with *z*-correlated random numbers from a multivariate normal distribution was generated. The random numbers were produced with the help of an external computer program (StatGraphics Plus 7.0, Manugistics Inc., USA). The horizontal correlation is ignored for both soil properties and Cd loads, i.e. their horizontal variograms are not considered. The vector of means and the covariance matrix are estimated from the data set of Non-Rigosols within the *WIA* (N=139). The Freundlich coefficients are estimated by using the *PTF 1a* (Chapter 7.4). The analysis of the simulation result is confined to the first and second moments of the model output (Profiles of *C* and *S*, Cd concentration in seepage water, Cd contents of sugar beet, potato and wheat). Note that the model output is not georeferenced.

RSC II

This approach is different from *RSC I* in that the four districts of the *WIA* are considered separately. Thus, the different Cd input histories as well as the different soil properties within each district are taken into account. For each district, the vector of means and the covariance matrix is estimated separately. 500

simulations were run for each district. Again, analysis of the simulation results is confined to the first and second moment of the model output.

RSC III

Both *RSC I* and *RSC II* approaches ignore the horizontal correlation of model input variables. However, as shown in Chapter 7, soil properties as well as Cd loads were found to be horizontally correlated. The *RSC III* modelling approach incorporates the spatial correlation of model input variables in all three dimensions. Therefore, *RSC III* combines the parallel soil column approach and the geostatistical method of "Conditional Simulation" (Chapter 3.3.2). The random input variables are generated as follows:

(1) A pool of 1D random soil columns (N=4,000) with multivariate normally distributed *p*H and multivariate lognormally distributed *OC* content is generated using the vector of means and covariance matrix as estimated from the measurements. Each soil column consists of 10 layers (0-0.3 m, 0.3-0.4 m, ..., 1.1-1.2 m).

(2) Variogram models of *p*H and *OC* content are fitted to experimental variograms at layers with largest spatial correlation length (*p*H: Layer 8 (0.9 to 1.0 m); *OC* content: Layer 1 (0 to 0.3 m) (Chapter 7.3). Moreover, a model is fitted to the experimental variogram of the Cd load (Chapter 7.1). The results are three independent 2D correlated random fields.

(3) 500 (x,y)-points are randomly drawn within the arable area of the *WIA*. At each point the depth of water table is set to its value according to the map of depths of water table.

(4) A Cd load, a *p*H value in Layer 8 and an *OC* content at Layer 1 are computed at each (x,y)-point by the method of conditional simulation. By that,

three two-dimensional random fields of horizontally correlated *p*H, *OC* contents and Cd loads are generated.

(5) Finally, soil columns which were generated in (1) are randomly joined to the two-dimensional fields. A matching soil column has to show within defined tolerances a similar *p*H and a similar *OC* content as the corresponding two-dimensional random field (*p*H: ± 0.05 *p*H; *OC* content: ± 5% difference between both values).

Note, since the 1D random soil columns and the 2D random fields are generated separately the ensemble of soil column produced is not truly but pseudo 3D correlated. In addition, each generated random field is only one possible realization of the region. Preliminary experiments had shown that at least 12 simulations are necessary to obtain a stable first moment of the averaged model output.

8.4 Model Parameterization

This subchapter gives a detailed summary of the parameters and variables used within the model *SEFAH*. The structure is similar to that of the Chapter 6. The first section deals with the water regime, the second with Cd displacement and the third with plant uptake of Cd. Model parameterization is based on external data, literature data and results of the present study.

8.4.1. Water Regime

According to data by the weather station Braunschweig-Völkenrode, in the period from 1957 to 1996 the average precipitation was 626 mm yr^{-1}. The irrigation rate varied over time. Until 1974 it amounted to 367 mm yr^{-1}, from 1975 to 1979 to 424 mm yr^{-1} and from 1980 to 1996 to 536 mm yr^{-1} (Streck, 1993).

Due to the high irrigation rates it can be assumed that optimal evaporation conditions exists all year round and that therefore the evapotranspiration *ET* can be approximated by the potential evapotranspiration *pET*. The annual *pET* of winter wheat and sugar beet was calculated according to Haude (1955) using the β-factors of Heger (1978) (Chapter 5.5). The *pET* of potato was taken from data of Dommermuth and Trampf (1990). From 1957 to 1996, the average *pET* was 539 mm yr^{-1} for winter wheat, 688 mm yr^{-1} for sugar beet and 536 mm yr^{-1} for potato.

The mean saturation deficit during the main vegetation period (Δe) was obtained by averaging hourly values (Chapter 5.5) for the period between 6:30 a.m. and 8:30 p.m. period during the main vegetation period (Ehlers, 1989). For winter wheat, Δe was taken as the average value between April 1st and July 31st, for sugar beet between April 15th and September 30th and for potato between April 15th and August 15th. From 1957 to 1996, the average value was 659 Pa for winter wheat, 692 Pa for sugar beet and 732 Pa for potato.

For potato and winter wheat k_P were taken from a study by Ehlers (1996), who gives for winter wheat a k_P of 4.0 Pa and for potato of 6.2 Pa. For sugar beet, no value for k_P could be found in the literature. Therefore, k_P had to be fitted and was estimated as 5.5 Pa (Chapter 7.5.2).

Historical crop yields from 1957 to 1996 in the *WIA* were reconstructed after Fischbeck (1993), who calculated average annual growth rates of several crop yields for West Germany from 1955 to 1990. According to this author, winter wheat yields increased annually by 1.08 dt ha^{-1}, potato yields by 3.8 dt ha^{-1} and sugar beet yields by 5.2 dt ha^{-1}. According to the *BMWA*, in 1996 the average yield of winter wheat was 62.5 dt ha^{-1}, that of sugar beet to 450 dt ha^{-1} and that of potato to 380 dt ha^{-1}. A retrospective calculation resulted for 1957 in a winter

wheat yield of 20.4 dt ha^{-1}, a sugar beet yield of 247 dt ha^{-1} and a potato yield of 232 dt ha^{-1}.

The empirical parameter ω, which describes the root distribution with depth (cf. Equation (45)), was calculated from the fraction of plant roots within the Ap horizon, $R(z_{Ap})$,

$$\omega = -\frac{\ln\left(1 - R(z_{Ap})\right)}{z_{Ap}} \tag{83}$$

where z_{Ap} stands for the thickness of Ap horizon (m). $R(z_{Ap})$ is generally available from literature data. In sandy soils $R(z_{Ap})$ was found to be 0.79 for winter wheat (Meuser et al., 1985), 0.93 for sugar beet (Kücke and Löffler, 1989) and 0.97 for potato (Schmidtke et al., 1999). These values correspond to a ω of 5.202 m^{-1} for winter wheat, of 8.864 m^{-1} for sugar beet and of 11.689 m^{-1} for potato.

Because heavy metal leaching is extremely insensitive to errors in the volumetric water content (Chapter 3.1), all simulations were run with a constant content of 16%, which corresponds to the average field capacity of sandy soils in Northern Germany (Zingk and Blume, 1987).

With regard to asparagus the data base for model parameterization was poor. Neither own measurements were carried out nor suitable data were found in literature. Therefore, parameterization could only be done with rough estimates. According to interviews with employees of the *BMWA* the average irrigation height at asparagus sites is about 100 mm yr^{-1}. The potential evapotranspiration was calculated according to Haude (1955) and was found to be 532 mm yr^{-1}. By rule of thumb, the annual transpiration was assumed as 125 mm. The fraction of roots within the first 0.3 m of the *R* horizon was estimated to be 80%. Moreover, it was assumed that the asparagus rhizome is planted 0.2 m below the soil sur-

face. The potential area of asparagus cultivations within the *WIA* was estimated as 15% (Chapter 7.2). Each site was assumed to be cropped with asparagus for 10 years followed by 20 years of recovery when it is cropped with wheat, sugar beet and potato. After the recovery phase the crop rotation starts again with a 10 year period of asparagus cropping.

8.4.2. Depth of Water Table

According to Bramm (1976) two aquifers are present within the *WIA*. The shallow aquifer is unconfined and its thickness is about 13 m. Below 15 m a nonpermeable clay layer of about 3 m thickness follows. The second aquifer reaches from roughly 18 to 33 m depth. The present study deals only with the shallow aquifer.

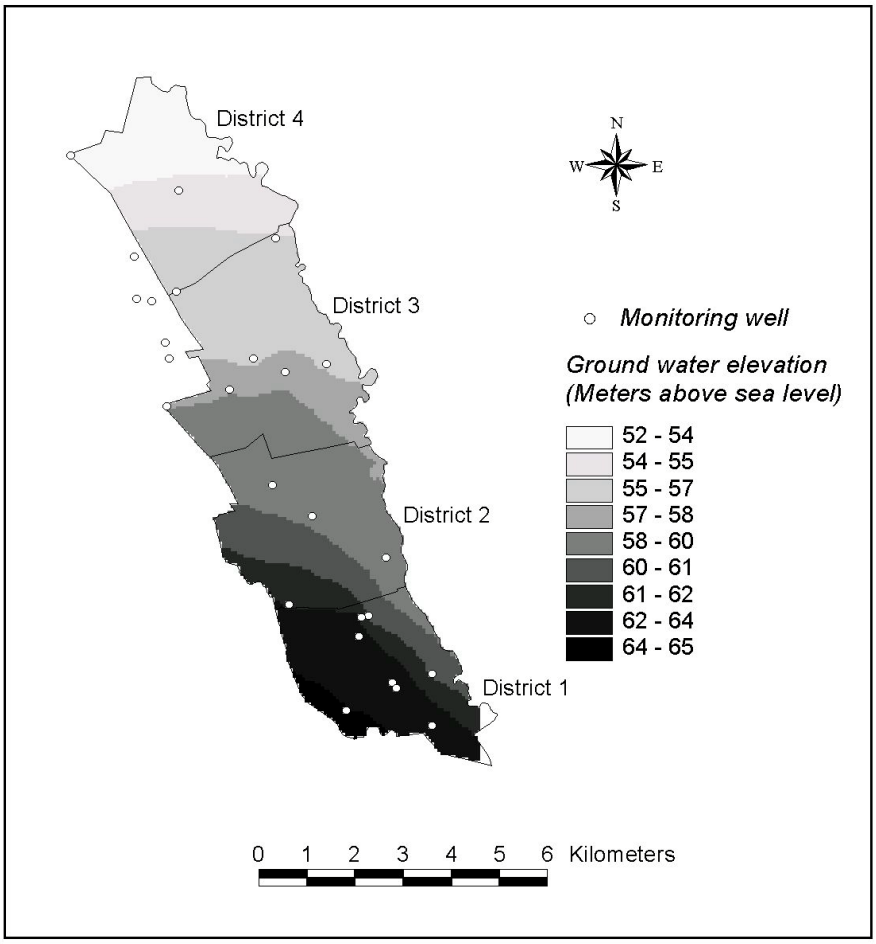

Figure 34: Map of ground water elevation.

On the basis of *BMWA* data a ground water elevation map was computed (Chapter 5.6). The ground water elevation drops gradually from south to north from 64.5 m to 52.5 m above sea level (Figure 34). Towards the north the direction of ground water flow gradually changes. In the south the ground water flows from southwest to northeast and in the north from south to north. Within the Districts 1 and 2 the direction of ground water flow appears to be affected by the river Oker. Within these two districts the hydraulic gradient is larger than in the northern districts. The effect of the river Erse on ground water flow seems to be negligible.

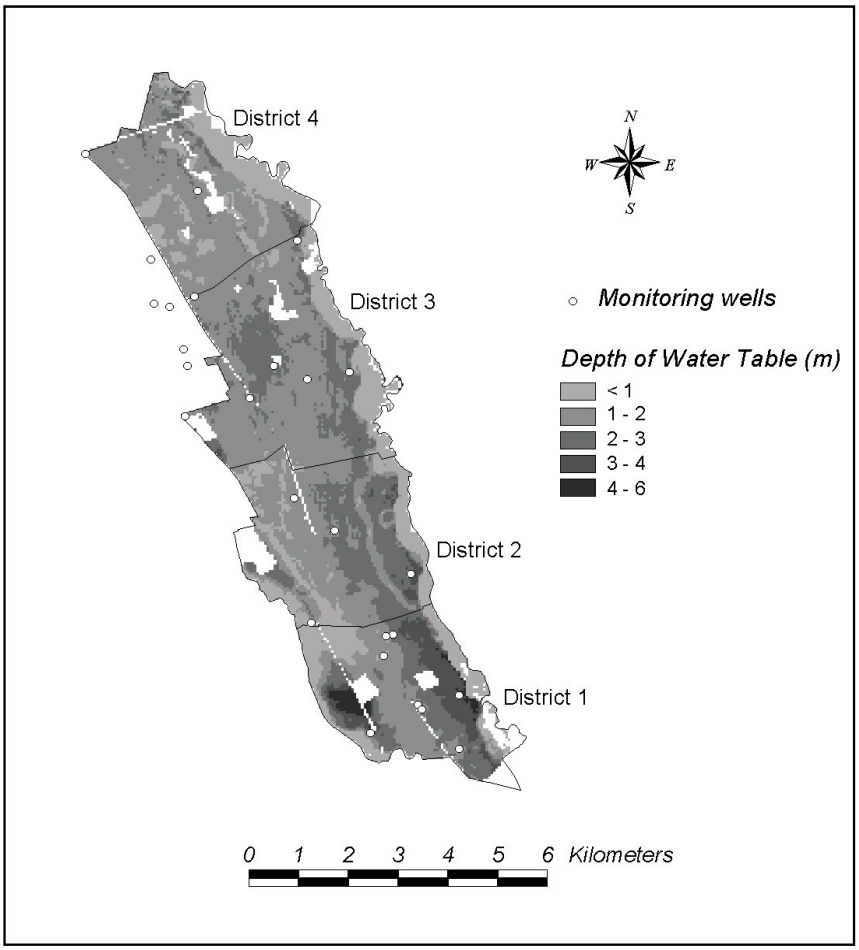

Figure 35: Map of the depths of water table.

Figure 35 depicts the depth of water table within the *WIA*. It decreases from south to north. Depths larger than 2 m are predominantly located in the eastern part except for small areas in the southwest, near Harvesse village, and in the

centre of District 3. Areas with low depths of water table (< 1 m) are located in the western parts of Districts 1, 2 and 4. In general, these sites are drained (about 340 ha). Within the *WIA* the depth of water table is 1.8 m on average, with a *CV* of 40%. Figure 36 gives for each district a histogram of water table depths.

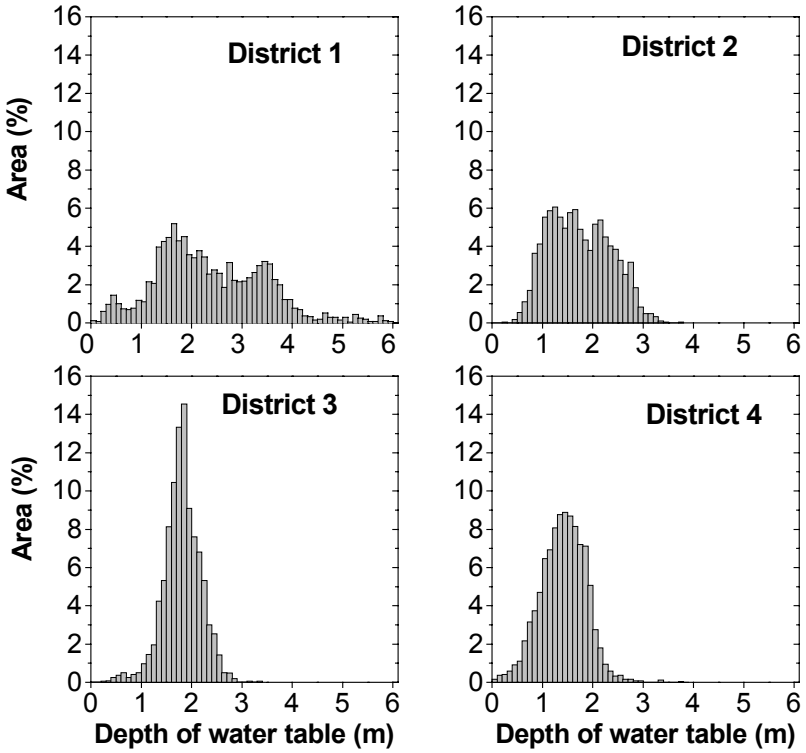

Figure 36: Histograms of the depths of water table for the four districts

Interpolations were validated using data by Dückel (1985). In February, March and April 1985, the author had recorded the ground water elevation of 46 monitoring wells, which include the 26 monitoring wells mentioned in Chapter 5.6. For the three months the depth of the water table was interpolated based on the data of the 26 wells. The ground water elevations of the remaining 20 monitoring wells were used for evaluating the goodness of interpolation. The average absolute difference between interpolated and measured depth of water table is 0.34 m, which is 19% of the regionally averaged depth of water table. The relative error is on average 23%.

8.4.3. Displacement

The parameters of *PTFs* applied were already given in Chapter 7.4. The Equation (51) for the apparent dispersion coefficient D_S ($m^2\ s^{-1}$) was parameterized as by Streck (1993) (b_D = 10; a_D = 0.006; D_0 = 0.0926 $m^2\ s^{-1}$; λ = 0.01 m). Mean bulk densities were set to 1.51 kg L^{-1} for the Ap and to 1.67 kg L^{-1} for the subsoil horizons. These values are based on investigations of the Soil Survey of Lower Saxony in the investigation area (Gehrt and Schäfer, pers. comm.).

The initial condition was set to the average Cd concentration of the 1.1-1.2 m layers of District 4 which was estimated as 0.1 µg L^{-1} (Chapter 7.2). In the hindcast simulations, each soil column received its Cd load exclusively by waste water irrigation, that is, Cd in the precipitation was ignored. For the period between 1957 and 1979 Cd concentrations in waste water were reconstructed from measured soil data (Chapter 7.1). For the period from 1980 to 1996 measured values could be used (Figure 5). In case of forecast simulations, Cd concentration in precipitation was calculated from data by Dämmgen et al. (1995) who measured at a location 5 km south of the *WIA* a bulk Cd deposition of 0.9 g $ha^{-1}\ yr^{-1}$.

For the *DSC* modelling approaches the lower boundary condition was directly taken from the interpolated map given in Figure 35. For the *RSC* approaches the depth of water table was randomly drawn according to the empirical distributions given in Chapter 8.4.2. When the depth of water table was below the sampling depth, the sorption characteristics of the unsampled soil zone were approximated by that of the deepest sampled layer.

From the late 1960s to the early 1980s, in soils of Lower Saxony the depth of ploughing had increased from 0.25 m to 0.35 m (Nieder et al., 1993). Since the early 1980s the depth of ploughing has been kept more or less constant. Based

on these data the deepening of tillage from 1967 to 1984 was interpolated as given in Figure 37. Because in 1996 the thickness of the Ap horizons sampled was on average 0.3 m the ploughing starts with an estimated thickness of 0.2 m.

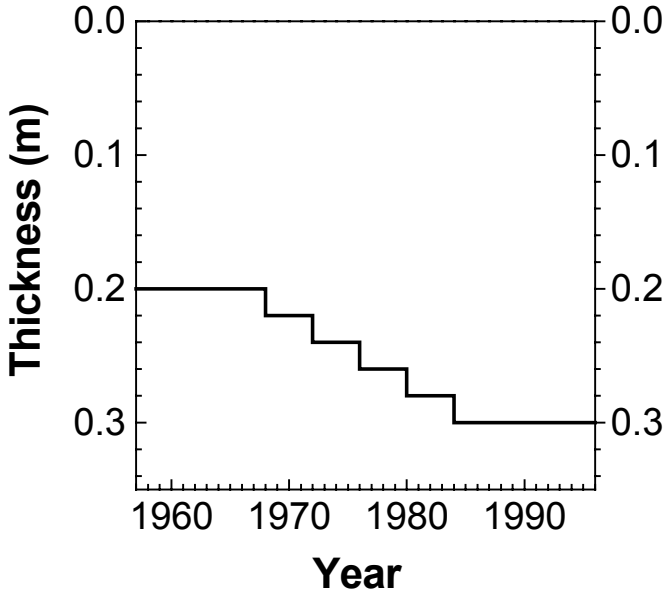

Figure 37: Deepening of tillage reconstructed according to Nieder et al. (1993)

For hindcast simulations of asparagus sites additional information about the year of deep ploughing was necessary. This information was collected through interviews with farmers. The soil exchange rates were determined as described in Chapter 7.2. Due to deep ploughing the *OC* content in Ap horizon is forced into a new, non-equilibrium state. In general, after deep ploughing the *OC* content in the Ap horizon is lower than before deep ploughing. Therefore, *OC* reaccumulates until the former or a new equilibrium state is reached. In the scope of this study the *OC* dynamic of Ap horizons could be modelled only in a very simplified manner. It was assumed that (1) at time of ploughing the *OC* regime is in equilibrium, (2) after ploughing the *OC* content linearly approaches the former *OC* content, (3) it takes 25 yr to reach the former equilibrium state (Gäth et al., 1997) and (4) the *OC* content of compartments below the Ap horizon is constant in time.

8.4.4. Plant Uptake

The parameters used in the plant uptake model are given in Table 11. The k_P's of winter wheat and potato as well as the parameter ω were taken from the literature (Chapter 8.4.1). All other parameters were either directly measured (Q_{HM}, Q_Y) or fitted by non-linear regression (k_P for sugar beet, η, K_{H+}, V_{H+}) (Chapter 7.5). With regard to potato only the Cluster *Alpha* was considered. All simulations were run using a schematic crop rotation of sugar beet, wheat, wheat, potato, wheat, wheat. The uptake of Cd by asparagus was ignored.

Table 11: Parameterization of the plant uptake model for winter wheat, sugar beet and potato

Crop	Q_{HM} ‡	Q_Y ‡	k_P	ω †	η ††	K_{H+} ††	V_{H+} ††
	—	—	— Pa —	— m^{-1} —	—	—	—
Wheat	2.1	0.98	4.0†	5.202	1	n.s.#	-
Sugar beet	4.2	0.37	5.5††	8.864	1	n.s.#	-
Potato§	20.9	0.092	6.2†	11.689	0.98	0.128	0.300
Potato&	11.8	0.133	6.2†	11.689	2.01	0.104	0.444

§ Cluster *Alpha.*
& Cluster *Beta.*
# n.s.: not different from zero at the 5% significance level (*t*-test).
‡ Measured.
† Literature data (see Chapter 8.4).
†† Fitted by non-linear regression.

8.5 Hindcast Simulations (1957-1996)

8.5.1. Cd Displacement

For the Non-Rigosol sites, Figure 38 shows observed and predicted solution phase concentration and total concentration profiles of Cd after up to 40 years of waste water irrigation. The agreement between observed and predicted data is fairly good. Particularly the solution phase concentration predicted in the Ap horizon agrees very well with measured data. The observed solution phase con-

centration in the Ap horizon is 1.76 µg L^{-1} and, and in dependence of different approaches, a concentration between 1.68 µg L^{-1} and 1.89 µg L^{-1} is predicted. The modelling efficiency (*EF*) of approaches applied varies between 72% and 85% with regard to predicted *C* profiles and between 98% and 99% with regard to the predicted C_T profiles (Table 12). The best results with the *DSC* approach were generally obtained by applying *Hybrid* approaches. Of the *RSC* simulations, the *RSC III* approach gave the best result.

A closer look reveals that for *RSC* approaches the solution phase concentrations in the Ap horizon decrease in the sequence *RSC I* (1.89 µg L^{-1}), *RSC II* (1.85 µg L^{-1}) and *RSC III* (1.71 µg L^{-1}). Hence, considering more details of spatial variability in the modelling approach leads to a slight decrease of the solution phase concentration in the Ap horizon and slightly reduced leaching of Cd. However, at the Non-Rigosol sites both *RSC* and *DSC* modelling approaches slightly overestimate Cd leaching. The displacement indices (*DI*) given in Table 12, range between 118% and 129%. It is conspicuous that particularly the concentrations in the layer 0.3 to 0.4 m are overpredicted by all approaches (Figure 38). In this layer, the smallest deviation between measured and predicted *C* and C_T occurs with the *DSC 1a Hybrid* modelling approach. Nevertheless, the deviation from measured *C* and *T* is still 0.38 µg L^{-1} (+59%) and 33.1 µg kg^{-1} (+49%), respectively.

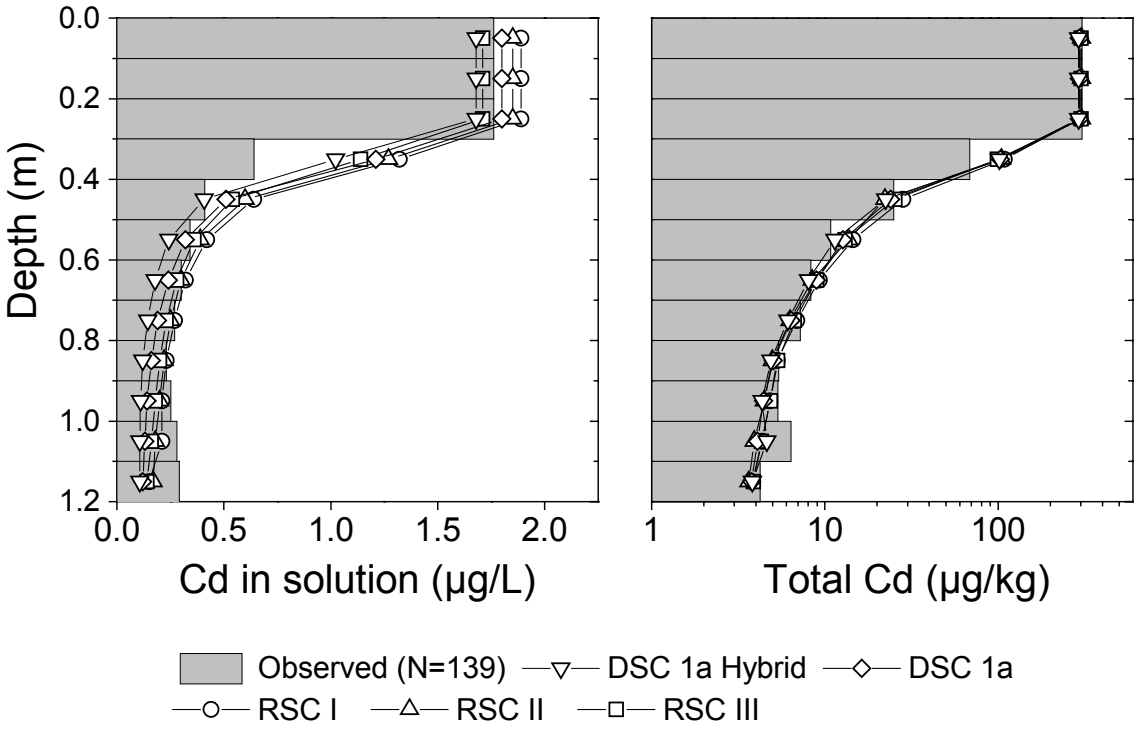

Figure 38: Observed and predicted profiles of averaged solution phase concentrations and total concentrations of Non-Rigosols.

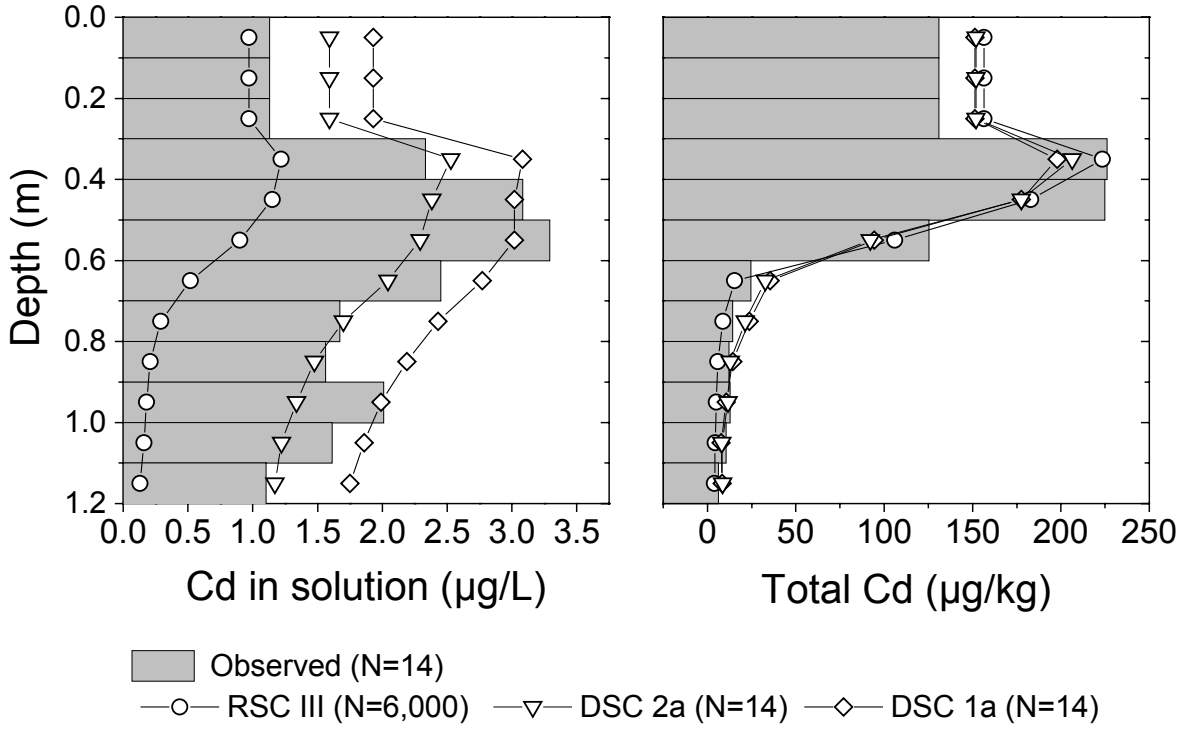

Figure 39: Observed and predicted profiles of averaged solution phase concentrations and total concentrations of Rigosols.

Table 12: Modelling conditions and results for the Non-Rigosol sites. Cd displacement was predicted with either deterministic soil column (DSC) or random soil column (RSC) modelling approaches using the local model SEFAH. The modelling efficiency (EF) and the displacement index (DI) are defined in Equation (40) and (41), respectively. C denotes the solution phase concentration and C_T the total concentration. The model assessment criteria were calculated for the averaged profiles (N=139).

	Modelling conditions				**Model assessment criteria**		
					EF		
Modelling approach	***PTF***[§]	**experimental *k* when available**[†]	**Model input variables**	***N***	***C***	***C_T***	***DI***
				—	—%—	—%—	—%—
DSC 1a	1a	no	observed	139	79	98	122
DSC 1b	1b	no	observed	139	78	98	121
DSC 2a	2a	no	observed	139	83	99	121
DSC 2b	2b	no	observed	139	82	99	122
1a Hybrid	1a	yes	observed	139	85	98	119
1b Hybrid	1b	yes	observed	139	83	99	118
2a Hybrid	2a	yes	observed	139	85	98	121
2b Hybrid	2b	yes	observed	139	84	98	121
RSC I	1a	no	1D correlated random	500	72	98	129
RSC II	1a	no	1D correlated random per district	4x500	77	98	122
RSC III	1a	no	3D correlated random	12x500	84	99	122

[§] *PTF*: Pedotransfer function.

[†] The Freundlich coefficient *k* of the Freundlich equation $S=kC^m$ was calculated using measured data when available (cf. Equation (32)).

For the Rigosol sites, Figure 39 depicts observed and predicted solution phase concentrations and total concentrations of Cd. The total concentrations are fairly well predicted by all modelling approaches. This finding indicates that the calculation of soil exchange rates using the measured *OC* profile is suited to model the transfer of soil between top and subsoil due to deep ploughing. However, the solution phase concentrations are acceptably predicted only by the *DSC* approaches (Table 13). The *RSC* approaches do not agree very well with the observed data. Even though the solution phase concentration is well predicted in the Ap horizon, the *RSC* approaches fail to predict the concentrations observed in subsoil. The deviation between observed and predicted values is mainly caused by different sorption properties of subsoils of the 14 Rigosols sampled and those of the random soil columns generated (N=500-6,000). There are two major reasons for this difference: (1) The vector of means and the covariance matrix of random variables for the *RSC* approaches were obtained from the Non-Rigosol sites (N=139) and not from the 14 Rigosol sites, (2) the mean of observed data as well as of *DSC* modelling approaches was taken over 14 observations only. Single profiles with exceptionally high solution phase concentrations in subsoil, like the Rigosols I09 and H17, did strongly affect the mean value. Hence, the number of Rigosols sampled is hardly sufficient to produce a stable regional mean.

Table 13: Modelling conditions and results for the Rigosol sites. Cd displacement was predicted with either deterministic soil column (DSC) or random soil column (RSC) modelling approaches using the local model SEFAH. The modelling efficiency (EF) and the displacement index (DI) are defined in Equation (40) and (41), respectively. C denotes the solution phase concentration and C_T the total concentration. The model assessment criteria were calculated for the averaged profile (N=14).

	Modelling conditions				**Model assessment criteria**		
					EF		
Modelling approach	***PTF*** [§]	**Experimental *k* when available** [†]	**Model input variables**	***N***	***C***	***C_T***	***DI***
				—	—%—	—%—	—%—
DSC 1a	1a	no	observed	14	47	94	87
DSC 1b	1b	no	observed	14	61	95	89
DSC 2a	2a	no	observed	14	68	93	86
DSC 2b	2b	no	observed	14	60	94	87
RSC I	1a	no	1D correlated random	500	-361	94	80
RSC II	1a	no	1D correlated random per district	4x500	-378	96	86
RSC III	1a	no	3D correlated random	12x500	-374	96	85

[§] *PTF*: Pedotransfer function.

[†] The Freundlich coefficient *k* of the Freundlich equation $S=kC^m$ was calculated using measured data when available (cf. Equation (32)).

Therefore, the deviation between the results of the *RSC* simulations and observed values does not necessarily indicate a failure of *RSC* modelling approaches. In contrast, the model outputs are in line with the measurements of Non-Rigosols. The averaged solution phase concentration of Non-Rigosols in Ap horizons is 1.76 µg L^{-1}. Even if top and subsoil were completely exchanged due to deep ploughing, the concentration in the subsoil would be at maximum the concentration of the former Ap horizon. Therefore, an average concentration of about 3.2 µg L^{-1} like observed in the 0.5 to 0.6 m layers from the 14 Rigosols sampled is not necessarily the "real" regional mean.

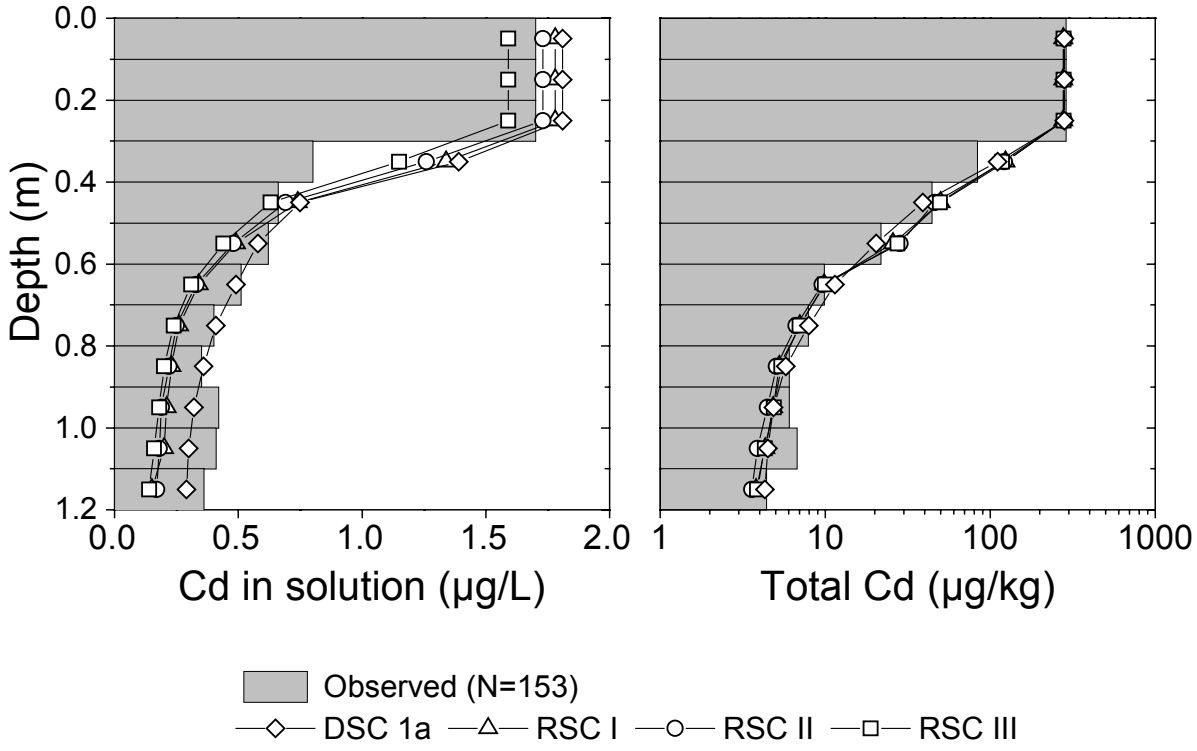

Figure 40: Observed and predicted profiles of averaged solution phase concentrations and total concentrations of Non-Rigosol and Rigosol sites.

To complete the picture the predicted regionally averaged solution phase concentrations and total concentrations of both Non-Rigosol and Rigosol sites are shown in Figure 40. Not surprisingly the predicted solution phase concentration below 0.5 m is highest for the *DSC 1a* modelling approach. The high solution phase concentrations of the 14 measured Rigosol profiles markedly affect the regionally averaged profile in the subsoil. The *EF* of the *DSC 1a* approach is 74% concerning *C* and the *DI* is 110%. The *EF* of *RSC* approaches ranges between 60% and 64% for *C* and the *DI* varies between 121% and 124% (Table 14).

Table 14: Modelling conditions and results for the Non-Rigosol and Rigosol sites. Cd displacement was predicted with either deterministic soil column (DSC) or random soil column (RSC) modelling approaches using the model SEFAH. The modelling efficiency (EF) and the displacement index (DI) are defined in Equation (40) and (41), respectively. C denotes the solution phase concentration and C_T the total concentration. The model assessment criteria were calculated for the averaged profile (N=153).

	Modelling conditions				**Model assessment criteria**		
					EF		
Modelling approach	***PTF***[§]	**experimental *k* when available**[†]	**Model input variables**	***N***	***C***	***C_T***	***DI***
				—	—%—	—%—	—%—
DSC 1a	1a	no	observed	153	74	99	110
DSC 1b	1b	no	observed	153	72	99	110
DSC 2a	2a	no	observed	153	79	99	109
DSC 2b	2b	no	observed	153	81	99	110
RSC I	1a	no	1D correlated random	500	60	97	124
RSC II	1a	no	1D correlated random per district	4x500	64	98	121
RSC III	1a	no	3D correlated random	12x500	63	98	121

[§] *PTF*: Pedotransfer function.

[†] The Freundlich coefficient *k* of the Freundlich equation $S=kC^m$ was calculated using measured data when available (cf. Equation (32)).

Between districts, the quality of simulation results is very different (Table 15). The best agreement between observed and predicted values was achieved for the soils of District 1. In contrast, for the soils of District 2 particularly the non-Hybrid approaches produced unsatisfactory simulation results (*EF* of *C*: -14-26%). For the soils of District 4 all approaches distinctly overestimated the displacement of Cd. The *DI* was up to 242% (Table 16) whereby the best *DI* values were obtained by applying the *DSC Hybrid* approaches, i.e. using measured data for calculating Freundlich coefficients when available.

Table 15: Modelling efficiencies (cf. Equation (40)) of district-averaged solution phase concentration (C) and total concentration (C_T) profiles of Non-Rigosol sites. The Cd displacement was predicted with either deterministic soil column (DSC) or random soil column (RSC) modelling approaches using the local model SEFAH.

	Modelling efficiency (*EF*)							
	District 1 (N=33)		**District 2** (N=35)		**District 3** (N=41)		**District 4** (N=30)	
Modelling approach	***C***	***C_T***	***C***	***C_T***	***C***	***C_T***	***C***	***C_T***
DSC 1a	84	99	10	96	72	97	64	95
DSC 1b	81	99	-14	95	71	97	62	94
DSC 2a	87	99	19	96	72	97	51	94
DSC 2b	85	99	12	96	71	97	49	94
DSC 1a Hybrid	90	98	49	99	78	96	82	97
DSC 1b Hybrid	89	99	41	99	75	96	79	97
DSC 2a Hybrid	89	99	49	99	78	96	81	97
DSC 2b Hybrid	89	99	46	99	77	96	80	97
RSC II	90	99	-7	96	52	96	42	94
RSC III	92	99	26	97	76	98	37	96

Table 16: Displacement indices (cf. Equation (41)) of district-averaged profiles of Non-Rigosol sites. Cd displacement was predicted with either deterministic soil column (DSC) or random soil column (RSC) modelling approaches using the local model SEFAH.

	Displacement index (*DI*)			
	District 1 (N=33)	**District 2** (N=35)	**District 3** (N=41)	**District 4** (N=30)
Observed	100	100	100	100
DSC 1a	116	87	140	231
DSC 1b	111	87	141	240
DSC 2a	110	83	146	237
DSC 2b	110	83	149	242
DSC 1a Hybrid	123	82	143	193
DSC 1b Hybrid	119	81	145	197
DSC 2a Hybrid	120	82	150	194
DSC 2b Hybrid	119	82	152	199
RSC II	103	80	147	240
RSC III	112	82	140	233

8.5.2. Cd Plant Uptake

Figure 41 shows simulated averaged Cd contents of wheat grain together with the saturation deficit between 1957 and 1996. The figure shows only the results of the *RSC* modelling approaches. The development of the Cd contents reflects the input history (Chapter 7.1), which is superimposed by the annual fluctuation of the saturation deficit. Before 1980, Cd contents gradually increased from about 0.01 mg kg^{-1} in 1957 to 0.075 mg kg^{-1} in 1979. Within 7 years only (1980-1986) the Cd content doubled from about 0.1 to 0.2 mg kg^{-1}. This period of strong increase is identically with the period of the highest Cd loads. Since late 1980s the continuous increase of Cd contents has stopped. Between 1987 and 1996 the Cd contents of wheat grain have fluctuated at a high level between 0.157 mg kg^{-1} and 0.257 mg kg^{-1}. Especially in 1989, 1992 and 1994, high saturation deficits led to very high Cd contents. Highest Cd contents were predicted by *RSC I* and lowest by *RSC III*.

Figure 42 shows simulated Cd contents of the processed plant parts of winter wheat, sugar beet and potato (Cluster *Alpha*). The model *SEFAH* was run with a constant mean saturation deficit of 659 Pa using the *RSC I* approach. Predicted Cd contents of all three plants show that contents were highest in the mid eighties while thereafter the contents slightly decreased. Highest contents was predicted for wheat grain followed by sugar beet hypocotyl. Simulated contents of potato tuber were lowest. Note, however, that using the parameter set for the Cluster *Beta* potato (cf. Chapter 7.5) would result in contents roughly twice as high.

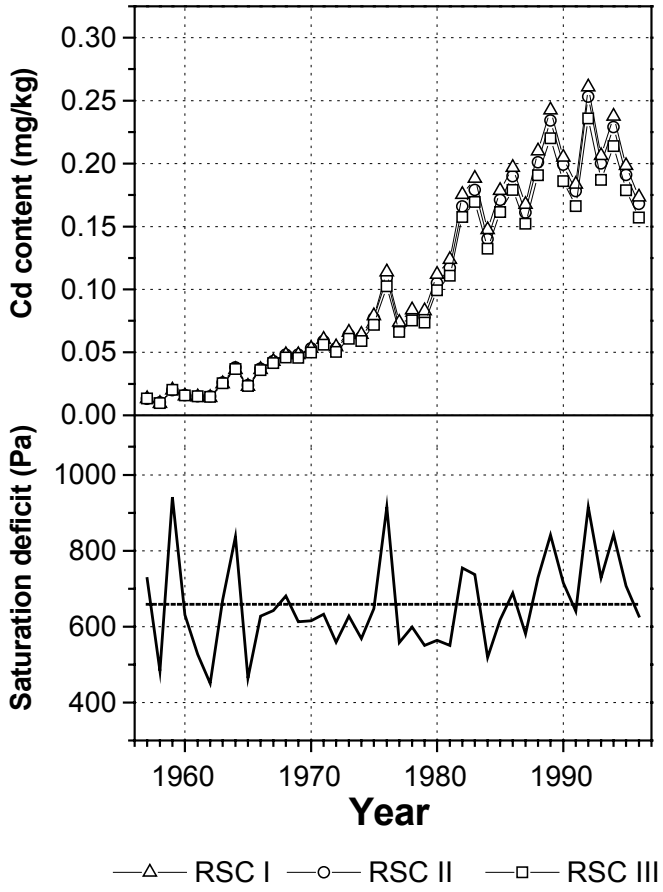

Figure 41: Simulated average Cd contents of wheat grain from 1957 to 1996 using the RSC modelling approaches (upper panel). The bottom of figure shows the saturation deficit of the air.

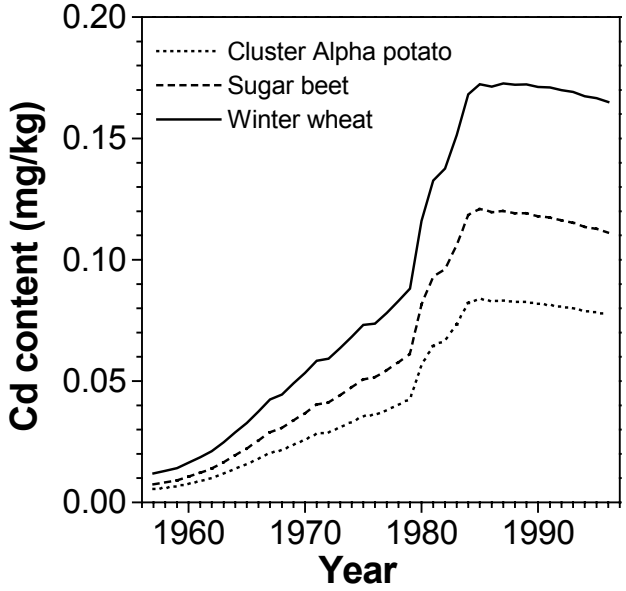

Figure 42: Simulated average Cd contents of processed plant parts of winter wheat, potato and sugar beet from 1957 to 1996 using the RSC I approach. For modelling constant mean saturation deficits were used.

8.6 Scenario Simulations

The model *SEFAH* was applied to look into the following questions:

- What would have happened if the Cd loads had not been reduced in the mid eighties?
- What would have happened if from 1957 to 1996 the Cd loads had been at the maximum level allowed by the German sewage sludge regulation?
- How will Cd pathways develop if the Cd loads from 1996 to 2046 are kept at the level of the year 1996?
- How would changes in soil *p*H affect the Cd uptake by winter wheat?

8.6.1. Scenario 1: What would have happened if Cd loads had not been reduced in the mid eighties?

In the mid 1980s the monitoring of illicit emissions to the municipal sewage canal system was enhanced and the sewage plant was equipped with a sewage press. Due to these two measures the Cd loads into the *WIA* have been markedly reduced (Chapter 4). Scenario 1 assumes that these countermeasures were not taken in the mid 1980s. In other words, Scenario 1 is a worst-case scenario. It is assumed that from 1985 to 1996 the Cd load of each district amounted to its mean between 1980 and 1984 (District 1: 98.5 g m^{-2}, District 2: 119.3 g m^{-2}, District 3: 156.5 g m^{-2}, District 4: 125.1 g m^{-2}). Scenario 1 was computed by applying the *DSC* approach using *DSC 1a Hybrid* for Non-Rigosols and *DSC 1a* Rigosols.

Figure 43 shows the model output of Scenario 1. If no countermeasures had been introduced in the mid 1980s, in 1996 the mean Cd content of wheat grain would have been 0.43 mg kg^{-1}. This value is markedly higher than twice the German food guideline value. The regional averages of the Cd solution phase

concentration and total concentration would have been 4 µg L^{-1} and 0.559 mg kg^{-1}, respectively. The ground water would not yet have been affected. In 1996, the averaged concentration in seepage water would have been 0.15 µg L^{-1}. But on the long run adverse effects on ground water quality would be unavoidably. This scenario demonstrates that the decision of the *BMWA* in the early 1980s to take measures against the high Cd inputs was fully reasonable. Without these measures, the impact on soil quality would have been tremendous. It is even questionable whether the soils of the *WIA* would still be suited for food production today.

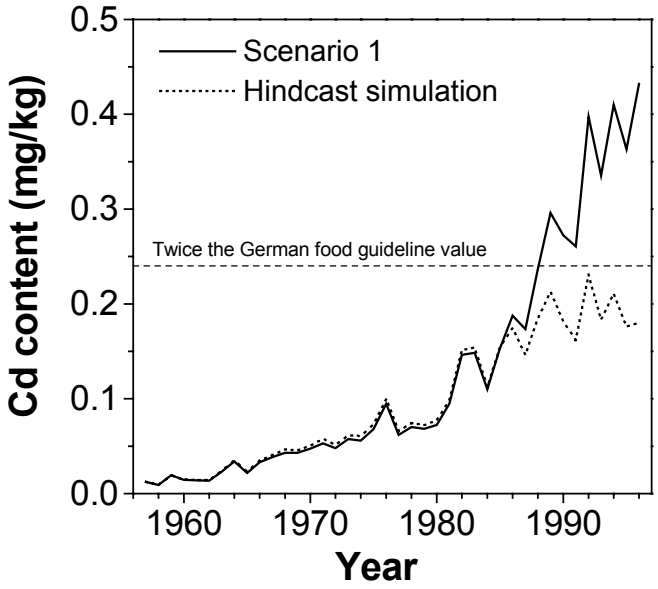

Figure 43: Cd content in wheat grain for Scenario 1 and a DSC hindcast simulation. Scenario 1 assumes that Cd loads had not been reduced in the mid 1980s.

8.6.2. Scenario 2: What would have happened if from 1957 to 1996 the Cd loads had been at the maximum level allowed by the German sewage sludge regulation?

According to the German sewage sludge regulation (AbfKlärV, 1992) the permitted Cd load is 8.33 g ha^{-1} yr^{-1}. The total atmospheric Cd deposition (wet and dry) was set to 0.9 g ha^{-1} yr^{-1} (cf. Chapter 8.4.3). Hence, the Cd load of each dis-

trict amounts to 9.23 g ha^{-1} yr^{-1}. In case of Non-Rigosols, the simulation was carried out with the *DSC 1a Hybrid* and in case of Rigosols with the *DSC 1a* approach.

Figure 44 presents the results for Scenario 2. At permitted Cd inputs the Cd content of wheat grain would have increased about linearly from 0.01 mg kg^{-1} in 1957 to 0.04 mg kg^{-1} in 1996. However, Cd accumulates slowly but continuously in soils until a steady state is reached.

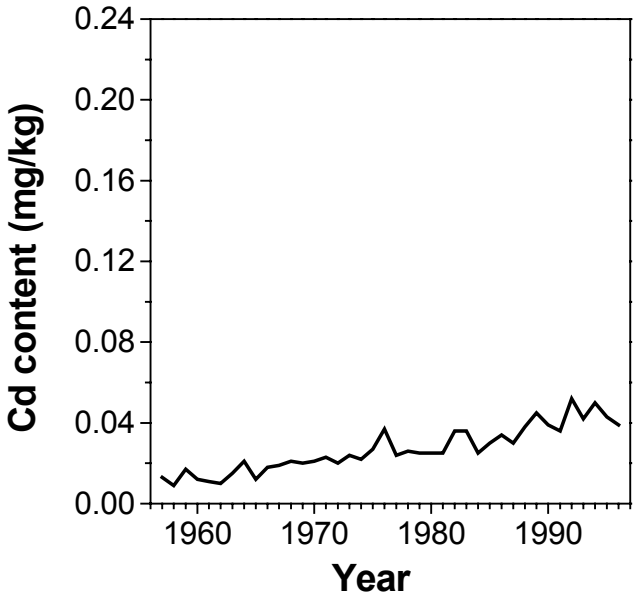

Figure 44: Cd content in wheat grain for Scenario 2: From 1957 to 1996 the Cd loads have been at the maximum level allowed by the German sewage sludge regulation.

In case of an uncontrolled Cd uptake by plants ($\eta = 1$) the steady state concentration can be calculated by performing a Cd balance for the Ap horizon. In steady state Cd inputs and Cd outputs of the Ap horizon are equal

$$Q_{Input} + Q_{Root} = Q_{Harvest} + Q_{Leaching} \tag{84}$$

where Q_{Input} (g ha^{-1} yr^{-1}) denotes the Cd input due to deposition and waste water irrigation, Q_{Root} (g ha^{-1} yr^{-1}) is the Cd flux from subsoil to the Ap horizon by plant uptake, $Q_{Harvest}$ (g ha^{-1} yr^{-1}) denotes the withdrawal with the harvest mate-

rial and $Q_{Leaching}$ (g ha^{-1} yr^{-1}) stands for the Cd leaving the Ap horizon by leaching.

If η equals unity the steady state concentration is constant with depth (cf. Chapter 9.5). Therefore, Q_{Root} can be written as (Chapter 6.3)

$$Q_{Root} = \frac{\Delta e\, Y\, C}{k_P\, \rho_w} \exp(-\omega\, z_{Ap}) \tag{85}$$

and the withdrawal with harvest material becomes

$$Q_{Harvest} = \frac{\Delta e\, Y\, C}{k_P\, \rho_w} (1 + Q_Y Q_{HM})^{-1} \tag{86}$$

The amount of Cd leaving the Ap horizon by leaching may be written as

$$Q_{Leaching} = \left(P + I - pET + \frac{\Delta e\, Y}{k_P\, \rho_w} \exp(-\omega\, z_{Ap}) \right) C \tag{87}$$

For symbols see the Appendix (Table A1). Inserting equations (85)-(87) into Equation (84) results in

$$C = \frac{Q_{Input}}{A_1 (1 + Q_Y Q_{HM})^{-1} + P + I - pET} \tag{88}$$

$$A_1 = \frac{\Delta e Y}{k_P \rho_w}$$

At a Q_{Input} of 9.23 g ha yr^{-1} and under the meteorological conditions of the *WIA* assuming a hypothetical monoculture of winter wheat (P=632 mm yr^{-1}, I=545 mm yr^{-1}, pET=540 mm yr^{-1}, Q_Y=0.98, Q_{HM}=2.1, Δe =658 Pa, k_P=4.0 Pa, Y=10830 kg ha^{-1} yr^{-1}) the Cd solution phase concentration at steady state is 1.3 µg L^{-1} and the content in wheat grain is 0.14 mg kg^{-1}. The annual Cd output by the withdrawal of harvest material and leaching at steady state would be 0.72 g ha^{-1} yr^{-1} and 8.51 g ha^{-1} yr^{-1}, respectively. That means, the Cd output by leaching is the

major sink (92%) and the Cd output by the withdrawal of harvest material is only of minor importance (8%). However, one of the specific features of the *WIA* is the high irrigation rate. If the irrigation rate would be only half of the current rate the steady state concentration and the Cd content in wheat grain would increase to 2.2 μg L^{-1} and 0.24 mg kg^{-1}, respectively. The withdrawal of harvest material would increase to 13% of total sinks.

8.6.3. Scenario 3 (1996-2246): How will Cd pathways develop if the Cd loads from 1996 to 2246 are kept at the level of the year 1996?

Scenario 3 is a "business as usual" scenario. Since the Cd displacement is generally very slow simulations were run from 1996 to 2246. Only after such a long simulation period a usable breakthrough curve was obtained. Scenario 3 assumes that from 1996 to 2246 Cd loads by waste water irrigation were at the level of the year 1996 (1.1 g ha yr^{-1}). The total atmospheric deposition was set to 0.9 g ha^{-1} yr^{-1} (cf. Chapter 8.4.3). The simulation was run with the *RSC III* modelling approach. Each model run was initiated with one of the twelve model outputs of the hindcast simulation *RSC III*. Climatic input variables (*N*, *pET*, Δe) were set to the averages of the period from 1957 to 1996. Crop yields beet were kept constant at the levels of the year 1996.

Figure 45 shows the development of Cd content in wheat grain from 1957 to 2046. After 1996 the simulation was run with a constant average saturation deficit. The Cd content decreases gradually from 0.16 mg kg^{-1} in 1996 to about 0.11 mg kg^{-1} in 2046. The solution phase concentration in the Ap horizon decreases from 1.7 μg L^{-1} in 1996 to about 0.9 μg L^{-1} in 2046. Moreover, in 2046 Cd is displaced to a depth below 1.2 m (Figure 46).

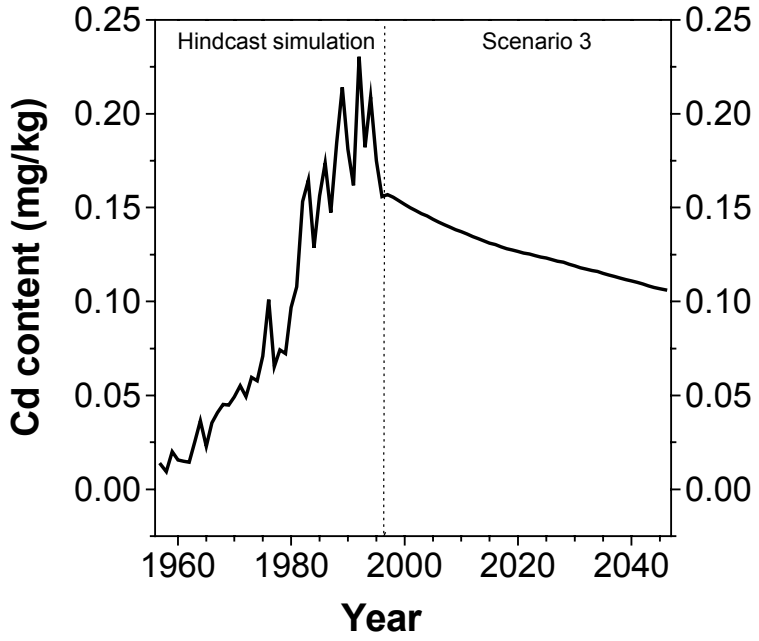

Figure 45: Simulated Cd content in wheat grain between 1957 and 2046. From 1996 to 2046 Cd loads were kept at the level of 1996 (Scenario 3). Simulations were carried out with the RSC III modelling approach.

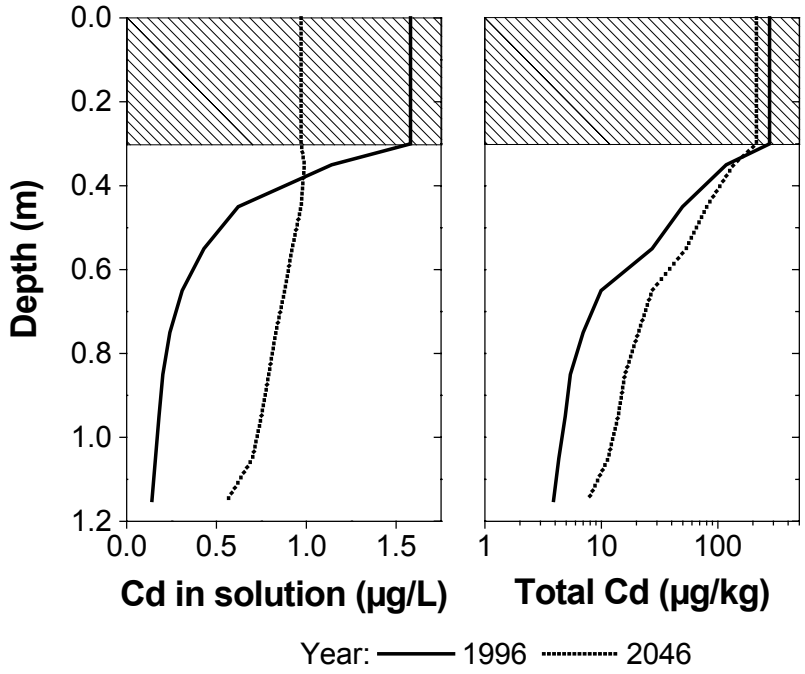

Figure 46: Simulated regionally averaged solution phase concentrations and total concentrations of Cd in 1996 and 2046. From 1996 to 2046 the Cd loads were kept at the level of 1996 (Scenario 3). Simulations were carried out with the RSC III modelling approach.

Figure 47 shows the regionally averaged breakthrough curve of Cd. Before 1980 the Cd concentration in seepage water is at the background level. After 1980 the Cd concentration increases gradually. The maximum (0.65 µg L^{-1}) is reached around 2100. After 2100 the Cd concentration decreases more or less linearly and is 0.55 µg L^{-1} in 2246.

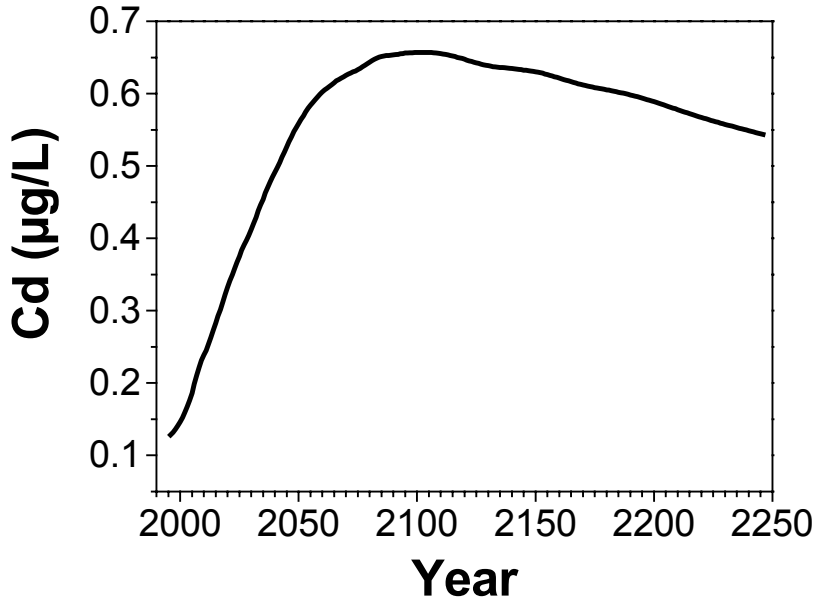

Figure 47: Predicted average Cd concentrations in seepage water at the depth of water table. From 1996 to 2246 the Cd loads were kept at the level of 1996 (Scenario 3). Simulations were carried out with the RSC III modelling approach.

8.6.4. Scenario 4 (1957-2046): How would changes in soil *p*H affect the Cd uptake by winter wheat?

Three different cases were investigated, whereby any changes were restricted to Ap horizons. At the beginning of simulations (a) the mean *p*H in Ap horizons was lowered from 5.78 to 5.5 (target *p*H of most soils in the *WIA*) and the standard deviation was not changed, (b) the standard deviation was lowered from ± 0.418 to ± 0.315 (-25%) whereby the mean *p*H was left unchanged, (c) like (b) but the standard deviation was lowered to ± 0.209 (-50%). Since in Scenarios 4b and 4c the standard deviation was changed the covariance matrix had to be

modified as well (Hartung, 1999). For calculation the correlation matrix of measured soil *p*H was used. Scenario 4 was computed with the *RSC I* modelling approach.

Figure 48 presents the results of different simulations. A decrease of the mean *p*H in Ap horizons from 5.78 to 5.5 increases the Cd content of wheat grain of about 35%. In 1996, at the *RSC I* hindcast simulation the average Cd content of grain was 0.20 mg kg^{-1} but 0.27 mg kg^{-1} at the Scenario 4a. In contrast, a reduction of the *p*H variability in Ap horizons had only a minor effect on Cd uptake. In Figure 44 the lines of the two scenarios and the *RSC I* hindcast simulation can hardly be distinguished from each other. A reduction of the *p*H variability of 50% leads to a decrease in the Cd content of grain of only 5%. Also the number of sites at which in 1996 the Cd content of grain exceeded the limit of 0.24 mg kg^{-1} is not strongly touched. In 1996, according to the *RSC I* hindcast simulation 24% of sites exceeded the limit whilst in Scenario 4b 22% and in Scenario 4c 20% of sites exceeded the limit.

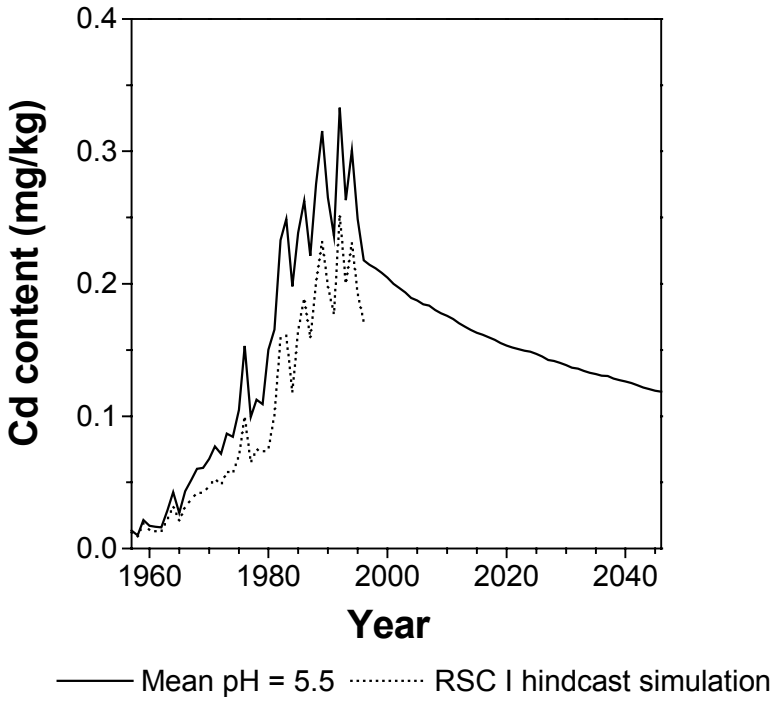

Figure 48: Cd content in wheat grain for scenario 4a. At the beginning of the simulation the mean pH in Ap horizons was lowered to 5.5 (target pH of most soils) and the standard deviation was not changed.

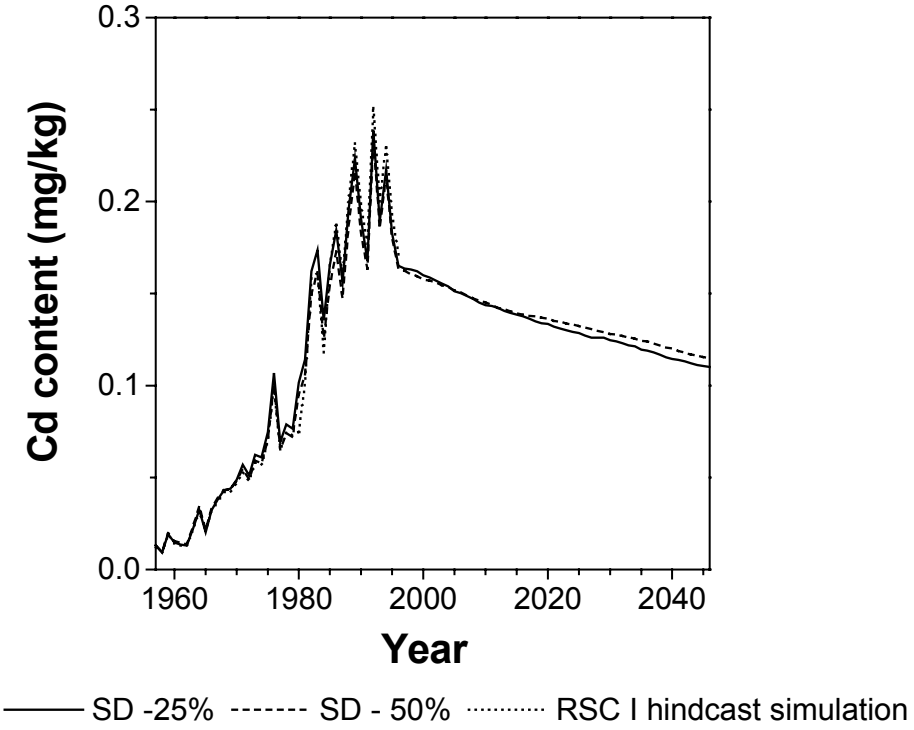

Figure 49: Cd content in wheat grain for scenario 4b and 4c. The mean pH in Ap horizons was not changed but the standard deviation was lowered by 25% and 50%.

8.7 Discussion

8.7.1. Displacement

For modelling the Cd movement it was assumed that the solute transport was convective-dispersive at the local scale and approximately stochastic-convective at the regional scale. It is beyond the scope of this study to prove or test these assumptions. The transport mechanism could be evaluated, for example, by monitoring solute spreading at progressive time by soil coring (Jury and Flühler, 1992). In case of strongly sorbing solutes like Cd the measurement intervals would have to be decades. However, there are sound arguments why to apply different approaches at different scales. As already mentioned in Chapter 3.1, the displacement velocity of a strongly sorbing solute is mainly controlled by the water flux and sorption characteristics of the soil. Streck and Richter (1997a)

observed at a field within the *WIA* that, for instance, soil *p*H was spatially correlated over a distance of about 30 to 60 m. As shown in the present study, at the regional scale the correlation length of these soil properties increases to distances of several hundred meters. On the assumption that the correlation length of displacement velocity is in the same range as that of the transport-relevant soil properties it seems unlikely that at the regional scale the transport distance, which is 1.8 m on average within the *WIA*, allows for a lateral mixing. Hence, at the regional scale it is likely that the movement of strongly sorbing solutes can be represented by a parallel soil column approach.

For the whole study the concentration in soil solution is of fundamental importance. In the present study Cd in soil solution was approximated by equilibrating soil with a 0.0025 M $CaCl_2$ background electrolyte. It is well known that ionic strength, chloride and calcium concentration affect Cd sorption (Boekhold et al., 1993). Therefore, the proper selection of the background electrolyte is essential in order to obtain reliable results. The composition of the background electrolyte should be similar to that of the soil solution, which depends on soil type, land use, climate etc. Moreover, short-term variation can be caused by fertilization or rainfall events. Hence, it is not surprising that the pertinent literature offers a wide spectrum of background electrolytes. Elzinga et al. (1999) evaluated batch sorption data from the literature and found that, for example, Ca^{2+} concentration in batch solutions ranged from 0.001 to 0.1 M. Thus the question arises, which is the correct background electrolyte? The experimental setup for generating sorption data has to be adjusted to the particular application. For instance, for the modelling of Cd transport in soil it is necessary to determine the total dissolved mobile Cd (e.g. free Cd^{2+} and complexed Cd^{2+}) and to consider the time scale at which heavy metal displacement occurs. There is evidence that disregarding short-term variation of the controlling variables of a long-term process is possible without producing a significant error. For example, when heavy metal

transport is modelled the simulation of the water regime under stationary conditions yields similar results as compared to simulations based on transient water flow (Swartjes, 1990). Therefore, it is most important to select the background electrolyte so that it represents the long-term composition of soil solution. For these reasons, a 0.0025 M $CaCl_2$ background electrolyte was used, which corresponds to the average ionic strength of the irrigation water as calculated from data by Fassbender and Steinert (1979). In addition, chloride is the main anion of the waste water, therefore complexation of Cd^{2+} by Cl^{-1} has to be taken into account. Last but not least, Streck and Richter (1997b) successfully used the same experimental procedure to model heavy metal displacement in a field within the *WIA*. To sum up, the method applied seems suitable to obtain reliable estimates of the concentrations in soil solution under the special conditions of the *WIA*.

Another very important methodical assumption is that the EDTA-extractable content represents the fraction of Cd which participates in sorption-desorption reactions. This assumption has already been used successfully by other authors (Filius et al., 1991; Schulte and Beese, 1994; Streck and Richter, 1997a). In addition, there are sound arguments for using the strongly complexing ion EDTA for this purpose. Firstly, EDTA does not extract Cd from the silicates (Brümmer et al., 1986), and secondly, EDTA reduces the free metal concentration by complexation to near zero, which should induce an almost quantitative desorption. Moreover, Gäbler et al. (1999) found in a recent study experimental evidence for the correctness of this assumption. The authors measured the amount of heavy metals participating in sorption-desorption reactions using an alternative method, the isotope dilution mass spectrometry. With regard to Cd, both methods, EDTA-extraction and isotope dilution mass spectrometry, led to comparable results.

The present study confirms the results of several other investigations carried out in the past: Heavy metal displacement is a very slow process (e.g. Dowdy et al., 1991; Cernik et al., 1994; Filius, 1993; Streck and Richter, 1997a). Even though conditions in the *WIA* are favourable to heavy metal transport (annual ploughing, sandy soils low in *p*H as well as *OC*, high water flux densities) after up to 40 years Cd has been displaced on average to little more than 0.5 m depth. However, displacement depths of Cd within the *WIA* are extremely variable. At some sites the observed displacement depth was up to 1.2 m. At other sites no Cd displacement was measurable below the Ap horizon. This minor displacement complicated the validation of the transport model. For example, for the averaged profiles the modelling criterion *EF* was mainly controlled by the three upper soil layers (0-0.5 m).

Especially the Cd concentrations in the 0.3 to 0.4 m layers showed a strong deviation between observed and simulated values. This may be explained to some degree by the sampling method used. As described in Chapter 5.1.1, first a sample of the Ap horizon was taken separately by digging a hole. Afterwards, a soil monolith was taken at the bottom of the hole with the help of a mechanical soil auger. In many cases, during drilling soil material of the Ap horizon contaminated the surface of soil core. Therefore, in these cases the first centimeter of the 0.3-0.4 m layer was excluded from sampling. Moreover, in several cases it was difficult to determine the exact boundary between the Ap horizon and the following layer. In addition, we have to bear in mind that the plough pan is a part of the first layer below the Ap horizon. It is therefore possible that the bulk density is higher than assumed. A higher bulk density would cause a higher retardation and thus a slower displacement.

Besides these methodical problems, modelling assumptions may also have caused the slight overestimation of Cd displacement at the Non-Rigosol sites.

For example, all modelling approaches applied assume that soil *p*H is constant in time. For agriculturally used soils this assumption seems reasonable. Particularly in Ap horizons, a regular liming of soils should keep *p*H more or less at a constant level provided the farmer acts like we expect. Indeed, even then there will be short-term fluctuations of *p*H within a crop rotation, but such short-term fluctuations would probably not significantly affect the long-term displacement. However, interviews with farmers and employees of the *BMWA* revealed that at the early 1980s the *BMWA* recommended to increase the soil *p*H to reduce heavy metal uptake by plants. After some years this recommendation was weakened, because it was observed that this method may also reduce the availability of essential plant nutrients like copper. This example demonstrates that the assumption of constant soil *p*H is probably too strict.

A further uncertainty in the modelling assumptions concerns the Cd loads by application of sewage sludge. While the Cd concentration in waste water as well as the amount of waste water irrigated has been measured since 1980, no detailed information is available on the use of the sludge for fertilization. Neither amount of sludge applied, nor the fields utilized nor the years of application were ever monitored. Thus, the reconstructed input history gives only a rough picture of reality.

The model *SEFAH* does not account for preferential flow. Preferential flow has been shown to arise from larger voids in the soil like vertical cracks or earthworm channels (Omoti and Wild, 1979; Ritchie et al., 1972). However, even sandy soils have been found to exhibit preferential flow, which originates from flow instabilities arising from transport across layered soil interfaces (fingering) and from funneling mechanisms (Kung, 1990). Experimental studies have been carried out predominantly with pesticides. Flury (1996) reviewed the literature and found that in worst case up to 5% of the applied mass can be leached by

preferential flow below the root zone. Indeed, particularly for pesticides preferential flow has serious environmental implications. Since biodegradation of pesticides occurs mainly within the Ap horizon, it is highly advisable to keep these compounds from migrating below this horizon. This issue is unimportant with regard to heavy metals, which are persistent. Even though Cd may be immobilized to some extent within the Ap horizon (Brümmer et al., 1988), the major part of Cd will generally move towards the ground water and it only depends on water flux density and sorption at which time Cd will arrive in the ground water.

At asparagus sites Cd displacement is mainly controlled by deep ploughing. Leaching is of minor importance. Due to deep ploughing high amounts of soil material, organic matter and heavy metals are instantly exchanged between topsoil and subsoil. A detailed investigation of the deep-ploughing process was beyond the scope of this study. Particularly the modelling of the *OC* regime is simplistic. Coupling the model *SEFAH* with a more detailed organic carbon model would probably improve the model. Moreover, an explanation for the deviation between the Monte-Carlo simulations and measurements could be subsoil acidification. This, however, would need further investigations and must be left to future work.

8.7.2. Plant Uptake

The transpiration-based model predicted the uptake of Cd by winter wheat, sugar beet and potato rather well. From the theoretical foundation of the model three serious practical implications become evident. First, the model assumes that the Cd uptake is directly proportional to the average saturation deficit of the air. Consequently, the higher the saturation deficit the higher the Cd uptake. Hence, in areas with different saturation deficits different limit values for soil Cd

content apply to protect plants against a harmful Cd pollution (cf. Figure 50A). Results of a study by Lübben (1993) support this conclusion. The author evaluated the results of identical pot experiments on the uptake of heavy metals carried out at four locations in Germany (Braunschweig, Giessen, Munich, Speyer). At the experimental site in Munich the Cd content of plants was significantly higher than at the other sites. Lübben (1993) postulated that at least in part this finding could be explained by an enhanced transpiration due to increased temperatures. Second, without information on the saturation deficit of the air an interpretation of the results as well as the comparison of different studies is difficult. Unfortunately, most soil scientific studies on the plant uptake of pollutants generally do not measure and report the saturation deficit of the air during the experiment. For example, within the *WIA* the saturation deficit during the main vegetation period of winter wheat was 692 Pa in 1998 and 917 Pa in 1999. According to the model, the climatic difference between both years may already cause a variation in Cd uptake of about 30%. Third, the variation in Cd uptake between plants species may be partly explained by their different water use efficiencies. The more water a plant transpires for producing a quantity of dry matter the higher is its uptake of heavy metals (cf. Figure 50B).

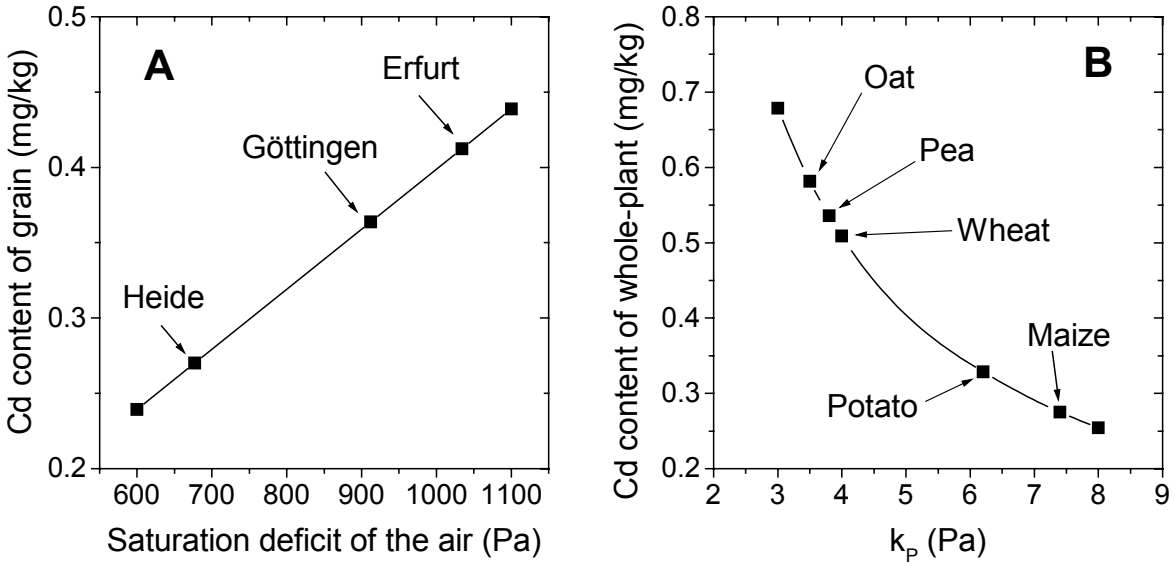

*Figure 50: Effects of **(A)** the average saturation deficit of the air and **(B)** k_P on Cd uptake by winter wheat according to the transpiration-based model. Values for Δe and k_P are taken from Ehlers (1996, Tab. 11.6). In panel A the solution phase concentration is set to 3 $\mu g\ L^{-1}$.*

The present study did not intend to explore the mechanism of Cd uptake by plants. In fact, it supplies only a rather coarse picture on how the uptake may work, based on the observation that the average saturation deficit of the air or rather the transpiration markedly affected the uptake of Cd. According to Bowling (1968) there is evidence that the latter finding indicates a non-metabolic (passive) uptake. This might explain why the supply mechanism by diffusion could be ignored in the plant uptake model. Diffusion requires a concentration gradient in the vicinity of the root. Such a gradient is generally created by an active uptake of ions by roots (Hendriks et al., 1981). When the uptake of a solute by the root or rather the demand of the plant is greater than what can be supplied by mass flow the concentration at the root surface is lowered and a concentration gradient arises. Note, however, that Cd is a strongly sorbing solute. The soil solution is highly buffered, i.e. the solution phase should be more or less protected from being depleted even in the vicinity of the root.

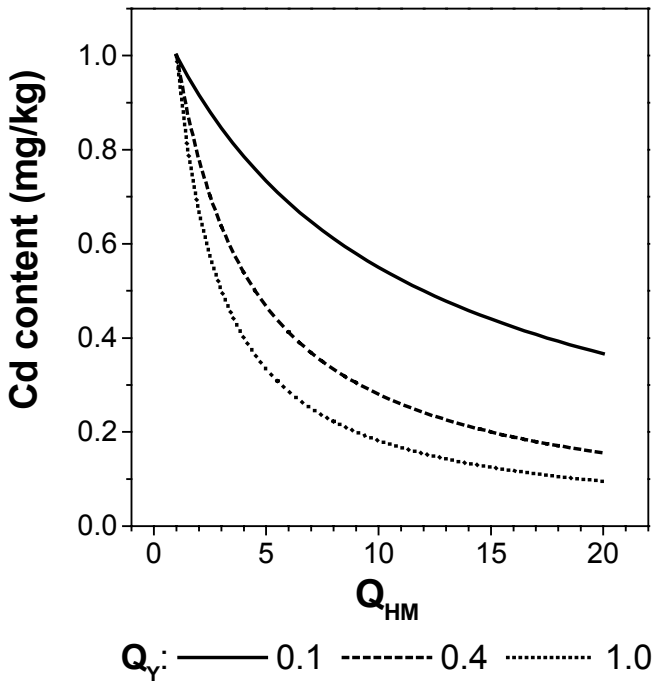

Figure 51: Effect of Q_{HM} and Q_Y on the Cd content of the processed plant part. Q_{HM} denotes the Cd content ratio and Q_Y the dry matter yield ratio between unprocessed and processed plant parts. The Cd content of the whole-plant is 1 mg kg^{-1}.

Florijn and Van Beusichem (1993) studied the genotypic variation in uptake and distribution in inbred lines of maize (*Zea mays* L.). They observed considerable variation in Cd content in shoots of the maize inbred lines while whole-plant Cd uptake was relatively constant. The authors concluded that internal distribution rather than uptake is causing the genotypic differences in shoot Cd content. The transpiration-based model considers internal distribution by the empirical quotient Q_{HM} and Q_Y (Figure 51). Both parameters were assumed to be constant. However, own measurements had shown that, for example, Q_{HM} for wheat varied between 1.1 and 4.0 and Q_Y between 0.8 and 1.2. This variation might have been caused by genotypic variation in internal distribution. However, at the regional scale modelling with constant Q_{HM} and Q_Y seems acceptable. At the field scale, we would possibly have to consider genotypic variation.

Many investigators observed that to a high degree Cd was retained in roots. For example, Jarvis et al. (1976) examined the uptake of Cd by the roots of plants and its transport to shoots using solution culture technique. They investigated 23 species and found that between 35% and 91% of Cd taken up was retained in the roots. Winter wheat, for example, retained 68%. The percentages given are probably much higher than under field conditions. The experiments did not last for a complete vegetation period. The authors examined the distribution between roots and shoots four days after a single, three-day exposure to a nutrient solution containing 10 $\mu g\ L^{-1}$ added Cd. However, Cataldo et al. (1981) have shown that especially at maturity high amounts of Cd are remobilized to the shoots or rather the seeds of plants. Reevaluating of wheat data from Lübben's pot experiments (Lübben, 1993, p.206-207) revealed that on average about 20% of the total Cd taken up was retained in roots. This might be a reason why the model, for example, overestimated the observed Cd contents of wheat grain by 12%. The model assumes that the Cd taken up is totally transported to the shoots. Consequently, if a part of the Cd is retained in the roots, the model overestimates the Cd content of shoots. Expanding the transpiration-based model by a root compartment would probably improve the results. Unfortunately, sampling as well as sample preparation of roots is extremely difficult under field conditions. However, for application to plants with considerable root-shoot barriers like soybean or bush beans the model would certainly have to be extended by such a compartment.

Several studies have shown that Zn and also other cations are able to inhibit Cd uptake (Cataldo et al., 1983; Jarvis et al., 1976; Shanker et al., 1996). However, whether competitive inhibition becomes important depends strongly on the concentration of competing cations. For example, Jarvis et al. (1976) observed a depression of the uptake of Cd by ryegrass at a Zn concentration of about 6,500 $\mu g\ L^{-1}$. In the present study at all sites except one, no evidence was found for a

depression of the uptake of Cd by Zn competition. In the soils of the *WIA* the Zn concentration in Ap horizons was at maximum about 350 µg L^{-1}. This concentration is markedly lower than that used in the study mentioned above.

Finally, it must be pointed out that the success of any future experiment to validate the plant uptake model will strongly depend on the accurate choice of the method to determine the concentration in soil solution. This issue, however, has already been discussed in connection with Cd displacement (see Chapter 8.7.1).

9 Simple Assessment Tools

9.1 Introduction

The next section presents two simple tools to assess the effect of soil Cd on ground water and food quality. These tools are simple in the sense that they do not use a numerical model, operate with simplified assumptions and need less input data. However, despite their simplicity these tools are based on the same physics as the model *SEFAH*.

In contrast to the German sewage sludge regulation (AbfKlärV, 1992), which prescribes limits in terms of aqua regia content, both tools are using the concentration in soil solution of the Ap horizon as a starting point. First of all, a threshold Cd concentration C_{th} is determined for the solution phase. This concentration should guarantee that a valuable function of soil (e.g. ground water protection) is not disturbed. Based on Freundlich sorption the amount of Cd which is involved in sorption-desorption reactions at the selected solution phase concentration is calculated. This amount will henceforth be labelled limit sorption capacity (*LSC*). A similar notion was already formulated by Brümmer (1978). The *LSC* can be transformed to an aqua regia content, henceforth labelled as tolerable total content (*TTC*), provided a statistical relationship between both variables can be set up. In order to test the suitability of the approach, the effect of calculated *TTCs* on ground water quality will be checked by numerical simulations using the model *SEFAH*. Finally, the *TTCs* will be compared with the limit of the German sewage sludge regulation (AbfKlärV, 1992).

Breakthrough times (*BTT*) of Cd to ground water are determined by means of a piston-flow approach. This approach is similar to that used by Gäth (1996). The accuracy of the procedure will also be tested by a comparison with the model

SEFAH. For both *TTC* and *BTT*, maps will be computed by means of block kriging. After investigating reliability and confidence of the maps an optimal sampling strategy will be derived. The field observations of the first sampling campaign (Chapter 5.1) supply the experimental database of this section.

9.2 Theory

9.2.1. Determination of the Threshold Concentration

A threshold concentration C_{th} should guarantee that a valuable function of soil is not disturbed. Important functions concern, for example, the protection of food and ground water quality. They may be defined as follows:

1) Ground water protection: A soil is capable to protect ground water against harmful Cd pollution as long as it is ensured that a specific concentration in ground water can be kept below a given limit, C_{gw}^{*} (µg L^{-1}).

2) Food protection: A soil is suitable for food production as long as the Cd content of a processed plant part is below a given limit, C_{f}^{*} (mg kg^{-1}).

The question now is which concentration in soil solution ensures these valuable soil functions. Let us start with the topic of ground water protection:

Assuming steady state and that the local dispersion is negligible the solute transport equation (Equation (50)) simplifies to

$$-\frac{\partial qC}{\partial z}-\phi=0 \tag{89}$$

Applying Equation (63) for the sink term ϕ yields after integration

$$qC-\eta T_P C\exp(-\varpi z)=const \tag{90}$$

Equation (90) states that the sum of convective solute flux and solute loss by plant uptake is constant. The constant can be calculated from the boundary condition. At z=0:

$$\left(qC - \eta T_P C \exp(-\varpi z)\right)_{z=0} = q_{\inf} C_{\inf} - f\eta T_P C \tag{91}$$

where f denotes the fraction of Cd taken up by plants which leaves the field by withdrawal of harvest material. The concentration in soil solution as a function of depth is thus given by

$$C(z) = \frac{q_{\inf} C_{\inf}}{q(z) - \eta T_P \left(\exp(-\varpi z) - f\right)} \tag{92}$$

If only processed plant parts are withdrawn from the field f is defined as

$$f = \frac{1}{1 + Q_Y Q_{HM}} \tag{93}$$

Inserting Equation (48) into Equation (92) yields

$$C(z) = \frac{q_{\inf} C_{\inf}}{P + I - E - T_P + (1-\eta) T_P \exp(-\varpi z) + f\eta T_P} \tag{94}$$

If the soil is ploughed Equation (94) splits into two terms

$$C(z) = \begin{cases} \dfrac{q_{\inf} C_{\inf}}{P + I - E - T_P + (1-\eta) T_P \exp(-\varpi z_{Ap}) + f\eta T_P} & 0 < z \le z_{Ap} \\ \dfrac{q_{\inf} C_{\inf}}{P + I - E - T_P + (1-\eta) T_P \exp(-\varpi z) + f\eta T_P} & z_{Ap} < z < \infty \end{cases} \tag{95}$$

According to Equation (95) three major cases can be distinguished when a soil is covered by plants (Figure 52): (1) If the uptake of Cd by a plant is directly proportional to the mass flow (η=1), the solution concentration is constant with depth, (2) if only water but no Cd is taken up by plants (η=0) the concentration increases below the Ap horizon and converges to a constant concentration below

the root zone, and (3) if the uptake of Cd is enhanced (η>1) the concentration decreases below the Ap horizon and reaches a constant concentration below the root zone.

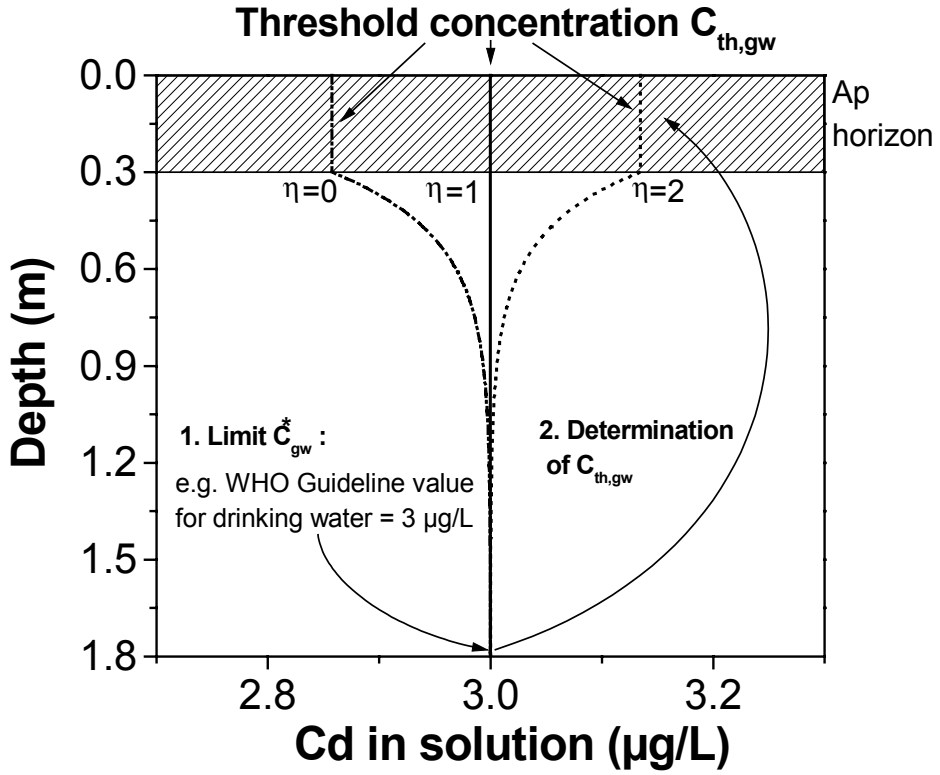

Figure 52: Which concentration in soil solution ensures that the concentration in seepage water at the depth of water table stays just below the limit C^*_{gw}? The figure gives steady state concentration profiles for η=0 (no plant uptake), η=1 (uncontrolled plant uptake) and η=2 (enhanced plant uptake). The climatic conditions were adjusted to average values of the WIA and the calculation was performed for winter wheat.

Assuming $\eta = 1$, as found for winter wheat and Cluster *Alpha* potato, a soil is capable of protecting ground water against harmful Cd pollution as long as the solution phase concentration in the Ap horizon does not exceed C^*_{gw}. Thus, the threshold concentration in soil with regard to ground water protection is

$$C_{th,gw} = C^*_{gw} \qquad for\ \eta = 1 \tag{96}$$

Now we consider the threshold concentration for food quality protection. Presuming that $\eta = 1$, the concentration is constant with depth, and thus, integration of Equation (70) yields

$$C_{th,f} = \frac{\rho_w k_P}{\Delta e} \frac{1 + Q_Y Q_{HM}}{1 + Q_Y} C_f^* \qquad for\ \eta = 1 \tag{97}$$

A soil is suitable for food production as long as the solution phase concentration in the Ap horizon does not exceed $C_{th,f}$.

9.2.2. Limit Sorption Capacity

The ability of soils to protect adjacent environmental compartments like ground water or plants against harmful Cd pollution is determined to a high degree by their sorption capacity. In weakly sorbing soils the same Cd immission leads to higher solution concentrations than in strongly sorbing soils. A physically based approach to quantify the sorption strength of soils is the concept of *LSC*. The *LSC* (mg kg^{-1}) is the amount of Cd which at C_{th} is buffered by a soil:

$$LSC = S + \frac{\theta}{\rho} C_{th} \tag{98}$$

Assuming Freundlich sorption, S can be written as

$$S = k\, C_{th}^m \tag{99}$$

and Equation (98) becomes

$$LSC = k\, C_{th}^m + \frac{\theta}{\rho} C_{th} \tag{100}$$

Since for strongly sorbing solutes (Streck, 1993)

$$k\, C_{th}^m >> \frac{\theta}{\rho} C_{th} \tag{101}$$

we may use the following approximation:

$$LSC \cong k\, C_{th}^{m} \tag{102}$$

The calculation of *LSC* always requires the specification of C_{th}. For example, in the following *LSC 3* denotes the *LSC* at the concentration in soil solution of 3 µg L^{-1}. Because of the dominant importance of the Ap horizon we restrict the calculation of *LSC* to topsoils.

To allow for a comparison with other limit or guideline values it is useful to convert the *LSC* into a aqua regia content. Here, converted *LSC* are labelled tolerable total contents (*TTC*). *TTC* values can only be specified if a statistical relationship between total concentration and aqua regia content can be established (e.g. Equation (75)).

9.2.3. Breakthrough Time

While the concept of *LSC* focuses on the topsoil, this section deals exclusively with the subsoil. By calculating breakthrough times (*BTT*) we aim at answering the question how fast Cd will be transported through the subsoil to the ground water at a constant infiltrating concentration. This time span depends mainly on sorption strength of subsoil and water flux. Using a "piston-flow" approach (Streck, 1993; Gäth, 1996) which neglects local dispersion the breakthrough time *BTT* (yr) of a solute through an unloaded subsoil to the ground water can be calculated by

$$BTT = \frac{1}{q}\sum_{i=1}^{n} h_i \left(\theta_i + \rho_i \frac{S_i(C_{\inf})}{C_{\inf}} \right) \tag{103}$$

where C_{inf} (µg L^{-1}) is a constant infiltrating concentration, usually a threshold concentration, and q is the water flux density (m s^{-1}). h_i is the thickness (m), ρ_i the bulk density (kg L^{-1}), θ_i the volumetric water content (% by volume) and S_i the sorbed phase concentration (µg kg^{-1}). The subscript i denotes the i-th soil

layer below the Ap horizon. The *n*-th layer is assumed to be bordered by ground water. Inserting Equation (99) and using Equation (101) yields

$$BTT \cong \frac{1}{qC_{\inf}^{1-m}} \sum_{i=1}^{n} h_i \rho_i k_i \qquad (104)$$

Calculations require the specification of the infiltrating concentration applied. For example, *BTT 3* denotes the *BTT* at a constant infiltrating concentration of 3 µg L^{-1}.

9.3 Application

9.3.1. General Preparations

The field observations of the first measuring campaign supply the experimental database for the following calculations. For C_f^* the doubled value of the German food guideline value for wheat grain (0.24 mg Cd kg^{-1}) and for C_{gw}^* the WHO guideline value for drinking water (3 µg Cd L^{-1}) were selected (Table 17). The parameter η was set to unity, and thus, $C_{th,gw}$ is 3 µg L^{-1} (cf. Equation (96)). Using Equation (97) with the parameters for wheat estimated in the present study $C_{th,f}$ becomes 2.1 µg L^{-1} (η=1, k_P=4.0 Pa, Q_{HM}=2.1, Q_Y=0.98, cf. Table 11).

In 38% of samples (N=616) the Freundlich coefficients could be determined experimentally. With the remaining samples, the concentration in soil solution was below the detection limit. In these cases the Freundlich coefficients *k* were calculated from *p*H and *OC* by the pedotransfer function *PTF 2b* (Chapters 5.3 and 7.4). The calculated *LSC* were transformed to tolerable total contents *TTC* by applying Equation (75).

Table 17: National and international drinking water and ground water guideline and limit values for Cd.

Guideline and limit values	**Cd**
	µg L^{-1}
Drinking water	
Limit of the German drinking water regulation (TrinkV, 1986)[§]	5
Guideline value for drinking water (WHO, 1993) [$]	3
Ground water	
Netherlands List (1994)	
- Reference value (S-value) [&]	0.4
- Intervention value (I-value) [#]	6
Anonymous (1993)	
- H-W value for ground water [‡]	1
- P-W value for ground water [†]	3
- P_{max} value for ground water [††]	8

[§] Limits are maximum values which, in general, may not be exceeded.

[$] The guideline value is intended to help to establish national limits.

[&] The reference value represents concentrations of "normal" unpolluted ground water.

[#] Measures of remediation are regarded as necessary.

[‡] Background concentration in unpolluted ground water.

[†] Trigger value to protect the ground water against harmful immissions from contaminated soils. Detailed investigations are necessary.

[††] Tolerance value to protect the ground water against harmful immissions by contaminated soils. Measures of remediation are regarded as necessary. Higher concentrations than the P_{max} value can be tolerated at a toxicologically low risk of human health.

For the calculation of breakthrough times the following assumptions were made: The mean water flow density was set to 570 mm yr^{-1} (Chapter 8.4.1). Mean bulk densities of 1.51 kg L^{-1} were assumed for the Ap and of 1.67 kg L^{-1} for the sub-soil horizons (Chapter 8.4.3). When the interpolated depth of water table (Chapter 8.4.2) was below the sampling depth, the sorption characteristic of the unsampled soil zone was approximated by that of the deepest sampled layer.

The environmental fate model *SEFAH* was used to test the assessment tools. The regional simulation was performed by applying the *DSC 1a Hybrid* modelling approach (Chapter 8.2). Deep ploughing due to asparagus cultivation (Chapter

6.2.3 and 7.2) was ignored in all simulations. The breakthrough time was defined as the time at which the concentration in seepage water reached 50% of the infiltrating concentration.

9.4 Results

9.4.1. Tolerable Total Contents

Calculated tolerable total Cd contents for different threshold concentrations are given in Table 18. Remember that the observed mean aqua regia Cd content in Ap horizons was 0.36 mg kg^{-1} (cf. Table 4). Comparison with the calculated *TTCs* shows that on the regional average neither the *TTC 2.1* (0.48 mg kg^{-1}) nor the *TTC 3* (0.61 mg kg^{-1}) is exceeded in Ap horizons of the *WIA*. However, the aqua regia content exceeds at 30% and 17% of sites the *TTC 2.1* and *TTC 3*, respectively. Thus, at the regional mean soils are still suited for wheat production as well as for ground water protection. Locally, however, both soil functions are partly restricted.

The limit according to the AbfKlärV (1992) of 1 mg kg^{-1} exceeds the calculated *TTC 2.1* and *TTC 3* in 97% and 90% of sites, respectively. Hence, in the sandy soils of the *WIA* the limit is neither suited to guarantee Cd contents in wheat grain below 0.24 mg kg^{-1} nor sufficient to ensure Cd concentrations in seepage water below 3 µg L^{-1}.

Table 18: Calculated tolerable total Cd contents for different threshold concentrations. 147 Ap horizons within the WIA were investigated.

Threshold concentration	**Tolerable total Cd content in the Ap horizons**					
	$\overline{X}$	$\overline{X}_{0.5}$	Min.	Max.	$C_{AR} > TTC$	Limit of AbfKlärV (1992) protects soil function [§]
— µg L^{-1} —	———— mg kg^{-1} ————				— % —	% of sites
1[†]	0.30	0.27	0.10	1.05	63	1
2.1[‡]	0.48	0.44	0.14	1.79	30	3
3[†]	0.61	0.56	0.17	2.32	17	10
5[†]	0.88	0.80	0.23	3.39	9	30
8[†]	1.23	1.11	0.31	4.80	3	56

[†] Possible threshold concentrations with regard to ground water protection

[‡] Threshold concentration for wheat production. According to the transpiration-based model the Cd content in wheat grain exceeds the limit of 0.24 mg/kg at a concentration in soil solution higher than 2.1 µg/L.

[§] The limit of the German sewage sludge regulation for sandy soils (clay content < 5% or 5 < *p*H < 6) is 1 mg kg^{-1}.

Figure 53A shows block kriging estimates of the mean *TTC 2.1* within 100 m x 100 m blocks. For kriging the log-transformed *TTC*'s an exponential variogram model with a sill of 0.229 and a practical range of 477 m was used. The map indicates that the most strongly sorbing soils are preferentially located in District 3 and District 4 and there particularly in the western areas. Large areas of weakly sorbing soils (*TTC 2.1* = 0.15-0.35 mg kg^{-1}) were observed especially in the centre of District 1 and District 2. Soils in these areas are particularly susceptible to Cd inputs. Figure 53B shows the blocks whose kriging estimates of the current total Cd content exceeds *TTC 2.1*. The map was produced by overlaying the maps of *TTC 2.1* and C_{AR} (see Figure 10A). In 233 blocks (8% of arable land) the aqua regia Cd content exceeds *TTC 2.1*. These blocks are mainly located in the proximity of the former sludge basins of District 1 and District 3.

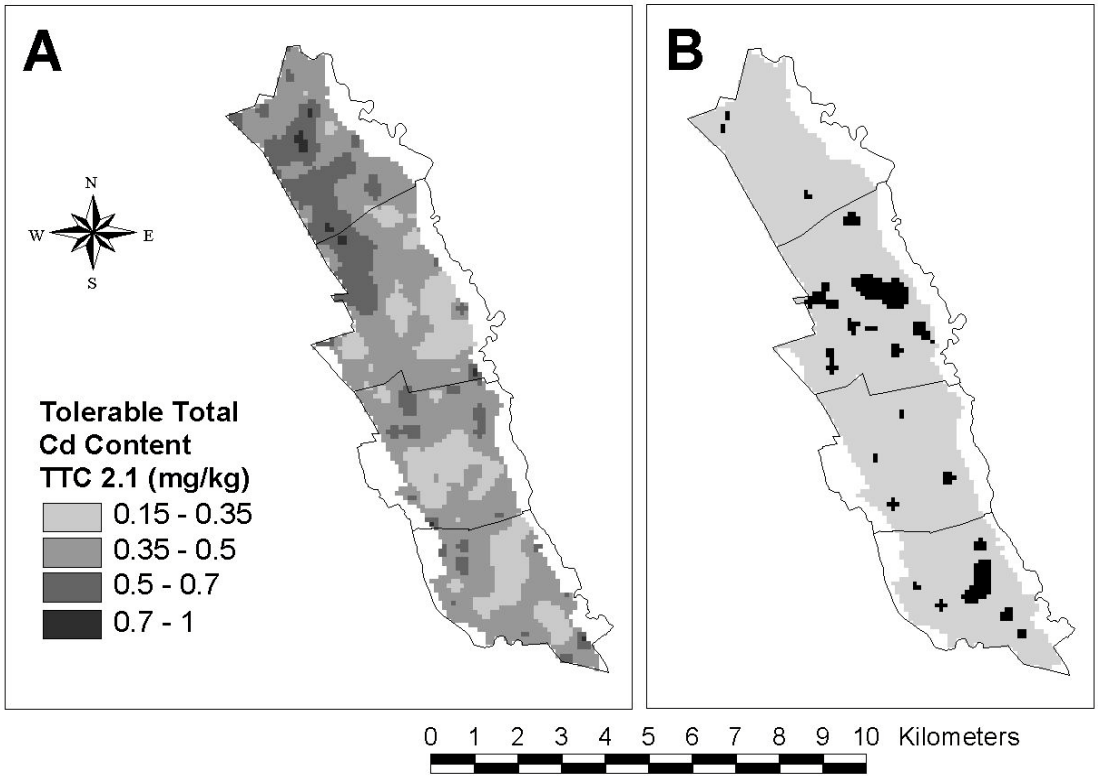

*Figure 53: **A)** Map of block kriging estimates of the mean TTC 2.1 within 100 m x 100 m blocks. **B)** Blocks whose kriging estimate of the current aqua regia Cd content exceeds TTC 2.1.*

Figure 54A shows block kriging estimates of the mean *TTC 3* within 100 m x 100 m blocks. For kriging the log-transformed *TTC 3* an exponential variogram model with a sill of 0.231 and a practical range of 517 m was used. The regional distribution pattern of *TTC 3* is similar to that of *TTC 2.1*. In 30 blocks (1% of arable land) the aqua regia content exceeds *TTC 3* (Figure 54B). Again, these blocks are mainly located in the vicinity of the former sludge basins of District 3 and District 4.

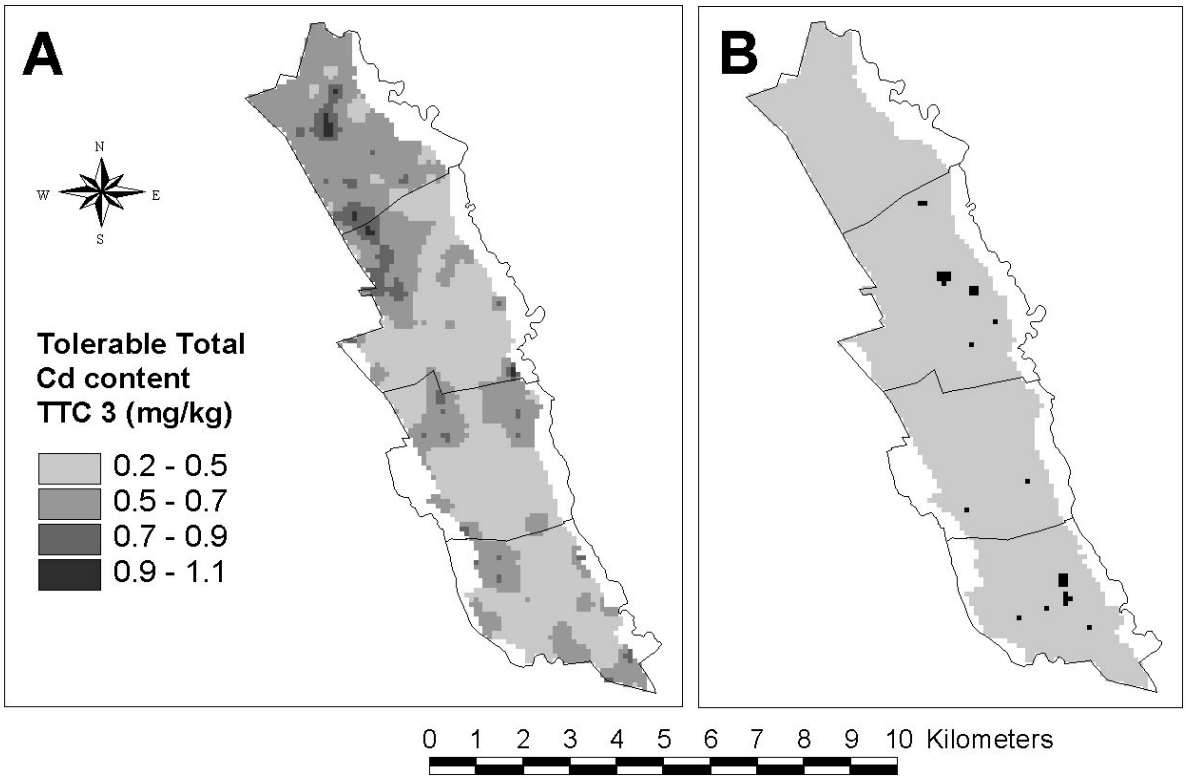

*Figure 54: **A)** Map of block kriging estimates of the mean TTC 3 within 100 m x 100 m blocks. **B)** Blocks whose kriging estimates of the current aqua regia Cd content exceeds TTC 3.*

By a numerical simulation it was tested whether the calculated *TTC 3* can ensure the defined ground water quality goal (3 µg Cd L^{-1}). For a comparison, a similar calculation was carried out using the current limit. Hence, two scenarios were simulated over a period of 200 years. Scenario A: During the entire simulation period the aqua regia Cd contents in Ap horizons were fixed at their *TTC 3*. Scenario B: During the entire simulation period the aqua regia Cd contents in Ap horizons were fixed at the limit of the sewage sludge regulation (1 mg Cd kg^{-1}). Figure 55 presents the results of the numerical simulations. If the aqua regia content of the Ap horizons is kept constant at the level of the soil-specific *TTC 3* (Scenario A) the average concentration in the seepage water at the depth of water table would approach asymptotically 3 µg L^{-1}. After 200 years the mean Cd concentration in the seepage water would increase on the average to 2.4 µg L^{-1} with a coefficient of variation of 50%. At a constant aqua regia Cd

content in Ap horizons of 1 mg kg^{-1} (Scenario B) the mean concentration in the seepage water after 44 years would be 3 µg L^{-1}. After 65 years the concentration of 5 µg L^{-1} would be exceeded and after 200 years the concentration in seepage water would be significantly above 8 µg L^{-1}. For this scenario the coefficient of variation of the concentration in seepage water was 104%. The highest local concentration in the seepage water would be 41 µg Cd L^{-1}.

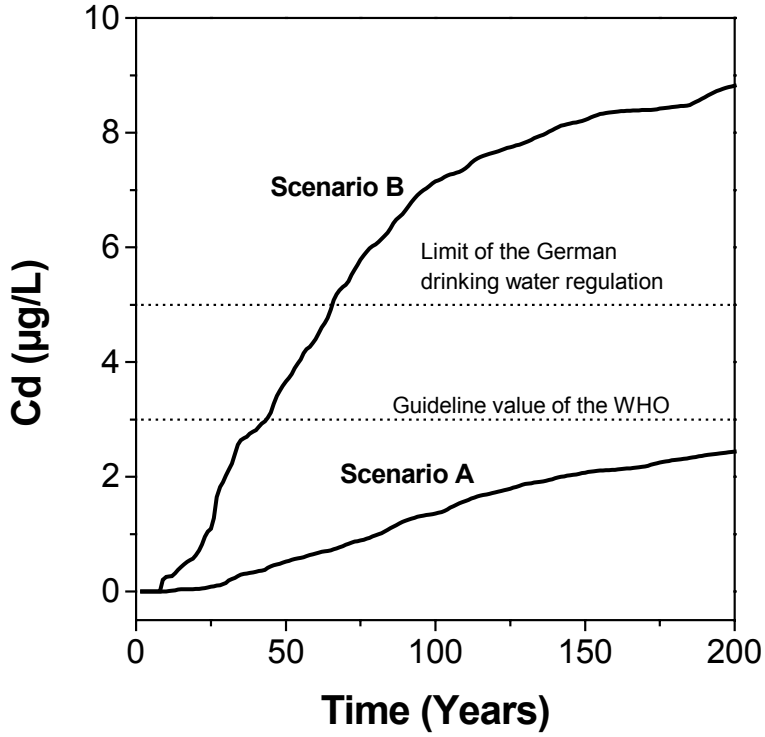

Figure 55: Averaged Cd concentrations in seepage water at the depth of water table. Scenario A: The aqua regia Cd content in Ap horizons is fixed at the site-specific TTC 3 (tolerable total content). Scenario B: The aqua regia Cd content in Ap horizons is kept at the limit of the German sewage sludge regulation (1 mg kg^{-1}).

9.4.2. Breakthrough Times

Based on the map of interpolated depths of water table (Figure 35), measured and estimated Freundlich coefficients, the *BTT* of Cd for an infiltrating concentration of 3 µg L^{-1} was calculated with Equation (104). The *BTT 3* in subsoils is lognormally distributed (*KS*-test, α=0.05). Mean and median are 141 years and

105 years, respectively. The *BTT 3* varies between 10 and 805 years and the interquartile range is 117 years. The accuracy of the piston flow approach was checked by a numerical simulation. The mean deviation between the results obtained by numerical simulation and the piston-flow approach was ± 2 years.

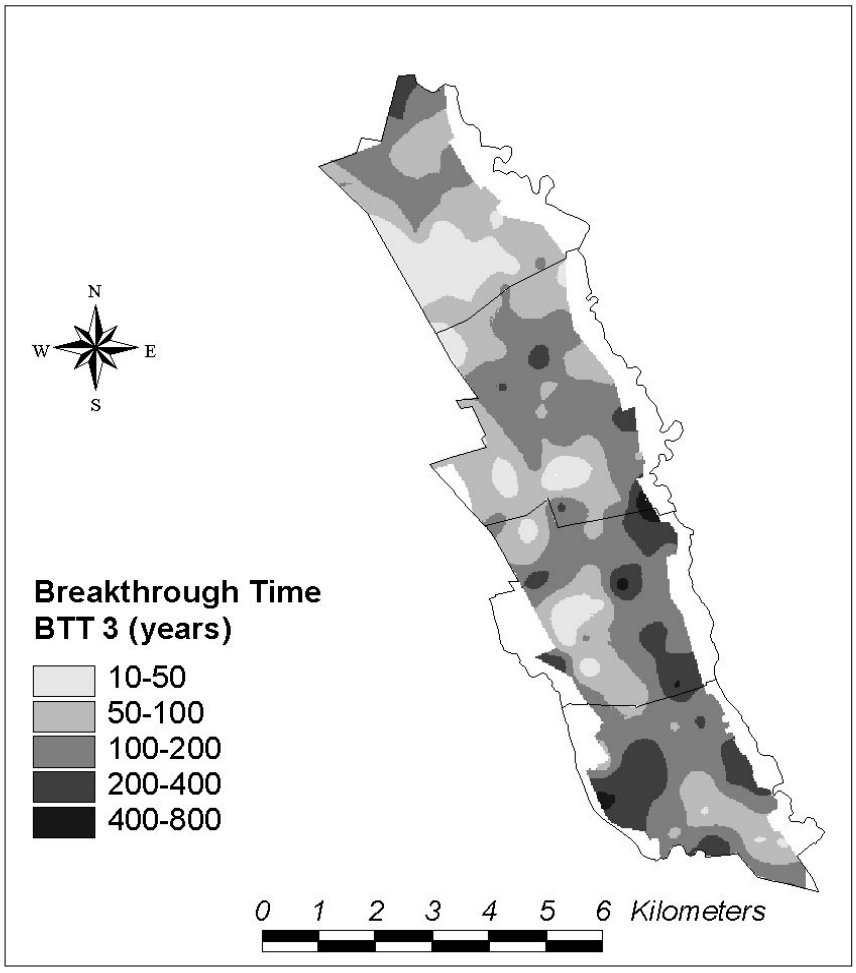

Figure 56: Map of the calculated breakthrough times of Cd for an infiltrating concentration of 3 µg L^{-1} (BTT 3). The mean water flux density was set to 570 mm yr^{-1}. The breakthrough times were calculated with a piston flow approach. Only the subsoil was considered in the calculation.

Figure 56 shows block kriging estimates of the mean *BTT 3* in subsoils within 100 m x 100 m blocks. Large areas with large *BTT 3* (200-800 years) are found in the south-western and eastern parts of the area. Areas with smaller *BTT 3,*

between 10 and 100 years, are estimated for the soils in the west of District 2 and 3 and for the soils in the south of District 4.

9.4.3. Error Analysis

In the previous chapters we estimated *TTC* and *BTT* in unsampled areas by block kriging. The estimates were used, among other things, for detecting areas which exceed a given threshold concentration. If such maps are to be used for management purposes it is particularly important to account for the uncertainty in the estimates. In the following, reliability and confidence of block kriging estimates (100 m x 100 m) for the Cd solution phase concentration in Ap horizons will be evaluated. Kriging was carried out using log-transformed data and an exponential variogram model with a sill of 0.6451 and a practical range of 472 m.

First, the uncertainty of estimates is assessed by confidence intervals (*CI*) (Chapter 3.3.1). Since we are only interested whether the mean of a block is with a given confidence either higher or less than the threshold concentration only one-tailed confidence intervals are computed. At the 10% significance level the one-tailed confidence interval becomes (see Equation (30))

$$CI = \pm 1.282\sigma_R \tag{105}$$

Figure 57 was created on the basis of block kriging estimates and block kriging variances obtained by using the 161 available sampling points. The figure shows the blocks whose mean is, on the 90% confidence level, either higher or less than the chosen threshold concentration of 2.1 µg L^{-1}. Only for 4% of the area a reliable statement is possible at this significance level and the current sample size. In 84 blocks the mean concentration is lower than 2.1 µg L^{-1}, while in 20

blocks it is higher than 2.1 µg L^{-1}. No statement is available about the remaining ≈2,700 blocks.

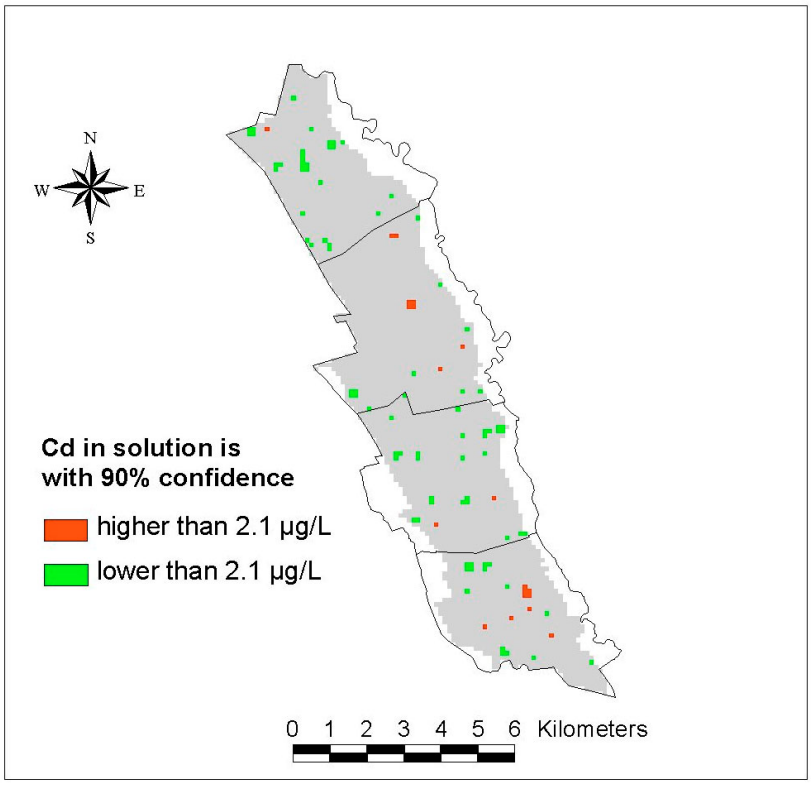

Figure 57: Block kriging estimates whose mean is with 90% confident either higher or less the threshold concentration of 2.1 µg L^{-1}.

Second, we use error maps to look into the question in as much an increase in sampling points would improve our estimation result. First of all, a conditional simulation was computed at 50,000 randomly drawn points within the *WIA*. On the basis of this point data set a reference map of block kriging estimates of the mean value within 100 m x 100 m blocks was computed. This map can be considered as one possible realization of the region. In the next step, different numbers of points (150, 250, 500, 1,000, 2,000, 4,000, 8,000, 16,000, 32,000) were randomly drawn from the point data set and were used for calculating block kriging estimates. The maps were then compared with the reference map and for each block it was determined whether 1) the estimator was correct, 2) the estimator was of Type I error (i.e. a block was falsely classified as not to exceed the

threshold), or 3) the estimator was of Type II error (i.e. a block was falsely classified as to exceed the threshold).

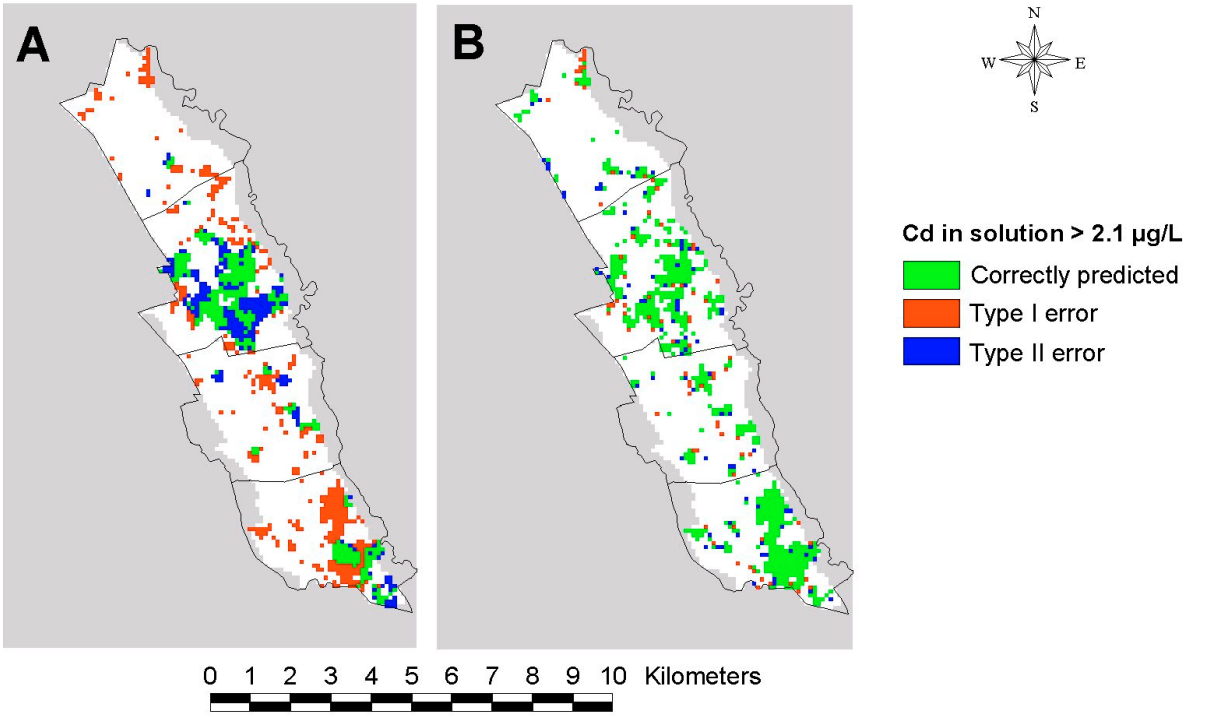

Figure 58: Error map of block kriging estimates for different sample sizes. ***A)*** *N=150.* ***B)*** *N=8000.*

Figure 58 shows the error maps of estimates on the basis of 150 and 8,000 points. The reference map contained 677 blocks (24% of arable land) whose mean is higher than the threshold concentration of 2.1 µg L^{-1}. On the basis of 150 sampling points 519 blocks were predicted to exceed the threshold concentration in total. Only 304 blocks (45%) were correctly predicted. Type I error occurred at 373 blocks, i.e. these blocks were falsely classified as not to exceed 2.1 µg L^{-1}. Type II error occurred with 215 blocks, i.e. these blocks were falsely classified as to exceed 2.1 µg L^{-1}. Increasing the sample size to 8,000 points, both Type I error and Type II error significantly decreased. Altogether 680 blocks were predicted to exceed the threshold concentration. From these 680 blocks 598 blocks (88%) were correctly predicted. Type I occurred at 79 blocks and Type II error was observed at 82 blocks.

Figure 59 gives a more detailed picture of the effect of increasing the sample size on the reliability of block kriging estimates. Both Type I and Type II error decrease strongly with increasing sample size (e.g. Type I error: 373 blocks at N=150 versus 22 blocks at N=32,000). To discover 90% of blocks whose mean is higher than 2.1 µg L^{-1} about 8,000 sampling points would be needed within the *WIA*, corresponding to about 3 points per hectare. If we are satisfied with a rate of correct classification of 75% we would still need 2,000 samplings points corresponding to a sampling density of about 0.7 points per hectare.

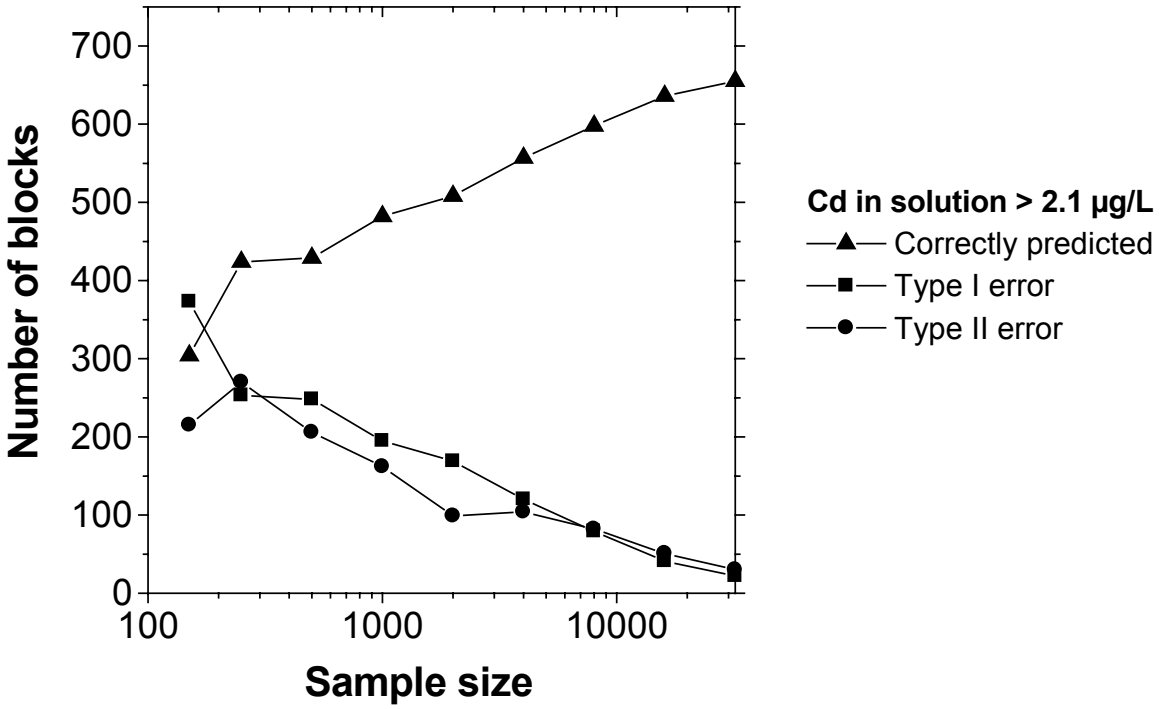

Figure 59: Reliability of block kriging estimates for different sample sizes. The conditional simulated region contained altogether 677 blocks whose mean solution phase concentration in the Ap horizon is higher than 2.1 µg L^{-1}.

9.5 Discussion

The concept of *LSC* permits a simple evaluation of the current and future effects of Cd immission on soils and adjacent environmental compartments. The calculation of *LSC* uses the concentration in soil solution as the starting point since both Cd transport in soil and uptake by plants are mainly controlled by the solution phase and not by a total (e.g. aqua regia) content. Also investigations from ecotoxicology (Van Gestel, 1997) refer to the outstanding role of the concentration in soil solution on the eco- and humantoxicological impact of heavy metals in soils. Consequently, it should be possible to apply the concept of *LSC* to this scientific field as well.

The calculation of the threshold concentrations presumes a mass-flow governed Cd uptake by plants with a η=1. As a consequence, the concentration profile in steady state is assumed constant with depth. Indeed, for winter wheat and Cluster *Alpha* potato we observed an η of unity. If η is smaller than unity, the sufficient threshold concentration is slightly lower. For example, if η is zero the threshold concentration in the Ap horizon has to be 2.86 µg L^{-1} to ensure that the Cd concentration at the depth of water table stays below the limit of 3 µg L^{-1}. However, the case of $\eta < 1$ was not observed in the present study. Instead, a η was observed to be about 2 for the Cluster *Beta* potato. In such a case the threshold concentration in the Ap horizon could be even slightly higher than 3 µg L^{-1}, in this case 3.13 µg L^{-1}.

The threshold concentration to guarantee a sufficient wheat quality (Cd content < 0.24 mg kg^{-1}) was found to be lower than the WHO guideline value for drinking water. According to this result the ground water is automatically protected against harmful Cd pollution as long as the overlaying soil is suitable for wheat production.

With regard to Cd, at the regional mean soils of the *WIA* are still suited for wheat production as well as for ground water protection. Locally, however, both soil functions are partly restricted. Particularly in the proximity of the former sludge basins it is very likely that the Cd content in wheat grain exceeds the limit of 0.24 mg kg^{-1} within larger areas. As explored in the error analysis a better sampling resolution would be necessary to reliably discover all these locations. Both the former sludge basins and the former storage basins were not sampled with sufficient intensity in the scope of this study. Only one sample was taken in the third campaign in 1999 inside the storage basin of District 1. But there is strong evidence that these sites are highly contaminated. If this suspicion should be confirmed in future investigations these sites should be completely excluded from agricultural use.

The error analysis of block kriging estimates shows that the maps presented are mainly suited for visualizing rough trends like, for example, the relationship between the vicinity to the former sewage sludge basins and high Cd loads. But the suitability of these maps for detecting single blocks, or rather fields, which are higher or below a certain threshold value is limited. On the current data basis (161 sampling points) the rate of correct classification is too poor (e.g. about 45% with regard to the solution phase concentration). The results suggest that due to the high spatial variability a sampling density of about 0.7 to 3 points per hectare is necessary to get a reliable overview at each location within the *WIA*. That is, before actions are taken, every single field must be sampled.

The calculated tolerable total Cd contents of the investigated soils were, on the average, 0.48 mg kg^{-1} with regard to food quality protection and 0.61 mg kg^{-1} with regard to ground water protection. The limit given in the AbfKlärV (1992), 1 mg kg^{-1}, is markedly higher than both *TTCs*. Consequently, in the sandy soils of the *WIA* the current limit is neither suited to keep the Cd concentration in

seepage water below the WHO guideline value, 3 μg L^{-1}, nor does it ensure that the Cd content of wheat grain stays below twice the German food guideline value, 0.24 mg kg^{-1}. In case of the sandy soils of the *WIA* it is therefore necessary to lower the Cd limit if a sustainable soil management and the long-term protection of valued soil functions is desired.

The solute transport model used for testing our concept considers neither kinetic sorption (Selim et al., 1992) nor long-term immobilization (Brümmer et al., 1988). The consequence of kinetic sorption would be an earlier increase of the concentration in seepage water, but the asymptotic concentration of the simulated scenarios would not be affected. Immobilization of Cd would lead to higher tolerable total contents in the long run. However, based on our present understanding a quantitative estimation of this process seems not yet possible.

The *BTT* calculated by the piston flow approach agree very well with the results of the numerical simulations. This agreement indicates that the time at which the concentration in seepage water reaches 50% of the input concentration can be calculated by the simple approach presented almost as well as by a rather complex solute transport model. It must be stressed, however, that the piston flow approach neglects local dispersion, so that this approach provides no information about any other parts of the breakthrough curve. A further restriction is that the application of the simplified approach is only possible for specific initial and boundary conditions. For instance, a *BTT* could not be computed in the case of a variable infiltrating concentration. Thus, this approach is primarily a simple tool to evaluate sorption characteristics of the subsoil. Nevertheless, the results show that despite the relatively homogeneous geo- and pedogenetic conditions the computed breakthrough times are highly variable in the investigation area. Moreover, it demonstrates that the effect of a Cd load on ground water quality is delayed by decades or even centuries.

10 Summary

Since the German Soil Protection Act has come into force in 1998, modelling of the environmental fate of heavy metals, with special emphasis given to the forecast of heavy metal concentrations in seepage water, has made a comeback. The present study aimed at investigating the environmental fate of Cd in the soils of the waste water irrigation area (*WIA*) of Braunschweig. The sandy acidic soils (28 km^2) within this region have undergone high loads of heavy metals by irrigation of municipal waste water for up to 40 years. 161 soil monoliths (0-1.2 m) were sampled to study the current status of Cd accumulation as well as the horizontal and vertical variability of sorption characteristics of soils. Moreover, Cd uptake was investigated at 40 potato, 40 sugar beet and 20 winter wheat fields. At each potato and sugar beet field a single plant was collected and soil monoliths were taken. At the winter wheat fields a plot of 0.25 m^2 was sampled.

All soil samples were analysed for *p*H, organic carbon (*OC*) content, EDTA-extractable content and Cd concentration in 0.0025 M $CaCl_2$. It was assumed that (1) the EDTA-extractable content represents the fraction of Cd which participates in sorption-desorption reactions and that (2) by a 24 h equilibration of soil with 0.0025 M $CaCl_2$ the concentration in soil solution can be approximated. Moreover, all topsoil samples were analysed for their aqua regia Cd content. Samples of processed and unprocessed plant parts were separately analysed for their Cd contents.

The Cd contents in soils showed a high spatial variability. The aqua regia Cd content in Ap horizons was 0.36 mg kg^{-1} on average. Particularly in the vicinity of the former sludge and storage basins high Cd contents were found. No relationship between the operation period of districts and Cd loads was observed.

Effects by different operation periods have probably been blurred by the transfer of sewage sludge between districts.

On average Cd has been displaced to about 0.5 m depth. However, Cd displacement is also highly variable. At some sites, even after 40 yr of waste water irrigation no displacement was measurable below the Ap horizon. In contrast, at some sites Cd has been displaced to below 1.2 m. At asparagus sites, Cd has mainly been displaced by deep ploughing and not by leaching. Deep ploughing leads to an instant exchange of soil material as well as of heavy metals between topsoil (0.0-0.3 m) and subsoil (0.3-0.6 m).

Soil *p*H in Ap horizons was both less variable and less continuous than in subsoils. The correlation length increased from about 500 m in Ap horizons to about 3,000 m in subsoils. This finding suggests that in Ap horizons soil *p*H is mainly controlled by agricultural cultivation (liming, fertilization, crop rotation etc.). With increasing depth soil *p*H is more and more controlled by hydro- and geological conditions (depth of water table, parent material etc.). In Ap horizons, the correlation length of *OC* contents was much higher (about 2,200 m) than that of soil *p*H. The *OC* distribution within the *WIA* could partly be traced back to the land use history.

There is evidence that the uptake of Cd by plants essentially depends on the amount of transpired water and hence the average saturation deficit of the air during the vegetation period. For example, the slope of regression between Cd concentration in soil solution and Cd content of wheat grain was 40% higher in a year with a 33% higher saturation deficit. This finding has three implications. Firstly, at locations with different saturation deficits different limits should be imposed to protect plants against harmful Cd pollution. Secondly, the comparability and interpretation of studies on the uptake of Cd by plants which do not report the saturation deficit of the air is limited. Thirdly, the variation in Cd up-

take between plant species may be partly explained by different water use efficiencies.

The model *SEFAH* was used to predict both the displacement of Cd (leaching, annual ploughing and deep ploughing) and its uptake by plants. Spatial variability of soil properties and boundary conditions was taken into account by using a parallel soil column approach. Simulations were performed either by deterministic one-dimensional simulations at points in the region where soil properties had been determined experimentally or by the Monte-Carlo method. Solute leaching in each column was modelled with the convection-dispersion equation. The sorption of Cd was described with an extended Freundlich equation as a function of spatially variable *p*H and *OC* content. Deep ploughing was computed by the use of soil exchange rates. The uptake of Cd by plants was modelled using a transpiration-based approach. The uptake was assumed to be proportional to mass-flow, i.e. the product of water transpired and Cd concentration in soil solution. The results of hindcast simulations agreed well with both the averaged profiles of measured Cd concentrations in soil and observed Cd contents in plants.

After validation through hindcast simulations, the model was used to calculate several retrospective and prospective scenarios with the following results:

(1) If Cd loads had not been reduced in the mid eighties the average Cd content of wheat grain would have been 0.43 mg kg^{-1} in 1996. Thus, the decision of the *BMWA* in the early eighties to take measures against the high Cd inputs was fully reasonable. Without these measures the impact on soil quality would have been tremendous and it is questionable whether the soils of the *WIA* would still be suited for food production today.

(2) If from 1957 to 1996 the Cd loads had been at the maximum level allowed by the AbfKlärV (1992), the Cd content in wheat grain would have been, on average, 0.04 mg kg^{-1} in 1996. By performing a Cd balance it was calculated that the steady state content in wheat grain would be 0.14 mg kg^{-1} under the conditions of the *WIA*.

(3) Presumed that Cd loads are kept at the current level, the average Cd content of wheat grain will gradually decrease from 0.16 mg kg^{-1} in 1996 to about 0.11 mg kg^{-1} in 2046. The mean solution phase concentration in Ap horizons will slowly decrease from 1.74 µg L^{-1} in 1996 to 0.9 µg L^{-1} in 2046. The mean concentration in seepage water will continuously increase in the next decades and reach its maximum (about 0.7 µg L^{-1}) about 2100. Afterwards the concentration will decrease to about 0.5 µg L^{-1} in 2246.

(4) A decrease of the current mean *p*H from 5.8 to 5.5 in Ap horizons would markedly affect the uptake of Cd by winter wheat. Lowering soil *p*H would increase Cd contents in grain by about 35%. In contrast, reducing the variability of *p*H in Ap horizons would have only a minor effect on Cd uptake.

Finally, two simple tools to assess the effect of soil Cd on ground water and food quality were presented, the determination of tolerable total Cd contents (*TTC*) and the calculation of breakthrough times (*BTT*). Both methods start with the selection of a threshold concentration C_{th} in the solution phase. A properly chosen value of C_{th} should guarantee that a valuable soil function (e.g. ground water protection) is not disturbed. Based on the WHO guideline value for drinking water and the German food guideline value for wheat grain values selected for C_{th} in Ap horizons were 2.1 µg L^{-1} and 3 µg L^{-1}, respectively. Limit sorption capacities (*LSCs*), defined as the amount of Cd which is involved in sorption-desorption reactions at the C_{th} selected were calculated assuming Freundlich sorption. The *LSCs* were transformed to total tolerable contents

(*TTCs*) by regression. Breakthrough times, *BTT*, of Cd through the subsoil to the ground water were determined by means of a simple piston-flow approach.

The regional average *BTT* for a Cd concentration of 3 $\mu g\ L^{-1}$ in the infiltrating water is 141 yr and varies between 10 and 805 yr. Thus, the effect of a Cd input on ground water quality is delayed by decades or even centuries.

As far as Cd is concerned at the regional mean the soils of the *WIA* are still suited for wheat production. Also, the quality of ground water is not at risk. Locally, however, soil functions may partly be restricted. Analysis of error of block kriging estimates revealed that based on the current sampling density only a small fraction of these locations can be identified with sufficient confidence. For example, conditional simulations showed that on the current data base only 45% of blocks (100 m x 100 m) whose mean solution phase concentration is higher than 2.1 $\mu g\ L^{-1}$ were correctly classified. Increasing the number of sampling points from 161 to 2,000 or even 8,000 would increase the fraction of correctly predicted blocks to 75% and 90%, respectively.

The tolerable total Cd contents calculated were, on the average, 0.48 $mg\ kg^{-1}$ with regard to food production (wheat) and 0.61 $mg\ kg^{-1}$ with regard to ground water protection. Hence, for the sandy soils of the *WIA* the limit of the German sewage sludge regulation (1 $mg\ kg^{-1}$) is neither suited to keep Cd contents in wheat grain below the legal limit (0.24 $mg\ kg^{-1}$) nor appropriate to ensure Cd concentrations in seepage water below the WHO guideline value for drinking water (3 $\mu g\ L^{-1}$).

Literature

AbfKlärV, 1992. Klärschlammverordnung vom 15.4.1992, BGBl. I, S. 912-934.

Abwasserverband Braunschweig (Editor), 1979. Reinigung und landwirtschaftliche Verwertung kommunaler Abwässer. Verlag Kurt Döring, Braunschweig.

Abwasserverband Braunschweig (Editor), 1995. Reinigung und landwirtschaftliche Verwertung kommunaler Abwässer. Druckerei Schiemann, Wendeburg.

Allen, H.E., 1993. The significance of trace metal speciation for water, sediment and soil quality criteria and standards. Science Total Environ., Supplement.

Ammoozegar-Fard, A., Nielsen, D.R. and Warrick, A.W., 1982. Soil solute concentration distributions for spatially varying pore water velocities and apparent diffusion coefficients. Soil Sci. Soc. Am. J., 46: 3-9.

Anonymous, 1993. Orientierungswerte für die Bearbeitung von Altlasten und Schadensfällen. Gemeinsame Verwaltungsvorschrift des Umweltministeriums und des Sozialministeriums Baden-Württemberg vom 16.9.1993, GABl. S. 1115.

Barber, S.A., 1976. Efficient fertilizer use. In: Agronomic research for food. Madison.

Barber, S.A., 1984. Soil nutrient bioavailability: A mechanistic approach. Wiley & Sons, New York.

Barber, S.A., Walker, J.M. and Vasey, E.H., 1963. Mechanisms for the movement of plant nutrients from the soil and fertilizer to the plant root. J. Agric. Food Chem., 11: 204-207.

BBodSchG, 1998. Gesetz zum Schutz vor schädlichen Bodenveränderungen und zur Sanierung von Altlasten (Bundes-Bodenschutzgesetz) vom 17. März 1998, BGBl. I.: S. 502.

Beven, K., Schulz, K. and Franks, S., 1999. Functional similarity in hydrological modelling at the landscape scale. In: J. Feyen and K. Wiyo (Editors), Modelling of transport processes in soils at various scales in time and space. Wageningen Pers, Wageningen, pp. 725-735.

Bierhuizen, S.F. and Slatyer, R.O., 1965. Effect of atmospheric concentration of water vapour and CO_2 in determining transpiration-photosynthesis relationships of cotton leaves. Agr. Meteorol., 2: 259-270.

Biggar, J.W. and Nielsen, D.R., 1976. Spatial variability of leaching characteristics of a field scale soil. Water Resour. Res., 12(1): 78-84.

Boekhold, A.E., Temminghoff, E.J.M. and Van der Zee, S.E.A.T.M., 1993. Influence of electrolyte composition and pH on cadmium sorption by an acid sandy soil. J. Soil Sci., 44: 85-96.

Boekhold, A.E. and Van der Zee, S.E.A.T.M., 1992. A scaled sorption model validated at the column scale to predict cadmium contents in a spatially variable field soil. Soil Sci., 154(2): 105-112.

Bowling, D.J.F., 1968. Active and passive ion transport in relation to transpiration in *Helianthus annuus*. Planta, 83: 53-59.

Bowling, D.J.F., 1976. Uptake of ions by plant roots. Chapman and Hall, London, 212 pp.

Bowling, D.J.F. and Weatherley, P.E., 1965. The relationship between transpiration and potassium uptake in *Ricinus communis*. Journal of Experimental Botany, 16: 732-741.

Bramm, A., 1976. Einflüsse der Abwasserlandbehandlung auf oberflächennahes Grundwasser - Untersuchungen im Abwasserverband Braunschweig. Ph.D. thesis, Kiel, 173 pp.

Broyer, T.C. and Hoagland, D.R., 1943. Metabolic activities of roots and their bearing on the relation to upward movement of salts and water in plants. American Journal of Botany, 30: 261-273.

Brümmer, G., 1978. Funktion des Bodens im Stoffhaushalt der Ökosphäre. In: G. Olschowy (Editor), Natur- und Umweltschutz in der Bundesrepublik Deutschland. Paul Parey, Hamburg, pp. 111-124.

Brümmer, G.W., Gerth, J. and Herms, U., 1986. Heavy metal species, mobility and availability in soils. Z. Pflanzenernähr. Bodenk., 149: 282-298.

Brümmer, G.W., Gerth, J. and Tiller, K.G., 1988. Reaction kinetics of the adsorption and desorption of nickel, zinc and cadmium by goethite. I. Adsorption and diffusion of metals. J. Soil Sci., 39: 37-52.

Butler, A.P. and Wheater, H.S., 1999. Modeling radionuclide transport and uptake in an integrated lysimeter experiment: I. Model development. J. Environ. Qual., 28: 1938-1946.

Cataldo, D.A., Garland, T.R. and Wildung, R.E., 1981. Cadmium distribution and chemical fate in soybean plants. Plant Physiol., 68: 835-839.

Cataldo, D.A., Garland, T.R. and Wildung, R.E., 1983. Cadmium uptake kinetics in intact soybean plants. Plant Physiol., 73: 844-848.

Cernik, M., Federer, P., Borkovec, M. and Sticher, H., 1994. Modeling of heavy metal transport in a contaminated soil. J. Environ. Qual., 23: 1239-1248.

Christensen, T. and Tjell, J., 1984. Interpretation of experimental results on cadmium crop uptake from sewage sludge amended soil. In: P.D. L'Hermite and H. Ott (Editors), Processing and use of sewage sludge. Reidel, Dodrecht, pp. 358-369.

Cushman, J.H., 1984. Nutrient transport inside and outside the root rhizosphere: Generalized model. Soil Sci., 138(2): 164-171.

Dagan, G. and Bresler, E., 1979. Solute dispersion in unsaturated heterogeneous soil at field scale: I. Theory. Soil Sci. Soc. Am. J., 43: 461-467.

Dämmgen, U., Küsters, A. and Max, W., 1995. Depositions-Wandermeßstelle Meßprogramm "Elm", Niedersächsisches Landesamt für Ökologie, Hildesheim.

Diehl, J.F. and Boppel, B., 1985. Dietary intake of cadmium: a reevaluation. Trace Elements in Med., 2: 167-174.

Djurhuus, J., Hansen, S., Schelde, K. and Jacobsen, O.H., 1999. Modelling mean nitrate leaching from spatially variable fields using effective hydraulic parameters. Geoderma, 87: 261-279.

Dommermuth, H. and Trampf, W., 1990. Die Verdunstung in der Bundesrepublik Deutschland Zeitraum 1951-1980. Selbstverlag des Deutschen Wetterdienstes, Offenbach am Main.

Dowdy, R.H., Latterell, J.J., Hinesly, R.B., Grossman, R.B. and Sullivan, D.L., 1991. Trace metal movement in an aeric ocharaqualf following 14 years of annual sludge application. J. Environ. Qual., 20: 119-123.

Draper, N.R. and Smith, H., 1966. Applied regression analysis. Wiley & Sons, New York.

Dückel, R., 1985. Hydrogeologische Untersuchungen im Bereich des Abwasserverbandes Braunschweig. Diplomarbeit. Braunschweig.

Ehlers, W., 1989. Transpiration efficiency of oat. Agron. J., 81: 810-817.

Ehlers, W., 1996. Wasserverbrauch von Kulturpflanzenbeständen. In: W. Ehlers (Editor), Wasser in Boden und Pflanze: Dynamik des Wasserhaushalts als Grundlage von Pflanzenwachstum und Ertrag. Ulmer, Stuttgart, pp. 105-131.

Elzinga, E.J., Van Grinsven, J.J.M. and Swartjes, F.A., 1999. General purpose Freundlich isotherms for cadmium, copper and zinc in soils. Eur. J. Soil Sci., 50: 139-149.

Epstein, E., 1966. Dual pattern of ion adsorption by plant cells and by plants. Nature, 212: 1324-1327.

Fassbender, H.W. and Steinert, B., 1979. Anfall und chemische Zusammensetzung der städtischen Abwässer von Wolfsburg und Braunschweig. Z. Pflanzenernähr. Bodenk., 142: 219-231.

Filius, A., 1993. Schwermetall-Sorption und -Verlagerung in Böden. Ph.D. thesis. Braunschweig.

Filius, A., Streck, T. and Richter, J., 1991. Freundlich-Isothermen für Schwermetalle bei landwirtschaftlich genutzten Böden. Z. angew. Geowiss., 10: 5-14.

Fischbeck, G., 1993. Einwicklungsphasen in der Steigerung der Hektarerträge wichtiger Kulturpflanzen des Ackerlandes in der Bundesrepublik Deutschland. Ber. Landw., 71: 567-579.

Florijn, P.J. and Van Beusichem, M.L., 1993. Uptake and distribution of cadmium in maize inbred lines. Plant and Soil, 150: 25-32.

Flury, M., 1996. Experimental evidence of transport of pesticides through field soils - A review. J. Environ. Qual., 25: 25-45.

Gäbler, H.-E., Bahr, A. and Mieke, B., 1999. Determination of the interchangeable heavy-metal fraction in soil by isotope dilution mass spectrometry. Fresenius. J. Anal. Chem., 365: 409-414.

Gäth, S., 1996. Verlagerungspotentiale für Schwermetalle in Böden. Forum Städte-Hygiene, 47: 353-357.

Gäth, S., Anthony, F., Becker, K.-W., Geries, H., Höper, H., Kersebaum, C. and Nieder, R. 1997. Bewertung des standörtlichen Denitrifikations- und Mineralisations-/Immobilisations-Potentials von Böden. Mitteilgn. Dtsch. Bodenkundl. Gesellsch., 85: 1373-1376.

Grifferty, A. and Barrington, S., 2000. Zinc uptake by young wheat plants under two transpiration regimes. J. Environ. Qual., 29: 443-446.

Hackenberg, S. and Wegener, H.-R., 1999. Schadstoffeinträge in Böden durch Wirtschafts- und Mineraldünger, Komposte und Klärschlamm sowie durch atmosphärische Deposition. Regionale Frachtenmodelle zur

Bewertung relevanter Schadstoffeinträge. Abfall-Wirtschaft - Neues aus Forschung und Praxis. M.I.C BAEZA-Verlag, Witzenhausen, 220-223 pp.

Hartung, A., 1999. Statistik. R. Oldenbourg Verlag, München.

Hatch, D.J., Jones, L.H.P. and Burau, R.G., 1988. The effect of pH on the uptake of cadmium by four plant species grown in flowing solution culture. Plant and Soil, 105: 121-126.

Haude, W., 1955. Zur Bestimmung der Verdunstung auf möglichst einfache Weise. Mitt. d. Dt. Wetterdienst, 11.

Heger, K., 1978. Bestimmung der potentiellen Evapotranspiration über unterschiedlichen landwirtschaftlichen Kulturen. Mitteilgn. Dtsch. Bodenkundl. Gesellsch., 26: 21-40.

Hendriks, L., Claasen, N. and Jungk, A., 1981. Phosphatverarmung des wurzelnahen Bodens und Phosphataufnahme von Mais und Raps. Z. Pflanzenernähr. Bodenk., 144: 486-499.

Hooymans, J.J.M., 1969. The influence of the transpiration rate on uptake and transport of potassium ions in barley plants. Planta, 88: 369-371.

Hornburg, V., 1991. Untersuchungen zur Mobilität und Verfügbarkeit von Cadmium, Zink, Mangan, Blei und Kupfer in Böden. Bonner Bodenkundliche Abhandlungen. Rheinische Friedrich-Wilhelm-Universität, Bonn.

Hylmö, B., 1953. Transpiration and ion absorption. Physiologia Plantarum, 6: 333-405.

Isaaks, E.H. and Srivastava, R.M., 1989. An introduction to applied geostatistics. Oxford University Press, New York.

Jarvis, S.C., Jones, L.H.P. and Hopper, M.J., 1976. Cadmium uptake from solution by plants and its transport from roots to shoots. Plant and Soil, 44: 179-191.

Jones, K.C., Symon, C.J. and Johnston, A.E., 1987. Retrospective analysis of an archived soil collection. II: Cadmium. Science Total Environ., 67: 75-89.

Journel, A.G. and Huijbregts, C.J., 1991. Mining geostatistics. Academic Press, London.

Jury, W.A. and Flühler, H., 1992. Transport of chemicals through soil: Mechanisms, models, and field applications. Adv. Agronomy, 47: 141-201.

Jury, W.A., Gardner, W.R. and Gardner, W.H., 1991. Soil Physics. Wiley & Sons, New York.

Kehres, B., 1994. Kompost und Stoffkreislauf. In: B.A.B. e.V. (Editor), Bodenschutz und Kompost, pp. 68-83.

KrWAbfG, 1994. Gesetz zur Förderung der Kreislaufwirtschaft und Sicherung der umweltverträglichen Beseitigung von Abfällen (Kreislaufwirtschafts- und Abfallgesetz) vom 27. September 1994, BGBl. I.

Kücke, M. and Löffler, P., 1989. Untersuchungen zum Wurzelwachstum von Getreide und Zuckerrüben auf unterschiedlich schweren Standorten. Mitteilgn. Dtsch. Bodenkundl. Gesellsch., 59: 741-744.

Kung, K.-J.S., 1990. Preferential flow in a sandy vadose zone. 2. Mechanism and implications. Geoderma, 46: 59-71.

Lenz, H.-M., Mull, R. and Kunst, S., 1998. Einfluß der landwirtschaftlichen Abwasserverwertung auf die Grundwasserqualität. Z. f. Kulturtechnik und Landentwicklung, 39: 17-22.

Lilliefors, H.W., 1967. On the Kolmogorov-Smirnov test for normality with mean and variance unknown. J. Amer. Statist. Assoc., 62: 399-402.

Loague, K. and Green, R.E., 1991. Statistical and graphical methods for evaluating solute transport models: Overview and application. J. Contam. Hydrol., 7: 51-73.

Lübben, S., 1993. Vergleichende Untersuchungen zur Schwermetallaufnahme verschiedener Kulturpflanzen aus klärschlammgedüngten Böden und deren Prognose durch Bodenextraktion. Landbauforschung Völkenrode, Sonderheft 140. Bundesforschungsanstalt für Landwirtschaft Braunschweig-Völkenrode, Braunschweig.

Maidment, D.R., 1993. Handbook of Hydrology. McGraw-Hill, New York.

Marquardt, H. and Schäfer, S.L. (Editors), 1994. Cadmium. Lehrbuch der Toxikologie. BI- Wiss. Verlag, Mannheim.

Mengel, K., 1991. Ernährung und Stoffwechsel der Pflanze. Gustav-Fischer Verlag, Jena.

Meuser, H., Litz, N., Renger, M. and Fleige, H., 1985. Untersuchung zur Wurzellänge und -oberfläche von Winterweizen auf unterschiedlichen Standorten. Mitteilgn. Dtsch. Bodenkundl. Gesellsch., 43: 661-666.

Mühlnickel, R., Sängerlaub, G. and Gebhardt, H., 1989. Schwermetallanreicherung in den Böden des Abwasserbehandlungsgebietes Braunschweig. Z. Pflanzenernähr. Bodenk., 152: 93-97.

Mullins, G.L., Sommers, L.E. and Barber, S.A., 1986. Modeling the plant uptake of cadmium and zinc from soils treated with sewage sludge. Soil Sci. Soc. Am. J., 50: 1245-1250.

Netherlands List, 1994. Interventions- (I-Werte) und Referenzwerte (S-Werte) für Böden und Grundwasser. In: Rosenkranz, D., Einsele, G. and Harress, H.-M. (Editors), Bodenschutz. Berlin, pp. 1-4.

Nieder, R., Scheithauer, U. and Richter, J., 1993. Dynamics of nitrogen after deeper tillage in arable loess soils of West Germany. Biol. Fertil. Soils, 16: 45-51.

Omoti, U. and Wild, A., 1979. Use of fluorescent dyes to mark the pathways of solute movement through soils under leaching conditions. 2. Field experiments. Soil Sci., 128: 93-104.

Parker, J.C. and Van Genuchten, M.T., 1984. Flux-averaged and volume-averaged concentrations in continuum approaches to solute transport. Water Resour. Res., 20: 866-872.

Pebesma, E.J. and Wesseling, C.G., 1998. GStat: A program for geostatistical modelling, prediction and simulation. Computers & Geosciences, 24(1): 17-31.

Press, J., Flannery, B.P., Teukolsky, S.A. and Vetterling, W.T., 1988. Numerical recipes in C: The art of scientific computing. Cambridge University Press, Cambridge.

Refsgaard, J.C. and Butts, M.B., 1999. Determination of grid scale parameters in catchment modelling by upscaling local scale parameters. In: J. Feyen and K. Wiyo (Editors), Modelling of transport processes in soils at variouns scales in time and space. Wageningen Pers, Leuven, pp. 650-665.

Ritchie, J.T., Kissel, D.E. and Burnett, E., 1972. Water movement in undisturbed swelling clay soil. Soil. Sci. Soc. Am. Proc., 36: 874-879.

Roth, D., Günther, R. and Roth, R., 1988. Transpirationskoeffizienten und Wassernutzungsraten von Getreide, Hackfrüchten und Silomais unter Feldbedingungen und in Gefäßversuchen. Arch. Acker-Pflanzenbau Bodenkd., 32: 397-403.

Schimmack, W. and Bunzl, K., 1986. Migration of solutes in a cultivated soil: effect of ploughing. Geoderma, 38: 155-163.

Schmidtke, K., Rauber, R., Stubbe, B., Homburg, M. and Heckemeier, K., 1999. Wurzelwachstum von Kartoffeln. Kartoffelbau, 50: 13-15.

Schulte, A. and Beese, F., 1994. Isotherms of Cadmium sorption density. J. Environ. Qual., 23: 712-718.

Selim, H.M., Buchter, B., Hinz, C. and Ma, L., 1992. Modeling the transport and retention of Cadmium in soils: Multireaction and multicomponent approaches. Soil Sci. Soc. Am. J., 56: 1004-1015.

Shanker, K., Mishra, S., Srivastava, S., Srivastava, R., Dass, S., Prakash, S. and Srivastava, M.M., 1996. Effect of selenite and selenate on plant uptake of cadmium by maize (*Zea mays*). Bull. Environ. Contam. Toxicol., 56: 419-424.

Smith, G.D., 1985. Numerical solution of partial differential equations: Finite difference methods. Clarendon Press, Oxford.

Springob, G. and Böttcher, J., 1998a. Parameterization and regionalization of Cd sorption characteristics of sandy soils. I. Freundlich type parameters. Z. Pflanzenernähr. Bodenk., 161: 681-687.

Springob, G. and Böttcher, J., 1998b. Parameterization and regionalization of Cd sorption characteristics of sandy soils. II. Regionalization: Freundlich *k*

estimates by pedotransfer functions. Z. Pflanzenernähr. Bodenk., 161: 689-696.

Streck, T., 1993. Schwermetallverlagerung in einem Sandboden im Feldmaßstab - Messung und Modellierung, Ph.D. thesis, Braunschweig.

Streck, T. and Piehler, H., 1998. On field-scale dispersion of strongly sorbing solutes in soils. Water Resour. Res., 34: 2769-2773.

Streck, T. and Richter, J., 1997a. Heavy metal displacement in a sandy soil at the field scale: I. Measurements and parameterization of sorption. J. Environ. Qual., 26: 49-56.

Streck, T. and Richter, J., 1997b. Heavy metal displacement in a sandy soil at the field scale: II. Modeling. J. Environ. Qual., 26: 56-62.

Swartjes, F.A., 1990. Numerische Simulation der eindimensionalen Schwermetallverlagerung im homogenen gesättigten/ungesättigten Böden, Ph.D. thesis, Berlin.

TA-Siedlungsabfall, 1993. Technische Anleitung zur Verwertung, Behandlung und sonstiger Entsorgung von Siedlungsabfällen vom 14. Mai 1993, BAnz. S. 4967.

Tiktak, A., Alkemade, J.R.M., Van Grinsven, J.J.M. and Makaske, G.B., 1998. Modelling cadmium accumulation at a regional scale in the netherlands. Nutrient Cycling in Agroecosystems, 50: 209-222.

Trapp, S. and Pussemier, L., 1991. Model calculations and measurements of uptake and translocation of carbamates by bean plants. Chemosphere, 22: 327-339.

TrinkV, 1986. Die Verordnung über Trinkwasser und Wasser für Lebensmittelbetriebe vom 22.05.1986, BGBl. I. S. 760.

Umweltbundesamt, 1997. Daten zur Umwelt. Erich Schmidt Verlag, Berlin.

Van der Zee, S.E.A.T.M. and Van Riemsdijk, W.H., 1987. Transport of reactive solute in spatially variable soil systems. Water Resour. Res., 23: 2059-2069.

Van Gestel, C.A.M., 1997. Scientific basis for extrapolating results from soil ecotoxity tests to field conditions and the use of bioassays. In: N.M. van Straalen and H. Løkke (Editors), Ecological Risk Assessments in Soil. Chapman and Hall, London, pp. 25-49.

Vázquez, M.D., Poschenrieder, C. and Barceló, J., 1992. Ultrastructural effects and localization of low cadmium concentrations in bean roots. New Phytol., 120: 215-226.

Weigel, H.-J., 1991. Zur Ökotoxikologie des Schwermetalls Cadmium: Untersuchungen über Aufnahme, Verteilung und Wirkung des Metalls bei Pflanze und Tier. Habilitationsschrift, Braunschweig.

WHO, 1972. Evaluation of certain food additives and contaminants mercury, lead and cadmium. Rep. No. 505, Joint FAO/WHO expert commitee on food additives, Geneva.

WHO, 1993. Guidelines for drinking water quality. Recommendations, Vol. 1, Geneva.

Zeien, H. and Brümmer, G.W., 1989. Chemische Extraktionen zur Bestimmung von Schwermetallbildungsformen in Böden. Mitteilgn. Dtsch. Bodenkdl. Gesellsch., 59: 505-510.

Zingk, M. and Blume, H.-P., 1987. Zur nutzbaren Feldkapazität von Sandböden. Mitteilgn. Dtsch. Bodenkdl. Gesellsch., 55: 265-268.

Appendix

Table A1: List of most important symbols.

Symbol	Definition	Unit
a	empirical parameter of the extended Freundlich equation	
ANOVA	one-way analysis of variance	
b	empirical parameter of the extended Freundlich equation	
BMWA	Braunschweig Municipal Waste Water Association	
BTT	breakthrough time	yr
C	concentration in soil solution	kg m^{-3}
C_{AR}	aqua regia content	mg kg^{-1}
C_{EDTA}	EDTA-extractable content	mg kg^{-1}
C_{inf}	concentration of infiltrating water	kg m^{-3}
C_P	content in processed plant parts	kg kg^{-1}
C_{Pr}	concentration in precipitation	kg m^{-3}
C_T	total concentration	mg kg^{-1}
C_{th}	threshold concentration	µg L^{-1}
$C_{th,f}$	threshold concentration with regard to food production	µg L^{-1}
$C_{th,gw}$	threshold concentration with regard to ground water protection	µg L^{-1}
C_U	content in unprocessed plant parts	kg kg^{-1}
C_W	concentration in waste water	kg m^{-3}

C^*_{gw}	limit in ground water	µg L^{-1}
C^*_f	limit in processed plant parts	mg kg^{-1}
CDE	convection-dispersion equation	
CV	coefficient of variation	%
D	effective dispersion coefficient	m^2 s^{-1}
D_S	apparent dispersion coefficient	m^2 s^{-1}
DI	displacement index	%
DSC	deterministic soil column	
E	evaporation rate	m s^{-1}
EF	modelling efficiency	%
f	fraction of Cd taken up by plants which leaves the field with the harvest material	%
h_i	thickness of layer *i*	m
I	irrigation rate	m s^{-1}
k	Freundlich coefficient	kg^{-m} m^{3m}
k^*	intrinsic Freundlich coefficient	kg^{-m} m^{3m}
k_P	crop-specific constant	Pa
KS-test	Kolmogorov-Smirnov test	
LSC	limit sorption capacity	mg kg^{-1}
m	Freundlich exponent	
OC	organic carbon	% by mass
P	precipitation rate	m s^{-1}
pET	potential evapotranspiration rate	m s^{-1}

PTF	Pedotransfer function	
q	volumetric water flux density	$m\ s^{-1}$
Q_{HM}	Cd content ratio between unprocessed (e.g. straw) and processed (e.g. grain) plant parts	
Q_Y	dry matter yield ratio between unprocessed (e.g. straw) and processed (e.g. grain) plant parts	
R	retardation factor	
$R(z_{Ap})$	fraction of plant roots within the Ap horizon	
R^2	coefficient of determination	
rH	relative humidity	%
RSC	random soil column	
S	sorbed phase concentration	$kg\ kg^{-1}$
SD	standard deviation	
t	time coordinate	s
T	temperature	°C
T_P	transpiration rate	$m\ s^{-1}$
TTC	tolerable total content	$mg\ kg^{-1}$
t-test	Student's t-test	
v	pore water velocity	$m\ s^{-1}$
WIA	waste water irrigation area	
Y	dry matter production	$kg\ m^{-2}\ s^{-1}$
z	space coordinate	m
z_{Ap}	thickness of Ap horizon	m

α_i	soil exchange rate between the Ap horizon and the *i*-th compartment	kg m^{-2}
ϕ	sink term	kg m^{-3} s^{-1}
ϕ_i	sink term of the *i*-th compartment	kg m^{2} s^{-1}
η	crop-specific empirical parameter	
λ	local dispersion length	m
ω	empirical parameter describing the root distribution with depth	m^{-1}
θ	volumetric water content	% by volume
ρ	bulk density	kg m^{-3}
ρ_w	density of water	kg m^{-3}
$\overline{C}$	average content of total dry matter	kg kg^{-1}
Δe	average saturation deficit of the air during the main vegetation period	Pa

Table A2: Measured data of the first sampling campaign in 1996. For space reasons, the table presents only data of Ap horizons. The complete data set including the subsoil data can be supplied on inquiry.

C_{AR}: Aqua regia Cd content.

C_{EDTA}: 0.025 M $(NH_4)_2$-EDTA-extractable Cd content.

C: Cd concentration in 0.0025 M $CaCl_2$ after 24 h of equilibration.

OC: Organic carbon.

		Gauß-Krüger-coordinates		Soil properties in Ap horizon				
ID	***District***	***X***	**Y**	C_{AR}	C_{EDTA}	C	***OC* content**	***p*H value**
——	——	—— m ——	—— m ——	µg kg^{-1}	µg kg^{-1}	µg L^{-1}	% by mass	——
J04	1	3594335	5802683	354	286	1.20	0.91	6.19
J05	1	3594440	5803075	423	356	2.17	1.16	5.75
K03	1	3594695	5802400	263	209	0.67	0.47	6.27
K04	1	3594695	5802840	364	292	3.40	0.67	5.79
K05	1	3594835	5803260	423	382	1.03	1.24	6.31
K06	1	3594875	5803760	258	214	0.20	1.40	5.85
L03	1	3595270	5802433	502	362	4.30	1.15	5.65
L04	1	3595435	5802780	283	209	0.93	1.98	5.88
L05	1	3595180	5803335	350	300	1.36	1.27	6.15
L06	1	3595288	5803815	111	96	0.37	0.51	6.30
M02	1	3595660	5801860	411	271	0.20	0.99	6.99
M03	1	3595785	5802250	267	232	1.22	1.39	5.97
M04	1	3595851	5802650	174	175	3.72	0.87	4.96
M05	1	3595740	5803340	195	125	1.06	0.97	5.66
M06	1	3595710	5803765	197	170	2.13	0.63	5.83
N02	1	3596330	5801745	304	326	1.11	1.31	6.33
N03	1	3596205	5802240	415	323	1.25	1.46	6.46
N04	1	3596285	5802815	805	691	5.39	0.88	5.50
N05	1	3596185	5803250	541	416	7.19	0.93	5.18
N06	1	3596140	5803835	493	379	3.15	0.81	5.99
N07	1	3596215	5804275	119	121	1.50	0.64	5.36
O01	1	3596720	5801415	191	153	0.64	0.84	6.54
O02	1	3596735	5801750	290	282	1.24	0.67	5.68
O03	1	3596740	5802220	354	208	3.89	0.61	5.22
O04	1	3596620	5802775	229	165	0.51	0.65	6.38
O05	1	3596690	5803385	407	324	1.65	0.69	5.93
O06	1	3596580	5803775	687	668	2.20	1.28	5.66
P01	1	3597190	5801110	416	367	0.84	0.99	6.19
P02	1	3597110	5801755	133	146	3.45	0.50	4.99
P03	1	3597150	5802330	338	277	1.87	1.00	5.76
P04	1	3597205	5802650	557	394	1.57	0.88	6.59
Q01	1	3597720	5801090	243	212	1.13	0.68	6.09
Q02	1	3597630	5801670	494	314	0.67	0.68	6.77
G09	2	3592865	5805200	392	345	0.70	0.91	6.48
H09	2	3593430	5805325	158	137	0.46	0.37	6.07
H10	2	3593188	5805768	257	227	0.94	0.63	5.72
H11	2	3593252	5806339	152	114	0.25	0.83	5.79
H12	2	3593145	5806653	340	369	2.38	0.61	5.53
H13	2	3593145	5807168	185	108	0.78	0.61	5.57
H14	2	3593419	5807662	316	199	0.79	1.00	6.30

Continuation of Table A2

I08	2	3593690	5804865	285	162	0.43	1.00	6.10
I09	2	3593824	5805279	267	157	2.71	0.44	5.16
I10	2	3593715	5805815	429	299	4.00	1.06	5.20
I11	2	3593750	5806310	325	191	0.41	0.79	6.24
I12	2	3593575	5807023	429	331	1.06	0.51	6.27
I12/1	2	3593651	5806810	465	377	1.33	0.71	6.20
I13	2	3593558	5807207	846	582	1.83	1.13	6.05
J07	2	3594100	5804275	447	374	0.79	0.80	6.21
J08	2	3594125	5804760	399	312	5.46	0.79	5.12
J09	2	3594075	5805295	< d.l.	102	0.52	0.62	6.38
J10	2	3594420	5805865	218	172	2.53	0.50	5.03
J10/1	2	3594420	5805866	197	175	1.60	0.74	5.27
J11	2	3594265	5806425	225	226	1.19	1.12	5.92
J12	2	3594340	5806789	561	416	2.94	0.94	5.90
J13	2	3594265	5807165	162	159	1.45	0.44	5.44
K07	2	3594735	5804295	304	242	1.71	0.85	5.60
K09	2	3594815	5805265	< d.l.	52	0.23	0.66	6.13
K10	2	3594677	5805739	166	147	1.44	0.51	5.29
K11	2	3594740	5806210	124	100	0.97	0.36	5.59
K12	2	3594740	5806725	263	240	1.03	1.12	5.68
K13	2	3594615	5807305	240	220	0.60	0.85	6.38
L07	2	3595135	5804400	388	247	1.41	0.70	5.76
L08	2	3595245	5804855	190	195	1.23	0.63	5.76
L09	2	3595205	5805390	365	344	1.79	0.80	6.14
L10	2	3595175	5805825	307	240	1.71	0.66	5.61
L11	2	3595245	5806341	314	267	0.78	1.19	6.24
L12	2	3595243	5806805	< d.l.	118	0.26	0.89	6.23
L13	2	3595087	5807330	320	285	1.34	0.76	5.63
M07	2	3595715	5804450	321	341	1.07	1.38	5.99
M08	2	3595670	5804790	352	310	1.80	0.51	5.78
M09	2	3595665	5805240	313	262	1.36	0.75	5.82
M12	2	3595590	5806880	< d.l.	104	0.33	0.36	5.90
N08	2	3596125	5804575	273	258	0.20	0.64	5.96
Z01	2	3595435	5805345	259	277	5.46	0.79	5.20
F14	3	3592310	5807700	m.v.	34	0.20	0.48	6.41
F15	3	3592285	5808285	119	76	1.37	0.90	4.92
F16	3	3592305	5808715	1167	150	1.00	1.63	5.78
F17	3	3592250	5809370	795	816	2.82	1.60	5.78
F18	3	3592315	5809785	531	464	1.65	1.74	5.87
F19	3	3592427	5810178	577	449	1.29	2.52	5.64
F20	3	3592085	5810671	516	710	1.81	1.08	5.54
G13	3	3592652	5807351	174	145	0.96	0.63	5.93
G14	3	3592730	5807775	598	432	3.91	1.38	5.56
G15	3	3592705	5808210	390	394	3.12	1.53	5.79
G16	3	3592758	5808817	499	336	1.54	1.71	5.82
G17	3	3592745	5809318	956	760	2.34	2.31	6.21
G18	3	3592658	5809675	784	716	3.27	1.62	5.50
G19	3	3592640	5810260	376	338	1.24	1.13	5.71
G20	3	3592695	5810720	295	246	0.95	1.18	6.15
H15	3	3593270	5808280	367	264	1.45	1.24	5.75
H16	3	3593263	5808730	515	466	2.59	2.51	5.73
H17	3	3593355	5809210	239	105	2.03	1.05	4.98
H18	3	3593415	5809695	643	336	2.91	1.24	5.66

Continuation of Table A2

H19	3	3593350	5810120	383	235	1.60	0.71	5.66
H20	3	3593395	5810830	395	268	1.22	0.80	5.55
H21	3	3593180	5811235	498	257	5.76	0.95	4.97
I14	3	3593684	5807600	380	237	1.44	1.00	5.96
I15	3	3593600	5808140	262	144	0.75	0.83	5.78
I16	3	3593753	5808710	676	491	2.35	1.47	5.79
I17	3	3593695	5809378	573	362	2.11	0.93	5.76
I18	3	3593645	5809685	1485	1135	6.16	1.06	5.45
I19	3	3593790	5810195	m.v.	334	1.38	0.83	6.13
I20	3	3593665	5810710	157	114	0.96	0.73	5.45
I21	3	3593720	5811271	254	196	1.28	0.70	5.67
I22	3	3593744	5811608	173	153	0.79	0.67	5.74
J14	3	3594335	5807753	396	332	2.40	1.22	5.40
J15	3	3594225	5808250	324	286	3.91	0.96	5.07
J16	3	3594178	5808715	176	185	1.07	0.92	5.86
J17	3	3594290	5809390	404	159	4.33	1.04	4.86
J18	3	3594183	5809755	369	291	2.96	1.62	5.15
J19	3	3594260	5810175	240	184	0.52	0.96	6.10
K14	3	3594733	5807715	100	86	0.52	0.66	5.63
K15	3	3594638	5808320	162	144	1.25	0.66	5.77
K16	3	3594755	5808770	461	345	4.74	1.12	5.10
K17	3	3594845	5809135	264	162	0.30	1.02	6.33
K18	3	3594622	5809810	176	123	2.03	0.68	4.80
L14	3	3595163	5807708	334	336	0.58	0.92	5.61
L15	3	3595085	5808460	376	317	2.55	0.81	5.55
Z02	3	3593360	5808720	202	212	1.92	0.96	5.75
A26	4	3590000	5813610	150	131	0.19	0.26	6.16
B25	4	3590213	5813270	511	498	3.35	1.30	5.75
B26	4	3590313	5813620	919	872	4.42	0.64	5.64
C23	4	3590830	5812229	318	280	1.29	4.94	5.21
C24	4	3590565	5812815	181	150	0.20	2.46	5.39
C25	4	3590635	5813241	505	327	1.96	0.72	5.63
C26	4	3590883	5813665	254	186	1.22	1.37	5.71
C27	4	3590910	5814340	267	185	0.63	0.49	6.58
D20	4	3591320	5811040	350	255	0.68	1.20	5.95
D21	4	3591265	5811146	203	131	0.97	1.81	5.24
D22	4	3591136	5811754	351	231	0.67	3.31	5.39
D23	4	3591125	5812370	516	384	2.06	1.96	5.37
D24	4	3591199	5812820	373	327	0.20	1.59	6.28
D25	4	3591111	5813099	325	276	0.55	0.88	5.87
D26	4	3591351	5813645	262	212	0.32	1.91	6.07
D27	4	3591244	5814060	308	213	1.66	0.94	5.39
E20	4	3591765	5810973	396	306	0.64	2.31	6.24
E21	4	3591670	5811154	296	219	0.57	1.68	6.24
E22	4	3591735	5811690	544	522	1.81	3.37	5.18
E23	4	3591528	5812450	203	154	0.58	2.59	5.97
E24	4	3591775	5812735	473	359	2.06	0.91	5.63
E25	4	3591799	5813266	135	101	0.20	0.37	5.63
E26	4	3591630	5813755	470	324	1.76	0.57	5.90
F21	4	3592108	5811160	434	444	1.52	3.20	5.52
F22	4	3592190	5811800	417	366	3.00	1.07	5.32
F23	4	3592120	5812290	249	239	0.70	1.28	5.94
F24	4	3592398	5812989	490	366	1.43	0.68	5.65

Continuation of Table A2

F25	4	3592046	5813330	281	241	1.26	0.39	5.72
G21	4	3592707	5811426	283	148	1.51	0.81	5.76
G22	4	3592830	5811738	519	391	1.05	0.86	5.62
G23	4	3592850	5812164	434	308	1.21	1.07	5.56
G24	4	3592598	5812633	375	323	1.72	0.85	5.53
H22	4	3593336	5811797	400	259	1.49	0.74	5.81
H23	4	3593149	5812159	226	133	0.64	0.58	5.66
D17	outside	3591193	5809318	418	301	4.28	0.81	5.23
D18	outside	3591415	5809582	129	94	0.30	0.82	6.17
D19	outside	3591303	5810155	101	57	0.60	0.68	5.52
E15	outside	3591695	5808470	244	196	0.26	0.82	6.36
E16	outside	3591620	5808665	138	114	0.60	0.74	5.72
E17	outside	3591675	5809335	220	143	0.37	1.12	5.84
E18	outside	3591770	5809711	109	383	0.32	1.38	5.96
E19	outside	3591663	5810120	127	53	< d.l.	1.33	5.73

< d.l.: value below detection limit.
m.v.: missing value.

Table A3: Measured data of the winter wheat sites investigated in 1998 (control plots of the *BMWA*) and 1999 (W01-W20). The average saturation deficit of the air during the main vegetation period was 591 Pa in 1998 and 785 Pa in 1999.

	Gauß-Krüger-coordinates		Cd content in plant parts		Dry matter		Cd concentration in soil solution			
ID	**X**	**Y**	**Grain**	**Straw**	**Grain**	**Straw**	**0-0.3 m**	**0.3-0.4 m**	**0.4-0.5 m**	**0.5-0.6 m**
——	— m —	— m —	mg kg^{-1}	mg kg^{-1}	g m^{-2}	g m^{-2}	µg L^{-1}	µg L^{-1}	µg L^{-1}	µg L^{-1}
I2			0.128†				2.96	0.64	0.14	< d.l.
I3			0.117†				1.59	0.16	< d.l.	< d.l.
II3			0.137†				1.84	0.22	< d.l.	< d.l.
II5			0.254†				0.80	0.30	< d.l.	0.26
III1a			0.623†				8.24	2.54	1.18	2.34
III1b			0.831†				7.62	0.50	0.25	0.21
III2a			0.375†				3.96	0.44	0.34	0.33
III2b			0.333†				4.45	0.38	0.46	0.93
III4			0.179†				1.29	< d.l.	< d.l.	< d.l.
III5			0.052†				1.18	0.19	< d.l.	< d.l.
IV1			0.083†				0.58	< d.l.	< d.l.	< d.l.
IV4			0.166†				0.82	0.32	0.18	< d.l.
IV5			0.094†				1.13	2.20	0.14	< d.l.
W01	3596194	5803115	2.735	10.063	854	937	72.23	32.66	27.03	23.03
W02	3593559	5809295	0.159	0.272	672	568	0.51	0.43	1.03	0.41
W03	3593773	5809336	0.248	0.490	803	809	2.73	1.27	0.35	0.23
W04	3593600	5809630	0.273	0.551	653	731	1.35	12.74	3.23	1.36
W05	3593270	5810157	0.229	0.422	904	749	1.95	0.27	< d.l.	< d.l.
W06	3594823	5809113	0.063	0.123	937	797	0.38	< d.l.	< d.l.	< d.l.
W07	3594948	5808135	0.088	0.285	816	740	1.37	0.28	< d.l.	< d.l.
W08	3596213	5804319	0.154	0.223	1027	1175	1.39	0.31	0.33	< d.l.
W09	3596990	5801810	0.166	0.666	817	657	3.05	4.07	2.86	2.06
W10	3595260	5802450	0.231	0.529	700	852	3.64	1.65	0.61	0.28
W11	3594644	5803993	0.092	0.129	1013	879	1.48	1.04	1.03	< d.l.
W12	3593320	5806245	0.478	1.171	813	666	5.28	1.66	< d.l.	< d.l.
W13	3593273	5807063	0.191	0.435	732	583	1.85	< d.l.	< d.l.	< d.l.
W14	3595374	5805408	0.131	0.339	925	1149	1.93	< d.l.	< d.l.	< d.l.
W15	m.v.	m.v.	0.223	0.524	853	966	1.47	0.88	< d.l.	< d.l.
W16	3591944	5810380	0.120	0.207	934	1022	1.24	0.13	< d.l.	0.15
W17	3592630	5812630	0.094	0.211	716	657	1.35	0.21	0.10	0.11
W18	3591905	5813575	0.153	0.199	844	852	0.78	0.82	1.24	< d.l.
W19	3591840	5812590	0.177	0.246	764	731	0.88	1.79	0.66	0.15
W20	3592035	5811165	0.115	0.131	576	598	1.11	0.34	0.40	0.14

< d.l.: value below detection limit.
m.v.: missing value.
†: Data of the Braunschweig Municipal Waste Water Association (*BMWA*). The identification numbers of the control plots are internally used by the *BMWA*.

Table A4: Measured data of the sugar beet sites investigated in 1998 (Z1-Z20) and 1999 (Z21-Z40). The average saturation deficit of the air during the main vegetation period was 614 Pa in 1998 and 898 Pa in 1999.

	Gauß-Krüger-coordinates		Cd content in plant parts		Dry matter per plant		Cd concentration in soil solution			
ID	X	Y	Leaves	Hypocotyl	Leaves	Hypocotyl	0-0.3 m	0.3-0.4 m	0.4-0.5 m	0.5-0.6 m
——	— m —	— m —	mg kg^{-1}	mg kg^{-1}	— g —	— g —	µg L^{-1}	µg L^{-1}	µg L^{-1}	µg L^{-1}
Z01	3596475	5801915	0.449	0.141	166	364	3.92	3.50	1.32	0.64
Z02	3596020	5803080	3.736	0.665	115	266	17.91	16.79	14.05	2.77
Z03	3595990	5803695	0.607	0.225	108	404	4.86	5.83	6.24	3.40
Z04	3595090	5803850	0.814	0.266	93	225	3.65	5.17	5.78	5.07
Z05	3594930	5803135	0.326	0.107	110	277	3.02	1.88	1.69	1.72
Z06	3593665	5804870	0.386	0.069	125	377	2.66	1.17	0.64	0.26
Z07	3593600	5805650	0.919	0.221	80	448	5.13	< d.l.	< d.l.	< d.l.
Z08	3593340	5807025	1.816	0.408	84	261	5.41	2.77	1.89	2.54
Z09	3594710	5806750	1.107	0.230	78	350	3.51	0.82	0.32	0.43
Z10	3594605	5805810	0.847	0.224	104	329	2.26	2.68	2.60	3.12
Z11	3594740	5807470	0.535	0.152	28	117	2.31	1.27	1.30	1.94
Z12	3594590	5807910	0.537	0.185	53	145	2.70	1.02	1.05	1.31
Z13	3593750	5809310	0.660	0.331	61	244	4.10	3.80	2.47	2.33
Z14	3593195	5810260	0.718	0.153	84	255	2.44	1.33	0.35	0.49
Z15	3592630	5807930	1.061	0.416	70	200	3.36	1.29	1.69	1.17
Z16	3592620	5811615	0.446	0.246	47	133	3.30	1.38	0.53	0.43
Z17	3591850	5812800	0.377	0.121	61	190	1.85	1.03	0.56	0.59
Z18	3591875	5913625	0.592	0.219	41	101	1.72	0.48	0.22	< d.l.
Z19	3590325	5814310	0.523	0.069	82	228	1.10	1.17	0.48	0.26
Z20	3591530	5811695	1.910	0.395	159	521	5.26	2.84	1.65	1.11
Z21	3596167	5801555	0.900	0.282	162	290	2.51	0.34	< d.l.	< d.l.
Z22	3596969	5802395	0.681	0.171	126	245	1.17	0.18	< d.l.	< d.l.
Z23	3595896	5803108	0.882	0.216	82	270	1.02	0.30	< d.l.	< d.l.
Z24	3593420	5809510	2.265	0.522	93	185	4.55	< d.l.	< d.l.	< d.l.
Z25	3593515	5809626	0.738	0.166	104	191	3.27	0.94	1.05	0.79
Z26	3594908	5803711	0.731	0.160	118	442	2.05	2.24	0.20	< d.l.
Z27	3594436	5802350	0.628	0.165	144	560	1.59	1.77	0.75	< d.l.
Z28	3593795	5804955	0.623	0.288	84	171	1.55	0.56	0.26	0.11
Z29	3593475	5806316	0.422	0.098	76	243	0.53	0.42	0.52	0.69
Z30	3594545	5805503	0.475	0.154	102	331	0.89	1.27	0.96	0.41
Z31	3596009	5804990	1.373	0.250	108	382	3.23	0.81	0.40	0.16
Z32	3595245	5806465	1.040	0.215	473	432	4.48	0.72	0.25	< d.l.
Z33	3592775	5809376	2.173	0.473	73	301	4.20	0.41	0.15	< d.l.
Z34	3593600	5809470	1.408	0.107	100	308	1.21	0.37	0.40	0.34
Z35	3593345	5810135	0.476	0.115	113	179	0.99	1.26	0.86	< d.l.
Z36	3592383	5812912	0.507	0.349	85	297	1.68	0.79	0.38	0.30
Z37	3591285	5813750	1.300	0.362	85	198	2.13	0.51	0.61	0.82
Z38	3590241	5813285	0.846	0.117	48	115	2.53	0.30	< d.l.	< d.l.
Z39	3592082	5811843	1.144	0.266	96	385	2.08	0.29	< d.l.	< d.l.
Z40	3591560	5811000	1.252	0.189	59	247	2.13	0.43	0.21	< d.l.

< d.l.: value below detection limit.

Table A5: Measured data of the potato sites investigated in 1998 (K01-K20) and 1999 (K21-K40). The average saturation deficit of the air during the main vegetation period was 692 Pa in 1998 and 917 Pa in 1999.

	Gauß-Krüger-coordinates		Cd content in plant parts		Dry matter per plant		Cd concentration in soil solution			
ID	X	Y	Straw	Tuber†	Straw	Tuber†	0-0.3 m	0.3-0.4 m	0.4-0.5 m	0.5-0.6 m
——	— m —	— m —	mg kg^{-1}	mg kg^{-1}	— g —	— g —	µg L^{-1}	µg L^{-1}	µg L^{-1}	µg L^{-1}
K01	3595495	5805160	2.675	0.104	72	558	3.10	0.10	< d.l.	< d.l.
K02	3595680	5805230	4.849	0.180	17	98	3.85	0.19	< d.l.	< d.l.
K03	m.v.	m.v.	4.317	0.243	30	218	3.29	1.62	0.34	0.20
K04	m.v.	m.v.	3.801	0.162	37	350	3.49	1.23	1.01	0.89
K05	m.v.	m.v.	5.122	0.184	45	525	6.33	0.10	< d.l.	< d.l.
K06	m.v.	m.v.	4.046	0.206	73	706	5.78	0.93	0.28	0.05
K07	3594970	5806790	2.118	0.125	23	356	2.63	2.80	1.86	1.88
K08	m.v.	m.v.	1.835	0.070	44	520	1.55	0.87	0.37	0.17
K09	m.v.	m.v.	2.386	0.145	35	596	2.80	1.04	0.43	0.34
K10	m.v.	m.v.	2.330	0.105	20	346	1.32	0.24	< d.l.	< d.l.
K11	m.v.	m.v.	4.956	0.236	22	243	7.05	0.30	0.20	0.14
K12	m.v.	m.v.	2.840	0.156	26	279	3.43	0.36	0.31	< d.l.
K13	m.v.	m.v.	2.732	0.132	61	411	3.29	0.18	< d.l.	< d.l.
K14	m.v.	m.v.	1.956	0.098	59	430	1.69	0.33	0.16	0.20
K15	m.v.	m.v.	1.613	0.128	33	344	1.22	0.37	0.28	0.09
K16	3592950	5812090	2.398	0.093	33	303	2.20	0.32	< d.l.	< d.l.
K17	m.v.	m.v.	1.409	0.067	32	339	2.04	0.25	0.07	< d.l.
K18	m.v.	m.v.	1.814	0.074	36	473	1.71	0.15	0.05	< d.l.
K19	m.v.	m.v.	2.837	0.151	14	259	2.51	0.12	0.05	< d.l.
K20	m.v.	m.v.	2.742	0.179	21	360	3.28	0.65	0.64	0.56
K21	3596175	5801765	6.096	0.194	26	343	1.93	0.25	< d.l.	< d.l.
K22	3596490	5802124	2.587	0.187	71	476	2.14	0.64	0.27	0.48
K23	3595677	5803395	1.361	0.226	35	302	0.81	0.57	0.86	1.18
K24	3595774	5803855	3.845	0.572	44	220	1.90	0.32	< d.l.	< d.l.
K25	3595509	5805450	7.239	0.663	64	478	7.32	0.81	< d.l.	< d.l.
K26	3594615	5807178	2.624	0.354	72	278	2.22	1.34	1.30	1.73
K27	3594275	5807998	2.393	0.440	37	332	2.20	1.12	0.50	< d.l.
K28	3594180	5809434	3.851	0.309	39	366	2.12	0.40	< d.l.	0.26
K29	3593616	5809603	2.569	0.467	71	505	2.97	< d.l.	< d.l.	< d.l.
K30	3593780	5811460	1.649	0.176	41	363	1.10	< d.l.	< d.l.	< d.l.
K31	3591505	5813896	0.671	0.087	52	305	0.43	0.39	< d.l.	< d.l.
K32	3590510	5813554	1.351	0.233	67	390	1.28	< d.l.	< d.l.	< d.l.
K33	3591839	5812493	1.917	0.102	44	382	1.20	< d.l.	< d.l.	< d.l.
K34	3592568	5807689	5.133	0.329	25	181	1.79	1.25	0.77	0.61
K35	3592798	5807025	1.566	0.268	77	751	1.10	2.97	5.38	5.95
K36	3592675	5807625	1.546	0.207	39	289	1.21	1.52	1.90	0.68
K37	3593230	5806610	3.643	0.346	90	480	1.96	< d.l.	< d.l.	< d.l.
K38	3589988	5813415	1.164	0.155	30	279	0.49	< d.l.	< d.l.	< d.l.
K39	3590915	5813478	2.407	0.241	59	499	1.19	0.48	0.29	0.33
K40	3595160	5807129	1.948	0.270	29	202	1.60	< d.l.	< d.l.	< d.l.

< d.l.: value below detection limit.
m.v.: missing value.
†: including the peel.

Danksagung

Für die sehr gute Betreuung der Arbeit bin ich PD Dr. Thilo Streck zu besonderem Dank verpflichtet. In einer Vielzahl von Diskussionen hat er mir und der Arbeit wichtige Impulse gegeben. Prof. Dr. O. Richter danke ich für die Übernahme des Koreferats.

Ohne die große Kooperationsbereitschaft des Abwasserverbandes Braunschweig hätte die vorliegende Arbeit nicht entstehen können. In diesem Zusammenhang möchte ich mich bei Herrn Eggers und Herrn Seeßelberg bedanken. Besonderen Dank gilt Herrn Blickwede. Sein Wissen über die Geschichte des Verregnungsgebietes hat mir bei der Interpretation der Daten sehr geholfen.

Ein Dankeschön auch an Dr. J. Utermann von der Bundesanstalt für Geowissenschaften und Rohstoffe, der die Königwasseraufschlüsse der Oberbodenproben ermöglicht hat.

Vielen Dank an Birgit Heine und Alwin Küsters, die mich tatkräftig bei der Laborarbeit unterstützt haben. In diesem Zusammenhang sei natürlich auch Carmen Marheineke und Deborah Müntner gedankt. Ihnen ist es zu verdanken, daß diese Arbeit auf einer soliden (Daten-) Basis aufbauen konnte.

Udo Lampe und Marko Kastens danke ich für die tatkräftige Unterstützung bei den umfangreichen und oft nicht ganz unanstrengenden Feldarbeiten. Die schöne Zeit der Probenahmen im Verregnungsgebiet wird mir immer, bestimmt auch mit etwas Wehmut, in Erinnerung bleiben!

Ein herzliches Dankeschön auch an Uschi. Sie hat mir bei meinem täglichen Ringen mit Formularen, Dienstreiseanträgen und vor allem der finanziellen Abwicklung des Projekts unermüdlich beigestanden.

Ein Dankeschön auch an Sylvia Mönickes. Ihre lebendige und frohe Art hat im Raum 408 für ein sehr angenehmes Arbeitsklima gesorgt. Dr. Sven Altfelder danke ich für die vielen sowohl fachlichen als auch "börsentechnischen" Diskussionen.

Dr. Marco Roelcke, Andreas Pacholski und Deirdre Jacob danke ich für das Korrekturlesen. Ohne Ihr aufmerksames Lesen wäre die Arbeit sicherlich um das eine oder andere Pidgin-Englisch "reicher".

Beim Bewältigen von Soft- und Hardware Problemen haben mich des Öfteren Wolfgang Max und Klaus Schmalstieg unterstützt. Danke!

Schließlich möchte ich mich bei den Studentinnen und Studenten bedanken, die als studentische Hilfskraft an dieser Arbeit mitgewirkt haben. Ein Dankeschön an Christof Beyer, Kerstin Gottschalk, Christamaria Kugge, Anja Kuczera, Selma Linder, Julia Münch, Claas Nendel, Vanessa Stauch und Grit Walther.

Zu guter Letzt sei der Deutschen Forschungsgemeinschaft für die finanzielle Unterstützung der Arbeit gedankt.

Lebenslauf

Persönliche Angaben:	Name: Joachim Ingwersen
	Geburtsort: Bargum (Schleswig-Holstein)
	Geburtstag: 25.02.1969
	Familienstand: verheiratet, 1 Kind
	Staatsangehörigkeit: deutsch
Schulbildung:	
Aug. 1975-Juni 1979	Grundschule Leck
Aug. 1979-Mai 1985	Realschule Leck
Aug. 1985-Juni 1988	Fachgymnasium Niebüll (Schwerpunkt Agrarwirtschaft)
Militärdienst:	
Juli 1988-Juni 1990	Zeitsoldat
Berufsausbildung:	
Okt. 1990-Juli 1996	Studium der Geoökologie an der Technischen Universität Braunschweig
Praktikum:	
Aug. 1994-Okt. 1994	Fraunhofer-Institut für Atmosphärische Umweltforschung, Garmisch-Partenkirchen
Berufspraxis:	
Aug. 1996 bis Aug. 2000	Wissenschaftlicher Mitarbeiter am Institut für Geoökologie, Technische Universität Braunschweig